



DREDGED MATERIAL RESEARCH PROGRAM



TECHNICAL REPORT D-77-14

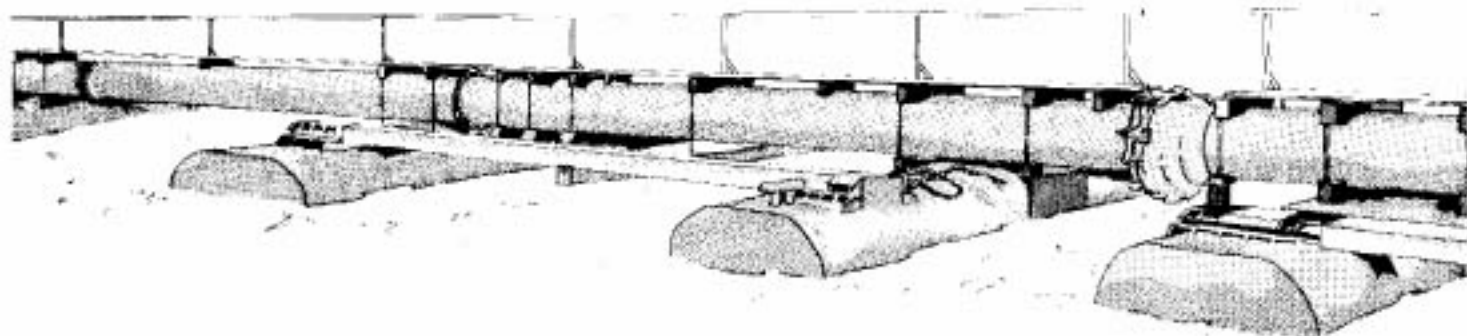
A LABORATORY STUDY OF THE TURBIDITY GENERATION POTENTIAL OF SEDIMENTS TO BE DREDGED

by

Barry A. Wechsler, David R. Cogley
Walden Division of Abcor, Inc.
850 Main St.
Wilmington, Massachusetts 01887

November 1977
Final Report

Approved For Public Release: Distribution Unlimited



Prepared for Office, Chief of Engineers, U. S. Army
Washington, D. C. 20314

Under Contract No. DACW39-75-C-0104
(DMRP Work Unit No. 6C01)

Monitored by Environmental Effects Laboratory
U. S. Army Engineer Waterways Experiment Station
P. O. Box 631, Vicksburg, Miss. 39180

Destroy this report when no longer needed. Do not return
it to the originator.



DEPARTMENT OF THE ARMY
WATERWAYS EXPERIMENT STATION, CORPS OF ENGINEERS
P. O. BOX 631
VICKSBURG, MISSISSIPPI 39180

IN REPLY REFER TO: WESYV

15 December 1977

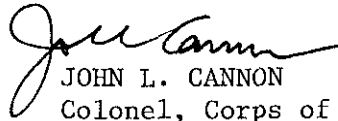
SUBJECT: Transmittal of Technical Report D-77-14

TO: All Report Recipients

1. The technical report transmitted herewith represents the results of one research effort (work unit) initiated as part of Task 6C (Turbidity Prediction and Control Research) of the Corps of Engineers' Dredged Material Research Program (DMRP). Task 6C, included as part of the Disposal Operations Projects of the DMRP, is concerned with investigating the problem of turbidity and developing methods to predict the nature, extent, and duration of turbidity around dredging and disposal operations. Equal emphasis is also placed on evaluating methods for controlling the generation and dispersion of turbidity.
2. Although there are still many questions about the direct and indirect effects of different levels of turbidity on aquatic organisms, turbidity generated by dredging and disposal operations can be aesthetically displeasing. Therefore, regardless of the ecological effects, high levels of turbidity generated by both dredging and disposal operations must be controlled when such measures are deemed necessary. However, before turbidity can be effectively controlled, the parameters controlling its generation and persistence in open-water environments must be evaluated. In addition, the development of a capability to predict the levels of turbidity that might be generated by dredging and/or disposal operations should provide a means for evaluating the necessity for different control measures.
3. This particular laboratory study undertaken by Walden Division of Abcor, Inc., Wilmington, Massachusetts, was concerned with the nature and amount of turbidity that a given sediment is likely to produce when re-suspended by a dredging or disposal operation. In addition, the relative importance of different sediment-water compositional factors which influence particle settling rates was also evaluated in a series of jar tests using three clay and eight natural sediments in a variety of test waters. The jar-test data also provided a quantitative evaluation of the duration of turbidity under various conditions. A turbidity plume model was developed to predict the extent of turbidity associated with the open-water pipeline discharge of dredged material slurry using the jar-test data to provide sediment settling velocity distributions.

SUBJECT: Transmittal of Technical Report D-77-14

4. This study addresses the settling aspects of dredged material suspensions and the relationship between these characteristics and the turbidity plumes that might be generated during a dredging or open-water disposal operation. This is the first of several studies concerned with the prediction of turbidity. Subsequent reports will present field data and further modeling of turbidity plumes generated by open-water pipeline disposal operations. Additional studies of turbidity-control techniques will provide information on silt curtains and the use of submerged pipeline discharge. Results of all studies conducted as part of Task 6C will be synthesized in one report that will give guidance on turbidity prediction and control.



JOHN L. CANNON

Colonel, Corps of Engineers
Commander and Director

REPORT DOCUMENTATION PAGE		READ INSTRUCTIONS BEFORE COMPLETING FORM	
1. REPORT NUMBER Technical Report D-77-14	2. GOVT ACCESSION NO.	3. RECIPIENT'S CATALOG NUMBER	
4. TITLE (and Subtitle) A LABORATORY STUDY OF THE TURBIDITY GENERATION POTENTIAL OF SEDIMENTS TO BE DREDGED		5. TYPE OF REPORT & PERIOD COVERED Final Report	
		6. PERFORMING ORG. REPORT NUMBER	
7. AUTHOR(s) Barry A. Wechsler David R. Cogley		8. CONTRACT OR GRANT NUMBER(s) Contract No. DACW39-75-C-0104	
9. PERFORMING ORGANIZATION NAME AND ADDRESS Walden Division of Abcor, Inc. 850 Main Street Wilmington, Massachusetts 01887		10. PROGRAM ELEMENT, PROJECT, TASK AREA & WORK UNIT NUMBERS DMRP Work Unit No. 6C01	
11. CONTROLLING OFFICE NAME AND ADDRESS Office, Chief of Engineers, U. S. Army Washington, D. C. 20314		12. REPORT DATE November 1977	
		13. NUMBER OF PAGES 177	
14. MONITORING AGENCY NAME & ADDRESS (if different from Controlling Office) U. S. Army Engineer Waterways Experiment Station Environmental Effects Laboratory P. O. Box 631, Vicksburg, Mississippi 39180		15. SECURITY CLASS. (of this report) Unclassified	
		15a. DECLASSIFICATION/DOWNGRADING SCHEDULE	
16. DISTRIBUTION STATEMENT (of this Report) Approved for public release; distribution unlimited.			
17. DISTRIBUTION STATEMENT (of the abstract entered in Block 20, if different from Report)			
18. SUPPLEMENTARY NOTES			
19. KEY WORDS (Continue on reverse side if necessary and identify by block number) Dredged material Sediment Dredging Settling Particles Turbidity			
20. ABSTRACT (Continue on reverse side if necessary and identify by block number) In order to understand the effects of physical and chemical factors which control particle settling rates and thereby develop the means to predict the extent of dredging-related turbidity, a series of laboratory jar tests was performed. The turbidity of suspensions of three pure clay samples and eight natural sediments was monitored as a function of time in waters of various salinity, hardness, and pH. The results were statistically analyzed to relate (Continued)			

20. ABSTRACT (Continued).

specific sediment and water compositional factors to observed settling rates and to evaluate their relative importance. Additional experiments were performed to characterize the nature of turbidity. While turbidity was found to be extremely persistent in soft fresh waters, hardness (200 mg/l) and particularly salinity (1-5 ppt) induced flocculation and consequently rapid settling. The organics content was the principal sediment component affecting turbidity, with higher organics levels correlated with more rapid settling in salt water. No significant segregation of sediment components was observed during settling, with the exception of coarser silt particles, which settled independently of clay-organic aggregates. A turbidity plume model was developed which accounts for flocculation in suspensions of dredged material.

Appendixes A-F were reproduced on microfiche and are enclosed in an envelope attached inside the back cover. Appendixes G and H follow the main text.

THE CONTENTS OF THIS REPORT ARE NOT TO
BE USED FOR ADVERTISING, PUBLICATION,
OR PROMOTIONAL PURPOSES. CITATION OF
TRADE NAMES DOES NOT CONSTITUTE AN OF-
FICIAL ENDORSEMENT OR APPROVAL OF THE
USE OF SUCH COMMERCIAL PRODUCTS.

SUMMARY

Turbidity generated by dredging and open-water disposal operations is objectionable for aesthetic reasons and for its potentially deleterious environmental effects. It would therefore be helpful to develop the means to predict the nature, duration, and extent of turbidity so that these problems can be minimized. This laboratory study was conducted to determine the nature and amount of turbidity that a given sediment is likely to produce when resuspended by dredging operations, and to evaluate the effects and relative importance of sediment and water compositional factors which influence particle settling rates.

A review of pertinent literature was performed to determine which sediment and water characteristics were likely to affect turbidity. Because of the colloidal nature of fine-grained silt, clay, and organic matter in suspensions of dredged material, the resultant turbidity is largely determined by particle agglomeration. Factors expected to be important based on previous studies included sediment composition (particle-size distribution, clay mineralogy, and organic content), water composition (salinity, hardness, and pH), and physical effects such as temperature and turbulence.

Laboratory jar tests were utilized to investigate the effects of sediment and water components on turbidity. Simple systems of pure clays and clay mixtures suspended in waters of various salinity, hardness, and pH were characterized first, followed by mixtures of clay with silt. Eight natural sediments were collected and extensively characterized concurrent with jar testing. The effect of initial sediment concentration was also studied. Turbidity data were statistically analyzed by stepwise linear regression techniques to determine which factors were significant in controlling turbidity.

Twenty-five experiments were replicated in a procedure designed to define the changes which take place over time as a given suspension flocculates and settles. Aliquots of the test suspensions taken at zero time and after significant settling had occurred were analyzed to determine the particle-size distribution, mineralogy, organic carbon

content, and zeta potential. This approach was utilized to obtain insight into possible mechanisms of particle agglomeration, physical interactions between various sediment components, differential settling rates of various components, and identifiable components responsible for persistent turbidity or rapid settling.

A wide variation in turbidity responses was observed for the range of sediments and waters examined. Turbidity was found to be quite persistent in soft fresh waters, but the presence of hardness levels typical of natural fresh waters (200 mg/l) led to slightly more rapid turbidity reduction. Low levels of salinity (1-5 ppt) were sufficient to induce flocculation and consequent rapid turbidity reduction.

The most important sediment compositional factor was the organics content (measured as % organic carbon), with higher organics levels correlated with more rapid settling in salt water. Clay mineralogy was not found to be a significant factor in experiments with natural sediments, although tests with pure clays did indicate disparities between different clay minerals. Increased initial sediment concentration also resulted in significantly more rapid settling.

No significant segregation of sediment components was observed during settling, with the exception of coarser silt particles, which settled independently. These and other results suggest that particle agglomeration in dredged material suspensions is strongly affected by the natural organics present and that clay-organic aggregates may be formed.

A simple plume model predicting the extent of turbidity associated with the discharge of dredged material slurry in open water was developed using jar-test data to provide particle settling-velocity distributions. Preliminary testing of the model by comparison of predicted plumes with field observations in Mobile Bay yielded favorable results. The results also suggest that significant variations in the extent of turbidity can be ascribed to sediment settling rates. Further testing is required to validate this model and to determine its effectiveness in providing useful estimates of turbidity plumes.

PREFACE

The work described in this report was performed under Contract DACW39-75-C-0104 entitled, "A Laboratory Study of the Turbidity Generation Potential of Sediments to be Dredged," dated 9 June 1975, between the U. S. Army Engineer Waterways Experiment Station (WES), Vicksburg, Mississippi, and the Walden Division of Abcor, Inc., Wilmington, Massachusetts. *67*

Work on this program was performed by Mr. Barry Wechsler and Ms. Perla Fickenschner under the management and supervision of Dr. David R. Cogley. Dr. Ralph D'Agostino, Associate Professor of Mathematics at Boston University, served as statistical consultant and is gratefully thanked for his patience and insight. Dr. John B. Southard, Associate Professor of Geology at Massachusetts Institute of Technology (M.I.T.), was primarily responsible for the derivation of the turbidity plume model, and Dr. W. Gilbert Strang, Professor of Mathematics at M.I.T., provided the numerical solution method. Mr. Kenneth Wiltsee of Walden wrote the plume model computer program. Dr. Robert L. Goldsmith, Director of the Technology Development Department at Walden, reviewed all phases of this program and provided valuable comments and direction. *Dr. Southard - 12/1/75*

This research was sponsored by the Dredged Material Research Program (DMRP) being administered by the Environmental Effects Laboratory (EEL) of WES. The study was conducted as part of the Disposal Operations Project (DOP), Task 6C, "Turbidity Prediction and Control," Work Unit 6C01. Dr. William D. Barnard was Manager of Task 6C; Mr. Charles C. Calhoun, Jr., was Manager of the DOP.

Directors of WES during the study and preparation of the report were COL G. H. Hilt, CE, and COL J. L. Cannon, CE. Technical Director was Mr. F. R. Brown.

Approved for Release by NSA on 05-08-2014 pursuant to E.O. 13526

BILL
10/1/75
E-1574

CONTENTS

	<u>Page</u>
SUMMARY.	2
PREFACE.	4
LIST OF FIGURES.	7
LIST OF TABLES	9
CONVERSION FACTORS	10
PART I: INTRODUCTION.	11
PART II: LITERATURE EVALUATION OF FACTORS CONTROLLING TURBIDITY.	13
The Nature of Turbidity	13
Factors Affecting the Settling of Suspended Sediments	15
PART III: EXPERIMENTAL DESIGN AND TEST PROCEDURES	25
Rationale and Approach.	25
Jar-Test Procedures	31
Test Plan and Sample Characterization	35
PART IV: TURBIDITY DATA AND ANALYSIS.	48
Preliminary and Subsidiary Tests.	48
Clays and Clay Mixtures	62
Silt Tests.	69
Natural Sediments	70
Summary and Discussion	80
PART V: TURBIDITY PLUME MODEL	86
Material Balance Relationship	86
Estimation of Settling Velocities from Jar-Test Data.	91
Numerical Solution of the Material Balance Equation	98
Computer Program and Sample Calculation	100
PART VI: APPLICATIONS TO FIELD USE.	113
Sediment and Water Sampling	113
Jar-Test Procedures	115
Turbidity Plume Modeling.	116

	<u>Page</u>
PART VII: CONCLUSIONS AND RECOMMENDATIONS.	118
Conclusions.	118
Recommendations.	120
REFERENCES.	122
APPENDIX A: SEDIMENT SAMPLING AND HANDLING DETAILS*	A1
APPENDIX B: SAMPLE CHARACTERIZATION PROCEDURES*	B1
APPENDIX C: COMPOSITION OF SYNTHETIC SEA SALT*	C1
APPENDIX D: TURBIDITY TESTING OF H ₂ O ₂ -TREATED SEDIMENTS*	D1
APPENDIX E: TURBIDITY DATA*	E1
APPENDIX F: REPLICATE TEST DATA*	F1
APPENDIX G: PLUME MODEL COMPUTER PROGRAM	G1
APPENDIX H: NOTATION	H1

* Appendixes A-F are reproduced on microfiche and are enclosed in an envelope attached to the inside of the back cover.

LIST OF FIGURES

<u>No.</u>		<u>Page</u>
1	Test plan matrix for clays and clay mixtures	41
2	Test plan matrix for silt tests.	41
3	Scanning electron micrographs of the <2 μ fraction of the Charles River sediment	44
4	Scanning electron micrographs of the Illinois River sediment.	45
5	Test plan matrix for natural sediments	46
6	Turbidity of kaolinite suspensions in two test waters at four wavelengths.	49
7	Turbidity of kaolinite suspensions in 0.5% sodium chloride solution, settling at three different temperatures	50
8	Turbidity of silt suspensions after 30 min of settling as a function of stirring rate during settling	52
9	Turbidity of kaolinite suspensions at various sea salt concentrations	54
10	Turbidity of illite suspensions at various sea salt concentrations	55
11	Turbidity of montmorillonite suspensions at various sea salt concentrations	56
12	Light attenuation as a function of suspended solids for clays and natural sediments.	58
13	Light scattering as a function of suspended solids for clays and natural sediments.	59
14	Light scattering as a function of light attenuation for clays and natural sediments	60
15	Turbidity of kaolinite suspensions in five test waters.	63

<u>No.</u>		<u>Page</u>
16	Turbidity of kaolinite, montmorillonite, and kaolinite + montmorillonite mixture in 0.5% sea salt solution	65
17	Turbidity of eight natural sediment suspensions in 0.1% sea salt solution	71
18	Residual turbidity (α/α_0) of eight natural sediment suspensions in 0.1% sea salt solution.	72
19	Turbidity of Mobile Bay sediment in 0.5% sea salt solution	94
20	Cumulative settling-velocity distribution for Mobile Bay sediment	95
21	Two-dimensional concentration distribution for one sediment fraction (no lateral spreading).	103
22	Summation of two-dimensional concentration distributions for all sediment fractions (no lateral spreading).	103
23	Table of lateral spreading factors	104
24	Surface concentration distribution	105
25	Comparison of predicted and observed center-line concentrations for Mobile Bay turbidity plumes	106
26	Predicted center-line turbidities at the surface for three different settling curves at two current velocities	110

LIST OF TABLES

<u>No.</u>		<u>Page</u>
1	Analytical Data for Clays and Natural Sediments	36
2	Mineralogy and Cation Exchange Capacity of Clays and the $<2 \mu$ Fraction of Natural Sediments	37
3	Regression Equations for α , FTU, and SS	61
4	Statistical Analysis of Clay and Clay-Mixture Data.	67
5	Evaluation of Preferential Settling of Sediment Components	74
6	Statistical Analysis of Natural Sediment Sedi- mentation Data	78
7	Settling-Velocity Distribution.	97

CONVERSION FACTORS, U. S. CUSTOMARY TO METRIC (SI)
UNITS OF MEASUREMENT

U. S. customary units of measurement used in this report can be converted to metric (SI) units as follows:

<u>Multiply</u>	<u>By</u>	<u>To Obtain</u>
angstroms	1.0×10^{-10}	meters
microns	0.000001	meters
inches	0.0254	meters
feet	0.3048	meters
yards	0.9144	meters
miles (U. S. statute)	1.609344	kilometers
miles (U. S. nautical)	1.852	kilometers
knots (international)	0.5144444	meters per second

A LABORATORY STUDY
OF THE TURBIDITY GENERATION POTENTIAL
OF SEDIMENTS TO BE DREDGED

PART I: INTRODUCTION

1. The Waterways Experiment Station (WES) is engaged in a comprehensive research program on the environmental effects of dredging and the disposal of dredged material. One aspect of this Dredged Material Research Program (Task 6C) deals specifically with the prediction and control of turbidity generated during both dredging and open-water disposal operations. While turbidity may have deleterious chemical and biological effects, it is also considered objectionable for aesthetic reasons. Research is needed to permit prediction of the nature, extent, and duration of turbidity resulting from dredging activities so that environmental impacts can be assessed and control measures can be implemented to minimize harmful effects.

2. Turbidity results from the resuspension and subsequent slow settling of fine-grained silt, clay, and organic matter in dredged material. These particles display colloidal properties and settle at rates which are largely dependent upon the chemical and physical characteristics of both the sediments and the water in which they are suspended. Thus, to understand the settling behavior of suspended dredged material, one must consider the sediment compositional factors, such as particle-size distribution, clay mineralogy, and organic content; water compositional factors including pH, salinity (in estuarine waters), and hardness (in fresh waters); and physical factors affecting coagulation and settling, such as temperature and turbulence.

3. The primary goals of this laboratory study were to determine the nature and amount of turbidity that a given sediment is likely to produce when resuspended by dredging operations, and to evaluate the effects and relative importance of the sediment-water compositional factors which influence particle settling rates. The factors controlling turbidity were determined in a series of jar tests on three clays

and eight natural sediments in a variety of test waters. These jar-test data also provided a quantitative evaluation of the duration of turbidity under various conditions. The nature of turbidity was determined through a series of measurements of particle-size distribution, mineralogy, zeta potential, and organic content. A turbidity plume model was developed to predict the extent of turbidity associated with the discharge of dredged material, using jar-test data to provide sediment settling-velocity distributions.

PART II: LITERATURE EVALUATION OF FACTORS CONTROLLING TURBIDITY

The Nature of Turbidity

4. Turbidity is a term describing the cloudy appearance of waters which contain sufficient suspended matter to prevent one's seeing through them clearly. To an observer outside the water, the visible turbidity is caused primarily by light scattered from suspended particles at or near the surface, while an underwater observer might notice a decrease in the intensity of transmitted light. This decrease, or light attenuation, results from the absorption of light by dissolved and suspended organic and inorganic substances in the water as well as the scattering by suspended particles.

5. Although turbidity is a visual phenomenon, it can be quantified by several types of measurements, including light transmission, scattering, and suspended solids concentration. The amount of scattering and absorption is controlled by the concentration of particles, their shape, size distribution, refractive index, and color. The quantitative measurement of turbidity by transmission or scattering is affected by parameters such as the instruments' angle of measurement, the size and shape of the optical beam, the volume of the sample, path length, and spectral distribution of the light source. Thus, for a given weight of suspended material, the turbidity measured optically may differ for various samples, depending on the physical properties of the particles and the instrumental configuration. In this study, turbidity was quantified by measuring % light transmission, light scattering, and suspended solids.

6. Dredged material consists of large particles (sand and gravel), silt, clay, and organics. The coarse-grained fractions ($>74 \mu$)* settle rapidly under normal conditions of water turbulence and thus do not contribute significantly to the turbid appearance of water. Silt comprises

* A table of factors for converting U. S. customary units of measurement to metric (SI) units is presented on page 10.

the nonclay mineral fraction of sediment with a grain size of 2-74 μ . Although silt particles, with settling rates as low as 1 cm/hr, may contribute to turbidity, in most cases the clay fraction is mainly responsible for the turbid appearance of water in the vicinity of dredging operations.

7. The clay fraction of sediments consists of fine particles which usually possess layered crystal structures. These clay particles, together with organic matter in sediments, display colloidal properties and settle at rates that are largely dependent upon the nature of the particles themselves as well as the chemical and physical characteristics of the water. The mineralogy, chemical composition, and size distribution of the suspended matter, as well as the composition, temperature, and shear rate of the fluid phase, all influence the settling behavior of the fine-grained sediment.

8. The stability (i.e., slow settling rate) of a colloidal suspension of clay particles is due to the small size and the negative surface charge of the particles. Because of the small particle size, settling is inhibited by the Brownian motion of the surrounding water molecules. Only when individual particles adhere to one another, producing relatively large agglomerates (\sim 50-100 μ), does settling occur at a more rapid rate (\sim 1-3 m/hr). The process by which such agglomerates are formed is referred to as coagulation or flocculation.

9. Because of the small size of the particles, surface charge effects exert a major influence on the behavior of clay suspensions. The primary negative surface charge on the faces of the clay "plates" is balanced by the formation of a layer of oriented water molecules around each clay particle. This particle-water interaction results in the formation of an electrical double layer at the interface between the clay particles and water. The clay particles are thus surrounded by an electric field which repels other similarly charged particles. In stable colloids, the short-range, attractive van der Waals forces are overcome by the repulsion arising from the electric field associated with the charged surfaces of the clay particles. In the absence of any flocculating agent, the repulsive forces extend far enough away from

the particles to prevent their close approach and subsequent agglomeration. In order for agglomeration to take place, the electric fields surrounding the particles must be reduced, allowing the attractive forces to act when interparticle collisions occur.

10. The agglomeration of dispersed particles in a colloid, then, depends on the collision frequency of the particles and the relative adhesiveness of the particles. Factors which influence the collision frequency, such as the concentration of suspended matter and the water agitation, and factors which affect the electrical forces associated with the particles, such as the solution composition, particle composition, the ion exchange properties of the particles, and their adsorption properties, determine the rate of agglomeration of the fine particulate matter. In the following sections, each of these factors and their importance under various environmental conditions is discussed more fully.

Factors Affecting the Settling of Suspended Sediments

Particle size

11. Sediment particle size influences the persistence of turbidity by determining particle settling rates. The effect of sediment particle size can be evaluated in terms of the settling velocity of equivalent spherical particles of equal density. The settling velocity of a small sphere in a viscous fluid is given by Stokes' Law:

$$w^* = \frac{gd^2(\rho_s - \rho_l)}{18\eta} \quad (1)$$

where w is the settling velocity; g is the gravitational acceleration (980.6 cm/sec^2); d is the diameter of the sphere; ρ_s ($\approx 2.5 \text{ g/cm}^3$) and

* For convenience, symbols and unusual abbreviations are listed and defined in the Notation (Appendix H).

ρ_1 are the densities of the sphere and liquid, respectively; and η is the coefficient of viscosity of the liquid (8.94×10^{-3} g/cm-sec for water at 25°C). The particle settling rate varies as the square of the particle radius, so that a 5 μ particle would settle twenty-five times as fast as a 1 μ particle. In other words, for nonagglomerating particles, turbidity due to 1 μ particles would persist twenty-five times longer than turbidity due to 5 μ particles.

12. For colloidal materials, turbidity persistence is often governed not by the settling of individual particles but by the settling of particle agglomerates. These agglomerates can achieve much higher settling velocities than individual particles because of their larger diameters (assuming densities of the same order of magnitude). Thus, in cases where coagulation takes place, turbidity persistence can be governed by the rate of particle agglomeration.

13. Theoretically, particle size should also influence the rate of agglomeration of fine-grained suspended material. This is a result of the fact that for a given weight of material the number of particles present is a function of the particle diameter and because the collision frequency of particles in a suspension increases proportionately with the number of particles present (see Equations 2, 3, and 5, below). The number of particles varies inversely with the cube of the particle diameter. Considering that fine sediments encountered during dredging may have mean particle sizes ranging over a factor of ten or more, the number of particles per unit weight can vary by at least a thousand times.

14. A study by Black and Vilaret¹ suggests that under certain circumstances the particle size of a suspension is important in determining the rate of agglomeration and, consequently, turbidity reduction. Their results indicate that for organic polymer flocculants and monodisperse (all particles of similar size) suspensions, smaller particle sizes favor more rapid agglomeration, although greater polymer dosages are required to yield optimum turbidity removal. However, polydispersity (the presence of a range of particle sizes) and the use of a metal salt coagulant (CaCl_2) which is of similar type, but not identical to

natural sea salt, apparently lessened or eliminated these effects. This suggests that the particle size may not be a major factor in determining the agglomeration rates of fine dredged material in natural waters.

Composition of the dispersed phase

15. The mineralogical composition of fine-grained dredged material may also have an important influence on the agglomeration and subsequent settling of suspended particles. Several studies have considered the relative stabilities of clay mineral dispersions using theoretical, experimental, and empirical methods and have concluded that settling rates for different clay minerals may vary significantly.

16. Hahn and Stumm² investigated the settling properties of illite, kaolinite, and montmorillonite in fresh and salt water bodies with different hydrodynamic properties from a theoretical viewpoint. Their calculations suggest that illite settles more rapidly than kaolinite, which in turn settles more rapidly than montmorillonite. The three clay dispersions were shown to have different stabilities at a given concentration of electrolyte due to differences in particle size and surface charge.

17. Edzwald et al.³ and Edzwald and O'Melia⁴ have evaluated the relative stabilities of illite, kaolinite and montmorillonite dispersions experimentally and have shown that the distribution of recent sediments in the Pamlico River Estuary, North Carolina, indicates that colloidal stability is a major factor controlling the sediment distribution in estuaries. The experimental results indicate that the relative stabilities for the three clays are as follows: illite > kaolinite > montmorillonite. This ranking applies over a wide range of salinities (2-19 ppt) but it is the reverse order of that predicted on the basis of theoretical arguments by Hahn and Stumm.

18. The clay distribution along the Pamlico River estuary supports the experimental determinations. The proportion of kaolinite in the clay fractions decreases downstream (toward higher salinity), while illite increases in abundance and montmorillonite is present only in minor amounts throughout. The illite-kaolinite trends apparently reflect the fact that kaolinite is less stable than illite and consequently

is removed from suspension more rapidly than illite. Illite, however, is more stable and remains in suspension for a longer time before it is destabilized by increasing salt concentration. Its proportion in the clay sediment fraction therefore increases with distance downstream.

19. This order of clay mineral stability is also consistent with the composition of suspended matter and recent sediments in the Gulf of Mexico and Caribbean Sea. Jacobs and Ewing⁵ reported that montmorillonite suspended in the Mississippi River flocculates and is deposited near the head of the Mississippi Delta, leaving the remaining water depleted in montmorillonite particles. Illitic clay discharged from the Amazon River remains in suspension as the Amazon water flows into the Atlantic Ocean and settles out of suspension as far north as the Caribbean and the Gulf of Mexico.

Composition of the fluid phase

20. According to the Derjaguin-Landau-Verwey-Overbeek (DLVO) theory of colloidal stability,⁶ destabilization occurs when the repulsive forces between like-charged particles are reduced enough to allow the attractive forces to dominate. The presence of electrolyte in solution tends to compress the electrical double layers surrounding clay particles in suspension and thereby promote coagulation. Not only is the ionic strength of the electrolyte an important factor in destabilizing colloids, but the valence of the cations present has a great effect on the concentration of ions required for flocculation. The concentrations of univalent, divalent, and trivalent cations required to flocculate a given dispersion are found to be approximately in the ratio 100:1.6:0.14.⁷ Apparently, the valence of the anion in the solution has no effect on the flocculation concentration. These results apply to a variety of colloidal materials including clays.

21. The experiments of Edzwald et al.³ have demonstrated the effects of ionic strength and solution composition on the coagulation kinetics of kaolinite, illite, and montmorillonite suspensions. The two solutions studied were a NaCl solution and a synthetic estuarine solution, each at three ionic strengths. In experiments with kaolinite suspensions, increasing ionic strength yielded more rapid coagulation

rates. In addition, the synthetic estuarine solution provided more rapid coagulation of the clay suspensions than did the simple NaCl solution, due to the presence of divalent cations (Mg^{2+} , Ca^{2+}). Edzwald and O'Melia⁴ further reported that the stability of all three clay colloids decreases with increasing salinity between 2-18 ppt salinity and that clays which are relatively more stable in low salinity waters are destabilized to a greater degree in waters of high salinity.

22. The presence of certain anions in solution can, under certain circumstances, stabilize low concentration clay suspensions and thereby lead to persistent turbidity. Swartzen-Allen and Matijevic⁸ report that montmorillonite and kaolinite have been shown to be deflocculated by the adsorption of hydroxide, phosphate, oxalate, sulfate, acetate, and chloride, among other anions. This is apparently caused by the disruption of edge-to-face agglomeration. The structure of the clay minerals leads to the presence of positively charged particle edges and negatively charged particle faces in many clay suspensions. The attraction between oppositely charged edges and faces of particles produces edge-to-face agglomeration in the absence of coagulants. However, the adsorption of anions from the solution on the positive edges of clay particles can interfere with the development of this structure at low concentrations and may redisperse the clay. Thus, in fresh water, the presence of certain anions can stabilize clay colloids and thereby cause persistent turbidity.

Influence of organic material

23. The organic matter present in dredged material is derived from many sources, including decomposition of terrestrial plants and animals, decomposition of aquatic plants and animals, sewage, and municipal and industrial wastes. Such organic matter may exist as relatively large masses, colloidal suspensions or in solution. Colloidal and soluble organic matter have the strongest effect on the sedimentation behavior of clays and clay-containing sediments.

24. Formation of clay-organic complexes. Clay and natural organics, when present together in an aqueous dispersion, can form complexes or aggregates which have colloidal properties different from one or both

of the component parts. These complexes form when attractive forces (e.g., ion-dipole forces, van der Waals forces, or hydrogen bonding) can overcome the electrostatic repulsive forces resulting from clay surface charges and the accompanying electrical double layers. It is instructive to compare the formation of clay-clay aggregates (coagulation) with the formation of clay-organic aggregates.

25. Coagulation of clay particles (without organics) is achieved by causing collapse of the diffuse double layers either by addition of divalent cations which adsorb on the clay, neutralizing the surface charge, or by increasing the ionic strength of the aqueous suspensions. Thus, clays coagulate in hard and saline waters. Organic materials can either destabilize or stabilize clay colloids, depending upon the specific properties and concentrations of various substances. The ionic or polar groups of the organic molecules may adsorb either on the negatively charged clay faces or on the positively charged clay edges. If several clay particles complex with a single organic molecule, the molecular weight of the aggregate can become high enough to render the repulsive electrostatic double layer forces ineffective. This interparticle bridging thus can result in flocculation of the clay particles. Under certain conditions the organic molecules can attach to and sometimes envelop, or form a coating around, clay particles, thereby masking the clay's usual properties and forming a stable protective colloid.

26. Behavior of clay-organic complexes. The response of clay-organic complexes to various water compositions can be strikingly different from that observed for pure clay suspensions. Whitehouse et al.⁹ characterized such differences for a wide range of organic compounds. The effects of charged and uncharged low molecular weight organic compounds on the settling of clays in artificial seawater of various strengths were measured. In general, the organic compounds tested changed the settling velocities of the clays by less than 50% and often less than 5%. In some cases, more marked effects were observed.

27. Narkis et al.¹⁰ investigated the effects of humic and fulvic acids, which are common organic constituents of natural waters, on the stabilities of several montmorillonite and kaolinite clay suspensions

in a dilute NaHCO_3 solution (soft water). It was found that varying degrees of interaction took place between humic acid and the clays, depending upon the clay type and composition. Adsorption of humate on Ca-montmorillonite particles led to increased stability of the suspension (smaller settling velocity), whereas the presence of humic acid had little or no effect on the agglomeration of other clays.

28. Neis and Hahn¹¹ also examined the effects of humic and fulvic acids, as well as lignosulfonic acid, on the stability of kaolinite suspensions in dilute CaCl_2 . Increasing concentrations of these organic acids were found to increase the stability of the kaolinite, with the exception of a destabilization which took place at high concentrations of humic acid. Lignosulfonic acid had the greatest effect on the clay stability, and humic acid had the least. The stabilizing effect of lignosulfonic acid is also consistent with the results of LeBell et al.,¹² who found that lignosulfonates greatly increase the stability of kaolinite suspended in NaCl solutions.

29. Conclusions regarding clay-organic interactions. The interaction of organic matter with clay particles introduces many complexities into the sedimentation behavior of colloidal suspensions of such materials. From the studies cited above, it is apparent that settling of the clay fraction in suspended dredged material can be greatly affected by the naturally occurring organic compounds. Depending upon the type and amounts of organics and clays present, aggregation of the clays in suspended sediments might be enhanced or hindered, with consequential effects on the settling rates of the suspensions. The sequence of flocculation of clays and the critical coagulant concentration (i.e., minimum salinity necessary to induce flocculation) in natural waters might be quite different from those expected for pure clays. Clays with the highest surface charge densities (montmorillonite) would be expected to interact most strongly with many organics.

Liquid shear

30. A prerequisite for particle agglomeration in colloidal suspensions is interparticle collision resulting from the Brownian motion of molecules in the suspending medium (water), internal shearing within

the medium, or the differential settling velocities of particles. While all three processes generally promote coagulation, high interparticle collision velocities or rapid liquid shear rates may cause disaggregation of agglomerates and resuspension of sediment.

31. Krone¹³ has discussed these three mechanisms and their relative importance in natural waters. The collision frequency of one particle with other particles due to thermal motions in the water I (Brownian motion) is given by:

$$I = \frac{4kTn}{3\eta} \quad (2)$$

where k is Boltzmann's constant; T is the absolute temperature; n is the particle number density (cm^{-3}); and η is the viscosity of the water. All particles are assumed to be the same size.

32. The collision frequency due to internal shearing in the liquid is given by the following expression:

$$J_j = \frac{4}{3} n_i R_{ij}^3 G \quad (3)$$

Here, J_j is the collision frequency on a particle of size j ; n_i is the number of particles of size i ; R_{ij} is the collision radius; and G is the local velocity gradient. The third power dependence of the collision frequency on R_{ij} results in the increasing efficiency of particle aggregates to gather small particles and grow still larger.

33. The ratio J/I gives a measure of the relative effectiveness of Brownian motion and liquid shear in promoting particle collisions. The resulting expression:

$$\frac{J}{I} = \frac{\eta R_{ij}^3 G}{kT} \quad (4)$$

indicates that even at very low shearing rates ($G = 1 \text{ sec}^{-1}$) and ambient temperatures, the ratio is unity for $R_{ij} = 0.77 \mu$. Thus, the two

mechanisms are equally important under these conditions for clay-sized particles. However, when larger particles or aggregates are present and/or the velocity gradients are higher, the shear-dependent collision rate predominates.

34. The collision rate of a settling particle P is given by:

$$P = \pi B R_{ij}^2 V_n \quad (5)$$

where B is the capture coefficient and V is the relative velocity between particles. This mechanism of particle capture is probably important when the local shearing rate is low. It may contribute significantly to the "sweeping out" of smaller particles by settling silt grains or clay aggregates.

35. A number of studies^{14,15} have shown that breakup of particle aggregates does occur at high liquid shear rates. This may be an important factor in determining the state of material discharged from a hydraulic pipeline dredge, since both flocculation and particle breakup can occur simultaneously due to turbulence within the pipeline. The ultimate fate of the dredged material is almost certainly dependent, at least in part, upon its state of aggregation when it is discharged into the receiving water.

Temperature

36. The settling velocity of a small sphere in a viscous fluid, as given by Stokes' Law (Equation 1), varies inversely with the viscosity of the fluid. The possible importance of this effect can be seen by comparing values for the viscosity of water over the range of temperature likely to be encountered in natural waters. At 30°C, $\eta = 0.7975$ centipoise, while at 4°C, $\eta = 1.567$ centipoises.¹⁶ Thus, the viscosity varies by about a factor of two, indicating that settling can be nearly twice as rapid in warm water as it is in cold water.

37. Temperature may also have some effect on the coagulation properties of clays, but its importance in natural waters is probably overwhelmed by other factors. The frequency of collisions induced by Brownian motion has been discussed above, where it was shown that the

collision frequency varies directly with the absolute temperature and inversely with the viscosity. Therefore, an increase in temperature should yield a somewhat higher collision frequency. However, the variation in absolute temperature of natural waters is only about 10% (~ 275 – 300 K), and the viscosity varies at most by a factor of two. The most important term in the expression for collision frequency, therefore, is the particle concentration, which may vary over several orders of magnitude. Furthermore, collisions induced by liquid shear may predominate over those caused by Brownian motion under many natural circumstances.

PART III: EXPERIMENTAL DESIGN AND TEST PROCEDURES

Rationale and Approach

Factors affecting the settling of dredged material

38. The dispersion of dredging-related turbidity is dependent upon the coagulation properties of sediment-water systems as well as bulk physical processes such as river, tidal, and wind-driven currents. The coagulation properties of such systems are important because the settling rates of suspended fine-grained dredged material may vary substantially in waters of differing composition. Furthermore, sediments of varying silt, clay, and organic content are likely to behave differently from one another under similar ambient water conditions.

39. The factors to be investigated experimentally in this study were chosen on the basis of the literature review presented above (Part II). The presence of dissolved electrolyte in waters in which dredged material is discharged enhances the coagulation of colloidal particles. In seawater or estuaries, salinity is the principal factor, whereas hardness is of concern in fresh water. The water pH was also considered to be of possible importance, as it may affect clay colloid stability and the nature of clay-organic interactions. Sediment factors expected to be of importance were the clay mineralogy (kaolinite, illite, montmorillonite, chlorite), particle-size distribution, and organic content. Since many complexities are involved in analyzing and classifying sediment organic constituents, it was felt that a single parameter, the wt.% organic carbon, would provide the simplest and most useful means of characterizing the sediment organics.

Correspondence of laboratory and field conditions

40. Several other factors, including the initial suspended solids concentration, the dissolved solids concentration, and the stirring history of the suspensions were considered in developing the test plan. Each of these parameters not only affects the flocculation of suspended particles, but also bears on the applicability of jar-test results to field conditions. In many cases, simple laboratory experiments cannot

adequately model situations encountered at actual dredging operations, but to the extent possible, test conditions were designed to simulate natural occurrences.

41. Sediment slurries discharged from hydraulic pipeline dredges typically contain from 0 to 20% solids by weight. The high concentrations of such slurries are beyond the optical turbidity measurement capability of the jar-test apparatus used, and lower concentrations had to be utilized. Since upwards of 95% of the discharged solids ordinarily settles rapidly to the bottom, however, concentrations on the order of 1% solids or less are to be expected quite near the discharge point. In fact, this prediction is confirmed by observations such as those of May.¹⁷ Therefore, sediment concentrations of 1 g/l and 5 g/l (0.1% and 0.5% solids) were utilized in jar tests. The use of two different concentration levels was intended to determine the effect of concentration on the flocculation and settling rates of dredged material suspensions.

42. The pH and hardness levels of jar-test waters were chosen to be appropriate to levels normally found in natural waters. Salinity levels of 1 g/l and 5 g/l sea salt were investigated in this study, although the salinity of estuarine or marine waters may often be significantly higher (seawater contains ~35 g/l salt). Previous studies (see Part II) and preliminary tests, however, suggested that even low salt concentrations were sufficient to flocculate suspended sediments and that increasing the concentration beyond about 5 g/l has relatively little additional effect.

43. Laboratory mixing conditions were intended to simulate those expected at actual dredging sites. These include rapid, turbulent mixing such as that in the dredge pipe followed by slower mixing as might be found downstream from the discharge. To accomplish this, jar test suspensions were first mixed rapidly (>100 rpm) for thirty minutes and were then mixed slowly (2-5 rpm) while the turbidity was monitored. The correspondence between laboratory and field mixing conditions is, of course, not exact. For example, sediment slurries transmitted through hydraulic pipelines may be subject to complex turbulence and variable flow regimes. This may affect the nature of

dispersal or flocculation of the material discharged from the pipe. In addition, the high solids content of dredged material slurries was not modeled during the rapid-stirring period in the laboratory jar tests. Rather than to model precisely the mixing encountered by dredged material, it was the intent of this investigation to determine the nature and relative importance of factors affecting the settling rates of suspended sediments. Therefore, exact correspondence between laboratory and field conditions was not attempted, and any differences must be accounted for when applying the results of this study to field situations.

Experimental approach

44. Factorial design. Laboratory jar tests were performed in a factorial design test plan to determine the effects of sediment-water factors and interactions on observed settling rates. Because the type of clay present was expected to be an important factor in determining turbidity, the first factorial experiment consisted of tests with three clay samples. Samples of kaolinite, illite, and montmorillonite, the three most common clays found in sediments, were tested singly and in two- and three-part mixtures in waters of varying salinity, hardness, and pH.

45. A second series of experiments was designed to determine the effects of silt and naturally occurring organic material on turbidity. Mixtures of silt with clay and silt with natural sediments were used to test for any interactions which might exist between clay and silt particles. An attempt was made to determine the effect of natural organics on turbidity by testing two natural sediments before and after treatment with hydrogen peroxide (H_2O_2) for removal of the organic fraction. However, organic carbon analyses of the sediments following H_2O_2 treatment indicated only a 30% reduction from the original organic carbon content. Furthermore, the H_2O_2 treatment may result in changes in the inorganic fraction¹⁸ and affect the settling behavior of the clays. The results obtained in this phase of the study are thus equivocal and cannot be used to specify the role of natural organics on the settling of sediment suspensions. Details of

the treatment and testing procedures are presented in Appendix D.

46. Finally, eight natural sediments (Appendix A) were tested in a factorial experiment. The sediments were obtained primarily from dredging sites and represented a broad spectrum of compositional characteristics. Four fresh waters and four saline waters were utilized in testing the natural sediments.

47. Settling curves. For each jar test, turbidity was monitored for a period of 60 minutes following an initial rapid-mix period. Curves of light attenuation vs. time were prepared which are a function of the coagulation and settling rates for each set of sediment and water conditions. For purposes of statistical analysis (see below), all results were characterized by a single parameter, the time to reach a 67% reduction from the initial turbidity. This approach represents a simple method of providing at least a relative ranking of settling rates for the factorial experiments.

48. Statistical analyses. Results of the jar tests for clays and natural sediments were analyzed by stepwise linear regression techniques to determine which sediment and water factors controlled the settling rates of the suspensions. A functional dependence of the following form was assumed:

$$Y = a + \sum_{i=1}^k b_i X_i + e \quad (6)$$

Y is the dependent variable, an experimentally estimated parameter proportional to the mean sediment settling rate; X_i is a set of independent variables corresponding to sediment and water variables; e is the random experimental error; and a and b_i are mathematically determined coefficients. Regressions are carried out in a stepwise fashion using a standard computerized statistical package.

49. In the first step, a single independent variable X_u is selected to provide an equation:

$$Y = a + b_u X_u \quad (7)$$

where X_u is the independent variable giving the greatest reduction in sum of squares of Y . An F-test of the null hypothesis $b_u = 0$ is applied. F is the ratio of the variances explained by the independent variable X_u to the unexplained variance. If the computed F value is greater than the corresponding tabulated $F_{0.01}$ value, the null hypothesis is rejected (i.e., there is less than 1% chance that $b_u = 0$), and the analysis is carried a step further.

50. In the second step another independent variable is selected to provide an equation:

$$Y = a + b_u X_u + b_v X_v \quad (8)$$

where X_v is the independent variable giving the next greatest reduction in sum of squares of Y . An F-test is applied to X_v and the procedure is repeated until a computed F value less than the corresponding tabulated $F_{0.01}$ value is obtained. This indicates an unacceptable linear regression step; i.e., the chances are greater than 1% that the reduction in variance assigned to the last selected independent variable could be due to chance.

51. The stepwise linear regression analysis is terminated and the penultimate regression equation is selected as the equation providing a statistically valid evaluation of the important factors controlling turbidity reduction. The correlation coefficient, standard error of the estimate, and standard errors of the coefficients are also provided. This approach may be termed a "step up method of stepwise linear regression utilizing an $F_{0.01}$ criterion." The resulting equations provide an estimate of the effects of controlling factors, and there is less than a 1% chance that functionally irrelevant factors have been specified. The results apply, of course, only to the range of sediments and waters tested; however, generalizations of sediment-water interactions can be made based on similarities in the behavior of different sediments.

52. Separate regressions were performed for two dependent variables (Y 's): the reciprocal of the settling time to 67% turbidity reduction in a jar test ($1/t_{67}$) and the natural logarithm of the reciprocal settling time. Both give a measure of the overall settling rate for

each test suspension, but the use of the natural logarithm has the effect of giving greater weight to small $1/t$ values than to large $1/t$ values. Since many of the large $1/t$ values (i.e., very short settling times) were based on extrapolation of experimental data, smaller $1/t$ values are in general expected to be more precisely determined. Thus $\ln(1/t)$ is, in effect, a weighted function giving higher weights to the more reliable data. It should also be noted that the 67% turbidity reduction criterion was chosen to minimize the amount of extrapolation necessary for both very short and very long settling times.

53. Replicate tests. Twenty-five experiments were replicated in a procedure designed to qualitatively and quantitatively define the changes which take place over time as a given suspension flocculates and settles. Aliquots of the test suspensions taken at zero time and after significant settling had occurred were qualitatively analyzed to determine the particle-size distribution, mineralogy, organic carbon content, and zeta potential. This approach was utilized to obtain insight into possible mechanisms of particle agglomeration, physical interactions between various sediment components, differential settling rates of various components, and identifiable components responsible for persistent turbidity or rapid settling. In addition, the tests were used to determine the correlation between light transmission, light scattering, and suspended solids concentration.

54. The choice of replicate tests was intended to provide both a comparison of the behavior of different sediments under similar water conditions and of individual sediments under different external conditions. Thus, replicate tests were run for all clay mixtures and natural sediments in a single water type (0.1% sea salt solution) at 1 g/l sediment concentration. In addition, the three-part clay mixture (kaolinite + illite + montmorillonite) and each of the natural sediments were tested under a second set of conditions (sediment concentration and/or water type) which produced substantially different settling behavior in the factorial jar tests.

55. Preliminary and subsidiary tests. Several experiments were performed which were outside the scope of the factorial test plan but

which were important to the proper interpretation of turbidity data. These included the effect of wavelength on the light transmission, the importance of temperature in determining the settling rate, and the possibility of turbulence and/or stratification during jar tests and their effects on the measured turbidity. The three clay samples were also tested over a wider range of sea salt concentrations than in the factorial plan to determine their responses to very high and very low salinities.

Jar-Test Procedures

Apparatus and turbidity measurements

56. A multiple jar-test apparatus was utilized in analyzing the settling characteristics of suspended sediments. The system includes a six-station stirring unit (Phipps & Bird, Richmond, Va.), stainless steel 1-l jars (with a height and diameter of 14.5 and 10.2 cm, respectively) fitted with fixed light probes (2-cm light path), and a Brinkmann probe colorimeter with a 48-in. fiber optic light guide. The light probe was fixed at a depth of 6 cm below the surface of the 1-l suspensions, while the 0.1- by 2.5- by 7.6-cm stirring blade was centered 2.5 cm below the surface. The stirring rate was variable between 0 and 100 rpm.

57. In order to ensure the equivalence of results obtained in all six jars, each beaker was standardized to 100% transmission with deionized water prior to every experimental run. This was done by reading the transmission through deionized water for each beaker and calculating the factor needed to raise this value to 100%. This calibration factor was then applied to subsequent transmission readings from each beaker. It was also noted that significant nonuniformity existed in the light probes, resulting in a dependency of the light transmission on the orientation of the fiber optic light guide with respect to the light probe. For this reason, readings were always taken with the light guide and probe in the same orientation, the exact orientation for each beaker having been determined initially by maximizing the observed transmission in deionized water.

58. Although the term "turbidity" may be used to signify several different physical properties, it is defined here to be a measure of the attenuation of a single wavelength (or narrow band) of light transmitted through a medium, relative to a deionized water standard. The attenuation is the sum of light absorption and scattering, the two processes which diminish the light intensity in a suspension. The attenuation coefficient, α , is hereby defined to be

$$\alpha = \frac{\ln(100/T)}{L} \quad (9)$$

where T is the % light transmission; L is the path length (m) through the suspension; and α is expressed in units of (m^{-1}) .¹⁹ All transmission data were gathered using an 880-nm filter in the colorimeter. It is important to remember that, in general, as the amount of material in suspension increases, the attenuation coefficient increases; however, the % transmission decreases.

59. The procedure for conducting jar tests consisted of first vigorously dispersing the clay or sediment suspensions during a rapid-mixing period, then measuring the light transmission at frequent intervals as settling occurred. The suspensions were stirred for 30 min at 100 rpm, and a transmission reading was taken immediately preceding the cessation of rapid mixing. The stirring rate was then reduced to 2-5 rpm, and transmission readings were taken at 5-min intervals for a total of 60 min. Transmission values were converted to α values and α vs. time curves were prepared for each experiment.

60. The Phipps and Bird stirring apparatus was somewhat unsteady at low stirring rates, and 2-5 rpm represents the range in stirring which was actually observed during the settling experiments. It should be noted that nonuniform liquid shear rates are obtained with a single stirring rate since the shear rate varies along the radius of the impeller blade. The shear rates thus obtained simulate the mixing in natural waters, which promotes flocculation without causing breakup of clay flocs or resuspension of settled material. The shear condition obtained corresponds to a velocity gradient in the range of 0.5 to 1.0 sec^{-1} .

Replicate tests

61. The procedure for preparing and conducting replicate tests was identical to that described previously for clay and natural sediment suspensions. For each replicate experiment, the light transmission of one jar was monitored for a full 60 min to compare its settling curve to previous determinations for the particular suspension. One control jar was also run for each replicate test. This consisted of a clay sample suspended in a standard salt solution and was prepared fresh for each run. In addition, other jars run simultaneously under the same conditions were sampled to obtain the desired qualitative data.

62. Samples of the suspensions were taken at the end of the rapid-stirring period (immediately preceding the start of slow stirring) and also after a period of settling defined by the decrease of the turbidity, α , to one-half of its initial value. All samples were analyzed for mineralogy, zeta potential, pH, light scattering, light transmission, suspended solids, particle-size distribution (dispersed), and particle morphology (by scanning electron microscopy).

63. Results of replicate test analyses are reported in Appendix F. Note that tests denoted by the letter "a" (1a, 2a, 3a, ..., 25a) indicate samples of the suspensions at zero time (prior to settling), while tests labeled "b" (1b, 2b, 3b, ..., 25b) represent samples taken after settling to one-half the initial turbidity. However, the mineralogy results (quartz, kaolinite + chlorite, illite, montmorillonite) and particle-size analyses (mean particle size and wt. % finer than 2 μ) for tests labeled "a" (zero time) were not obtained on actual aliquots of the test suspensions at zero time. The procedure for these two assays will be described in detail below. All other assays were performed on aliquots of the test suspensions.

64. Samples for analysis were obtained by draining the top half of each suspension. A few drops of suspension were filtered immediately on a 0.45 μ pore size Millipore filter and reserved for later scanning electron microscopy. The pH of the samples was measured within one minute of the sampling time and the samples were kept stirring until the zeta potential could be measured, ordinarily within 1 hr. Light

scattering was measured using a Hach 2100A Turbidimeter within 48 hrs after sampling and was reported as Formazin turbidity units (FTU). A light transmission measurement was made immediately following the turbidimeter reading and the same sample was later analyzed for suspended solids.

65. Samples for X-ray diffraction (mineralogical analysis) were prepared in the same manner as the $<2 \mu$ fraction of the sediments (see Appendix B), except that samples were not H_2O_2 -treated. In obtaining the "zero time" sample for X-ray analysis, the sediment being tested was suspended in deionized water and was allowed to settle the same period of time as the test suspensions which were sampled after settling to one-half the initial turbidity. For example, the sample for X-ray diffraction of test 8a was obtained by sampling a suspension of the sediment in deionized water after settling for 8-3/4 min. The mineralogy reported for test 8b was done on a sample of the sediment suspended in the test water (0.1% sea salt), also after settling for 8-3/4 min. This procedure allows the relatively coarse, nonflocculating silt particles (mostly quartz) to settle out equally in both "a" and "b" suspensions, and permits a direct comparison of the mineralogy of flocculated and unflocculated suspensions. Changes in the mineralogy which result from simple gravity settling of coarse particles (which is assumed to be the same in test solutions and deionized water) are thus not considered here. The results do point out any differences in settling behavior which result from flocculation in the test suspensions as opposed to the absence of flocculation in deionized water.

66. Note that for replicate test samples no attempt was made to distinguish kaolinite from chlorite in the X-ray diffraction patterns, and these two clay types are thus considered together. This differs from the X-ray diffraction results for the natural sediments (discussed below), where kaolinite and chlorite were distinguished.

67. The particle-size distribution of the suspended sediments was obtained after filtering the solids on a Millipore filter and redispersing them with sodium hexametaphosphate in 350 ml of deionized water. The pipet analyses were carried out in a 1000-ml graduated

cylinder. For analyses listed as "zero time," the particle-size distributions were performed directly on samples of the natural sediments, not on aliquots removed from test suspensions.

Test Plan and Sample Characterization

68. A stepwise approach was used to investigate the important sediment and water factors and interactions controlling turbidity. Simple systems of pure clays and clay mixtures suspended in waters of various salinity, hardness, and pH were studied first, followed by mixtures of clay with silt. Finally, eight natural sediments typical of those encountered at actual dredging sites were tested.

69. The physical and compositional characteristics of the samples which were expected to be of possible importance in affecting their settling properties were determined by a variety of techniques. These included the particle-size distribution (natural and dispersed), mineralogy (X-ray diffraction), zeta potential, % organic carbon, cation exchange capacity, moisture content, and pH. Samples were also examined by scanning electron microscopy to obtain qualitative information on particle agglomeration. Details of sample preparation and analytical techniques are presented in Appendix B. Results of these analyses are summarized in Tables 1 and 2.

Waters

70. Turbidity testing was carried out in a variety of fresh and salt waters in order to examine the effects of water hardness, salinity, and pH on the settling behavior of sediment suspensions. The four fresh waters chosen for study were as follows:

- soft water, pH 6.8
- hard water, pH 6.8
- soft water, pH 8.3
- hard water, pH 7.5

Table 1

Analytical Data for Clays and Natural Sediments

Sample	% Moisture	* pH	** pH	Organic carbon† (wt.%)	Zeta potential †† range(mv)	Zeta potential average(mv)	Natural		Dispersed	
							Mean particle size (μ)	Wt.% finer than 2 μ	Mean particle size (μ)	Wt.% finer than 2 μ
<u>Clays</u>										
Kaolinite	---	5.8	0.02	uniform	-21.6	2.5	43	<2	60	
Illite	---	8.2	0.57	uniform	-19.7	14.6	14	15.6	13	
Montmorillonite	---	9.7	0.19	uniform	-36.4	<2	72	<2	59	
<u>Silt</u>										
VIX	32.7	8.2	0.02	-14 to -26	-16.7	20.6	<1	---	---	
<u>Natural Sediments</u>										
Mobile Bay	68.8	7.3	1.48	-23 to -41	-26.7	8.7	30	2.0	50	
San Francisco Bay	58.3	7.6	0.87	-30 to -45	-33.4	5.2	38	3.2	41	
Boston Harbor	57.3	6.6	2.44	-32 to -37	-34.5	26.3	13	15.6	23	
Charleston Harbor	68.4	8.2	1.80	-24 to -28	-25.6	23.7	18	22.1	32	
Illinois River	40.2	7.8	0.72	-13 to -23	-18.3	19.9	15	17.3	19	
Toledo Harbor	57.1	8.4	2.09	-14 to -24	-16.8	14.6	30	3.9	38	
Rouge River	40.5	9.6	4.85	-16 to -25	-18.1	23.7	13	6.8	30	
Charles River	75.1	7.1	7.72	uniform	-29.3	>62.5	4	62.5	9	

* (weight of water)/(wet weight of sediment)

** pH of 0.1% suspension in deionized water

† dry weight basis

†† measured in deionized water

Table 2
Mineralogy and Cation Exchange Capacity of Clays
and the <2 μ Fraction of Natural Sediments

<u>Sample</u>	<u>Wt. % Kaolinite</u>	<u>Wt. % Illite</u>	<u>Wt. % Montmorillonite</u>	<u>Wt. % Chlorite</u>	<u>C.E.C. (meq/100g)</u>
<u>Clays</u>					
Kaolinite	100	0	0	0	14
Illite	0	100	0	0	20
Montmoril- lonite	0	0	100	0	97
<u>Natural Sediments</u>					
Mobile Bay	30	9	55	6	65
San Fran- cisco Bay	0	25	35	40	62
Boston Harbor	4	74	0	22	35
Charleston Harbor	54	8	31	7	54
Illinois River	14	27	52	7	67
Toledo Harbor	3	65	7	25	41
Rouge River	0	71	0	29	33
Charles River	2	62	0	36	41

The four saline waters were:

- 0.1% sea salt solution
- 0.1% sea salt + hard water
- 0.5% sea salt solution
- 0.5% sea salt + hard water

71. The basic soft water was prepared by adding 0.144 g/l of NaHCO_3 to deionized water, yielding a pH of 8.3. An equivalent soft water at acidic pH was made by adding CO_2 -saturated water to the basic NaHCO_3 solution until the pH was reduced to 6.8. The synthetic hard water was designed to simulate natural hard waters and was prepared to contain 150 mg/l of $\text{Ca}(\text{HCO}_3)_2$ and 50 mg/l of MgSO_4 , with a pH of 7.5. The water was actually prepared by dissolving 68.5 mg/l of $\text{Ca}(\text{OH})_2$, 50 mg/l of MgSO_4 , and adding enough CO_2 -saturated water to bring the pH to 7.5 or 6.8. Stock solutions of $\text{Ca}(\text{OH})_2$ and MgSO_4 were utilized, while CO_2 -saturated water was prepared before each run by bubbling CO_2 through deionized water.

72. Sea salt solutions were made by adding 1 g or 5 g of synthetic sea salt (Aquarium Systems, Inc., Eastlake, Ohio) per liter of deionized water. The manufacturer's chemical analysis of the sea salt is listed in Appendix C. Sea salt + hard water solutions were chosen to simulate the natural mixing of hard freshwater with seawater in estuaries. In preparing these solutions, the $\text{Ca}(\text{OH})_2$, MgSO_4 , and solid sea salt were first dissolved in deionized water, and CO_2 -saturated water was then added to bring the pH to 7.5.

Clays

73. Sample characterization. Samples of the three clay types which are the predominant constituents of the clay fractions of natural sediments were obtained for use in settling experiments. Kaolinite (Georgia Kaolin Co., #6494 SAF) and Wyoming montmorillonite (American Colloid Co.) were obtained in powdered form. Since illite was unavailable in pure powdered form, the illite used here was ground from a shale specimen (Ward's Natural Science Co.).

74. The montmorillonite was the most fine-grained of the clay samples, with more than 70% finer than 2μ in diameter. The kaolinite sample was also moderately fine-grained, with a mean particle size (undispersed) of 2.5μ . The illite sample was considerably coarser than either the kaolinite or montmorillonite samples, having a mean particle size near 15μ .

75. The kaolinite sample was virtually organic free, with 0.02% organic carbon. However, the other clays apparently had small quantities of organic matter present, with 0.19% organic carbon in the montmorillonite sample and 0.57% organic carbon in the illite sample. The estimated standard errors for these measurements are on the order of $\pm 4\%$ of the reported value for the higher levels, probably somewhat greater for the low value of kaolinite.

76. X-ray diffraction patterns of the clay samples indicated no major mineral impurities in the kaolinite and montmorillonite samples. The illite pattern suggests the possible presence of some quartz in that sample, but due to the overlap of quartz and illite diffraction peaks the evidence is not conclusive.

77. The cation exchange capacities (C.E.C.) of the kaolinite, illite, and montmorillonite samples were 14, 20, and 97 meq/100 g. These values compare favorably with other determinations for these minerals reported in the literature.²⁰⁻²³ Kaolinite is typically in the range of 5-15 meq/100 g, illite from 20-40 meq/100 g, and montmorillonite ordinarily from 90-110 meq/100 g.

78. The zeta potential is a measure of the effective charge difference between a colloidal particle and its surrounding fluid, and it is an indicator of the relative stability of a dispersion. Kaolinite, illite, and montmorillonite suspensions in deionized water had zeta potentials of -22 mv, -20 mv, and -36 mv, respectively. Generally, zeta potentials in the range of -10 to -30 mv are indicative of incipient instability, while values greater (more negative) than -30 mv are indicative of moderate to excellent stability.

79. Jar-test conditions. The three clay samples, kaolinite (K), illite (I), and montmorillonite (M), were tested singly and in all two-

and three-part mixtures (in equal proportions by weight) with the suspended solids concentration fixed at 1 g/l throughout. Each of the clays and clay mixtures was tested in five water types (Figure 1): soft waters at acidic and basic pH, 0.1% and 0.5% sea salt solutions, and hard water at basic pH. The stirring rate for all experiments was 2-5 rpm. Turbidity values (α), expressed as a percentage of the initial value at various times, are tabulated in Appendix E.

80. Replicate tests. Five replicate tests were run using clay mixtures (Figure 1). Each of the two-part clay mixtures (KI, KM, IM) as well as the three-part clay mixture (KIM) were run in 0.1% sea salt solutions. In addition, the KIM mixture in hard water was also run as a replicate test.

Silt tests

81. Sample characterization. The possibility that clay-silt interactions might exist and affect the settling of suspended sediments was evaluated by testing mixtures of silt with clay and silt added to several natural sediments. The sample utilized in these experiments was a soil obtained from a roadcut in Vicksburg, Mississippi (VIX). Essentially all the particles were in the silt size range and consisted primarily of quartz, dolomite, and feldspar. Organic carbon was extremely low (0.02 wt. %). Zeta potential measurements indicated the presence of particles with charges in the range of -14 to -26 mv, although whether these particles were clay minerals or not is unknown. Impurities and surface defects in non-clay minerals can also account for the charged particles. No determination of cation exchange capacity was made for this sample.

82. Jar-test conditions. Silt (VIX) was added to equal weights of the three-part clay mixture (KIM), Boston Harbor sediment (BH), and Charles River sediment (CR) and tested in the five water types used in the testing of clays (Figure 2). Total sediment concentration was 1 g/l for all tests, and the stirring rate was 2-5 rpm. Results are tabulated in Appendix E.

Natural sediments

83. Sample characterization. Natural sediments were obtained

Clay Type*	Water Type**				
	Soft 6.8	Soft 8.3	0.1% Salt	0.5% Salt	Hard 7.5
K	F [†]	F	F	F	F
I	F	F	F	F	F
M	F	F	F	F	F
KI	F	F	F,R	F	F
KM	F	F	F,R	F	F
IM	F	F	F,R	F	F
KIM	F	F	F,R	F	F,R

* Clay types:
 K - kaolinite
 I - illite
 M - montmorillonite
 KI, KM, IM, KIM - clay mixtures

** Refer to paragraphs 70-72 for water compositions

† F indicates factorial experiments;
 R indicates replicate tests

FIGURE 1. TEST PLAN MATRIX FOR CLAYS AND CLAY MIXTURES

Mixture*	Water Type**				
	Soft 6.8	Soft 8.3	0.1% Salt	0.5% Salt	Hard 7.5
VIX + KIM	F [†]	F	F	F	F
VIX + BH			F	F	
VIX + CR	F	F	F	F	F

* Samples:
 VIX - Vicksburg silt
 KIM - kaolinite, illite, montmorillonite clay mixture
 BH - Boston Harbor
 CR - Charles River

** Refer to paragraphs 70-72 for water compositions

† F indicates factorial experiments

FIGURE 2. TEST PLAN MATRIX FOR SILT TESTS

from four estuarine and four freshwater locations. The sites were chosen to encompass a broad geographic distribution and to ensure adequate variation in sediment compositional characteristics. The four estuarine areas sampled were Boston Harbor (BH), Charleston Harbor (CH), Mobile Bay (MB), and San Francisco Bay (SF). Freshwater sediments were obtained from the Charles River (CR), in Boston; the Illinois River (IR); Toledo Harbor (TH), Ohio; and the Rouge River (RR), in Detroit. In all areas except Boston Harbor and Charles River, the samples were taken from within dredged channels maintained by the Army Corps of Engineers. Details of sample locations are presented in Appendix A.

84. The sampling device used was a Petersen grab sampler, and bottom sediments were taken at from three to five separate sites at each locality. Portions of each discrete sample were retained for future reference, and the remainders of the samples from each locality were combined and thoroughly mixed to form a composite sample. It is the composite sample from each area which was subsequently used in all laboratory tests. All samples were kept refrigerated (4°C) to minimize degradation of the organic material present, but were not frozen.

85. The qualitative sediment analyses indicate that a broad range in compositional characteristics was represented in the samples tested. The mean particle size of the natural sediments (undispersed) ranged from about 5-63 μ , while the clay fraction (defined as wt. % finer than 2 μ , dispersed) varied from 9% to 50%.

86. The Illinois River sediment had the lowest organic carbon content, 0.72%, while the highest organic carbon level was found in the Charles River sample, 7.72%. A rough estimate of the total organic matter present can be obtained by assuming the organic material has the formula CH_2O . With this assumption, the organic carbon determinations would correspond to a range of total organic matter from about 2-19 wt. % in the samples studied.

87. The mineralogy of the $<2 \mu$ fraction of the sediments was also found to be diverse. Kaolinite was the predominant constituent ($>50\%$) of the Charleston Harbor sediment; illite was the major component in Boston Harbor, Toledo Harbor, Rouge River, and Charles River; and

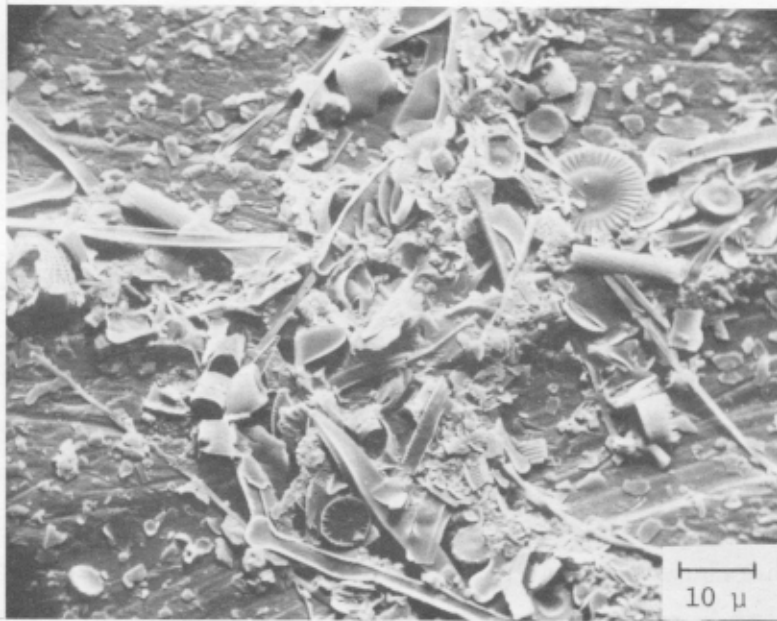
montmorillonite was the most important clay in Mobile Bay and the Illinois River. Chlorite was the major clay mineral in the San Francisco Bay sediment (40%) and was also found to be significant in several other samples.

88. The measured cation exchange capacity of the $<2 \mu$ fraction of the sediments varied from 33 to 65 meq/100 g and is consistent with the clay mineralogy as determined by X-ray diffraction techniques. The zeta potential of natural sediment suspensions in deionized water was found to range from about -17 mv to -35 mv. Most samples displayed a range in zeta potentials, as would be expected for polydisperse systems.

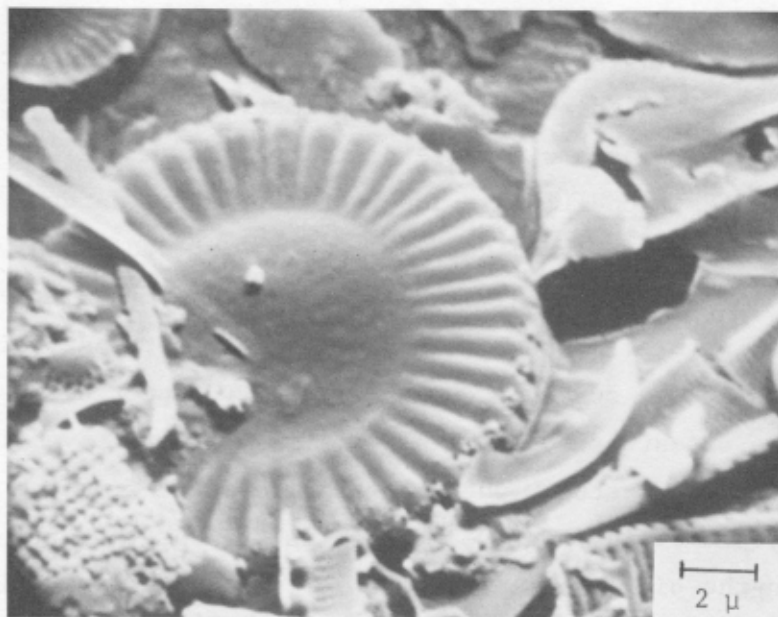
89. The range in sediment characteristics observed for the eight samples studied here is depicted clearly by the scanning electron micrographs of Figures 3 and 4. The Charles River sediment, the most organic-rich of those sampled, is seen to consist largely of material of biological origin, with a variety of organisms present. Some clay particles are also visible. The Illinois River sediment was the cleanest of the sediments studied and consisted primarily of inorganic silt and clay particles covering a wide size distribution.

90. Jar-test conditions. The test matrix for natural sediments encompassed 96 experiments (Figure 5). All eight sediments were tested in four saline waters, but only the freshwater sediments were tested in the four fresh waters. Estuarine sediments were not tested in fresh waters because it was considered unrealistic to expect disposal of dredged marine or estuarine sediments in fresh water. Even in the case of a well-stratified estuary where material dredged from the bottom might be disposed of in relatively fresh water near the surface, the salt water in the pipeline slurry (~80% or more water) as well as interstitial water in the dredged material would probably be sufficient to render the receiving water saline and induce flocculation.

91. All sediment-water combinations were tested at two sediment concentration levels, 1 g/l and 5 g/l (dry weight basis). Results are tabulated in Appendix E. When preparing the test suspensions, wet sediment was used, with the actual sample weight being determined by its

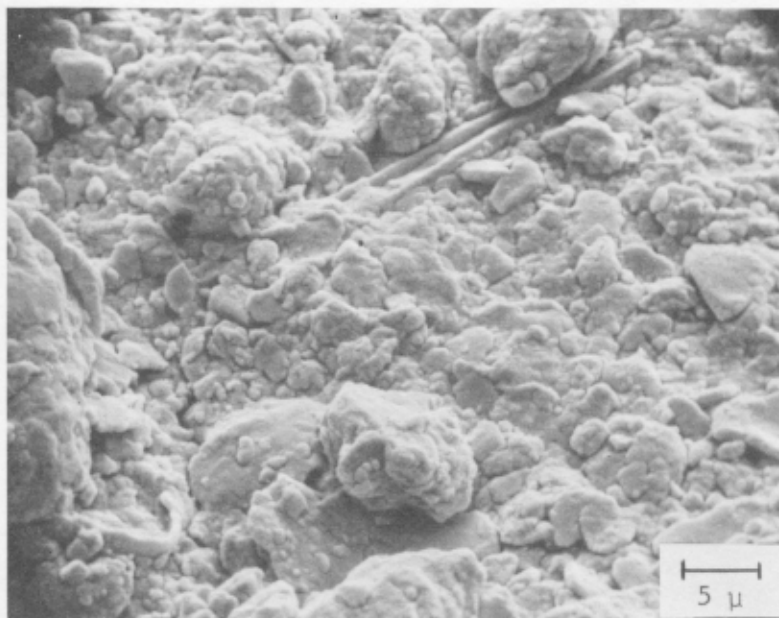


a. 1000 X magnification

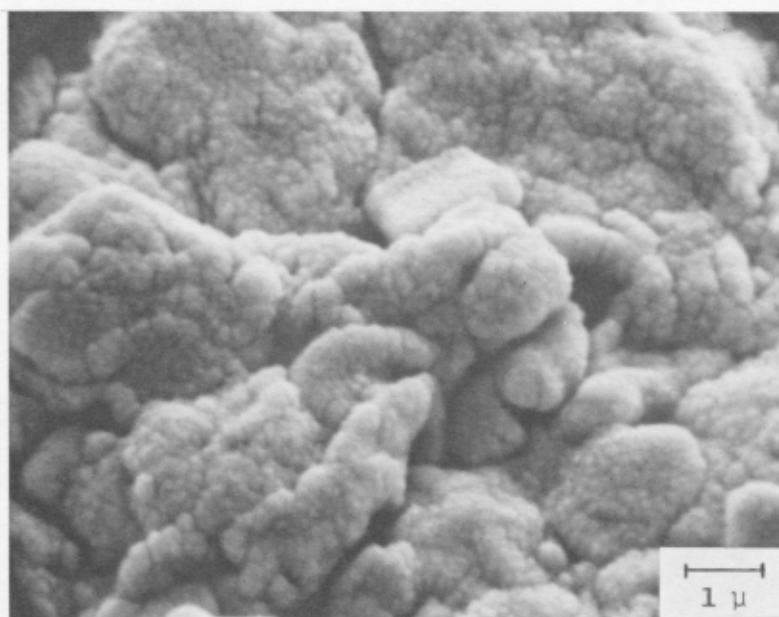


b. 5000 X magnification

FIGURE 3. SCANNING ELECTRON MICROGRAPHS OF THE $< 2 \mu$ FRACTION OF THE CHARLES RIVER SEDIMENT



a. 2000 X magnification



b. 10000 X magnification

FIGURE 4. SCANNING ELECTRON MICROGRAPHS OF THE ILLINOIS RIVER SEDIMENT

Sediment	Sed.* Conc.	Water Type**											
		0.1% Salt		0.1% Salt		0.5% Salt		0.5% Salt		Hard		Hard	
		F,R [†]	F,R	F	F	F	F	F	F	F	F	F	F
Mobile Bay	1	F,R [†]	F,R	F	F	F	F	F	F	F	F	F	F
San Francisco Bay	1	F,R	F	F	F	F	F	F	F	F	F	F	F
Boston Harbor	1	F,R	F	F	F	F	F	F	F	F	F	F	F
Charleston Harbor	1	F,R	F	F	F	F	F	F	F	F	F	F	F
Illinois River	1	F,R	F	F	F	F	F	F	F	F	F	F	F,R
Toledo Harbor	1	F,R	F	F	F	F	F	F	F	F	F	F	F,R
Rouge River	1	F,R	F	F	F	F	F	F	F	F	F	F	F,R
Charles River	1	F,R	F	F	F	F	F	F	F	F	F	F	F,R
Mobile Bay	5	F	F	F	F	F	F	F	F	F	F	F	F
San Francisco Bay	5	F	F,R	F	F	F	F	F	F	F	F	F	F
Boston Harbor	5	F,R	F	F	F	F	F	F	F	F	F	F	F
Charleston Harbor	5	F,R	F	F	F	F	F	F	F	F	F	F	F
Illinois River	5	F	F	F	F	F	F	F	F	F	F	F	F
Toledo Harbor	5	F	F	F	F	F	F	F	F	F	F	F	F
Rouge River	5	F	F	F	F	F	F	F	F	F	F	F	F
Charles River	5	F	F	F	F	F	F	F	F	F	F	F	F

* Initial sediment concentration (g/%)

** Refer to paragraphs 70-72 for water compositions

† F indicates factorial experiments; R indicates replicate tests

FIGURE 5. TEST PLAN MATRIX FOR NATURAL SEDIMENTS

moisture content and the desired suspended solids level. The stirring rate was 2-5 rpm throughout.

92. Replicate tests. Sixteen replicate tests were run using natural sediments, two for each of the eight samples (Figure 5). All sediments were tested in 0.1% sea salt solution at 1 g/l sediment concentration and again under various sediment-water conditions.

PART IV: TURBIDITY DATA AND ANALYSIS

Preliminary and Subsidiary Tests

Effect of wavelength

93. The light transmission through a given suspension was found to be wavelength-dependent. This is probably due primarily to the greater scattering of shorter wavelengths by fine particles in the suspensions. Figure 6 illustrates the effect of using various wavelength filters on the turbidity measured for kaolinite suspensions. Since the shape of α vs. time curves during settling experiments was apparently unaffected by the wavelength, all turbidity data were collected using light of 880-nm wavelength, which provided maximum transmission for the suspensions tested.

Effect of temperature

94. The effect of liquid temperature on the settling rate of kaolinite was studied by monitoring the turbidity of the clay in 0.5% NaCl at three different temperatures. As Figure 7 demonstrates, the settling rate is markedly higher at 59°C than at 4°C. This is consistent with the theoretical prediction of Stokes' Law that the settling velocity of a small sphere in a viscous fluid is inversely proportional to the viscosity. However, for the water temperature range encountered in dredging operations, the effect on turbidity removal is likely to be minimal. Furthermore, the limited temperature variation of perhaps 5°C in laboratory jar tests could not cause significant errors in turbidity data. Note that the crossing of the 59°C and 40°C curves in Figure 7 is due to random fluctuations and is not significant.

Turbulence in jar tests

95. The jar tests were designed to characterize the settling properties of representative sediments in a simplified laboratory situation that involved water compositions and shear rates that are realistic in terms of the natural environment. An important consideration in use of the jar-test data is the relative importance of downward flux of sediment due to gravitational settling and upward flux due

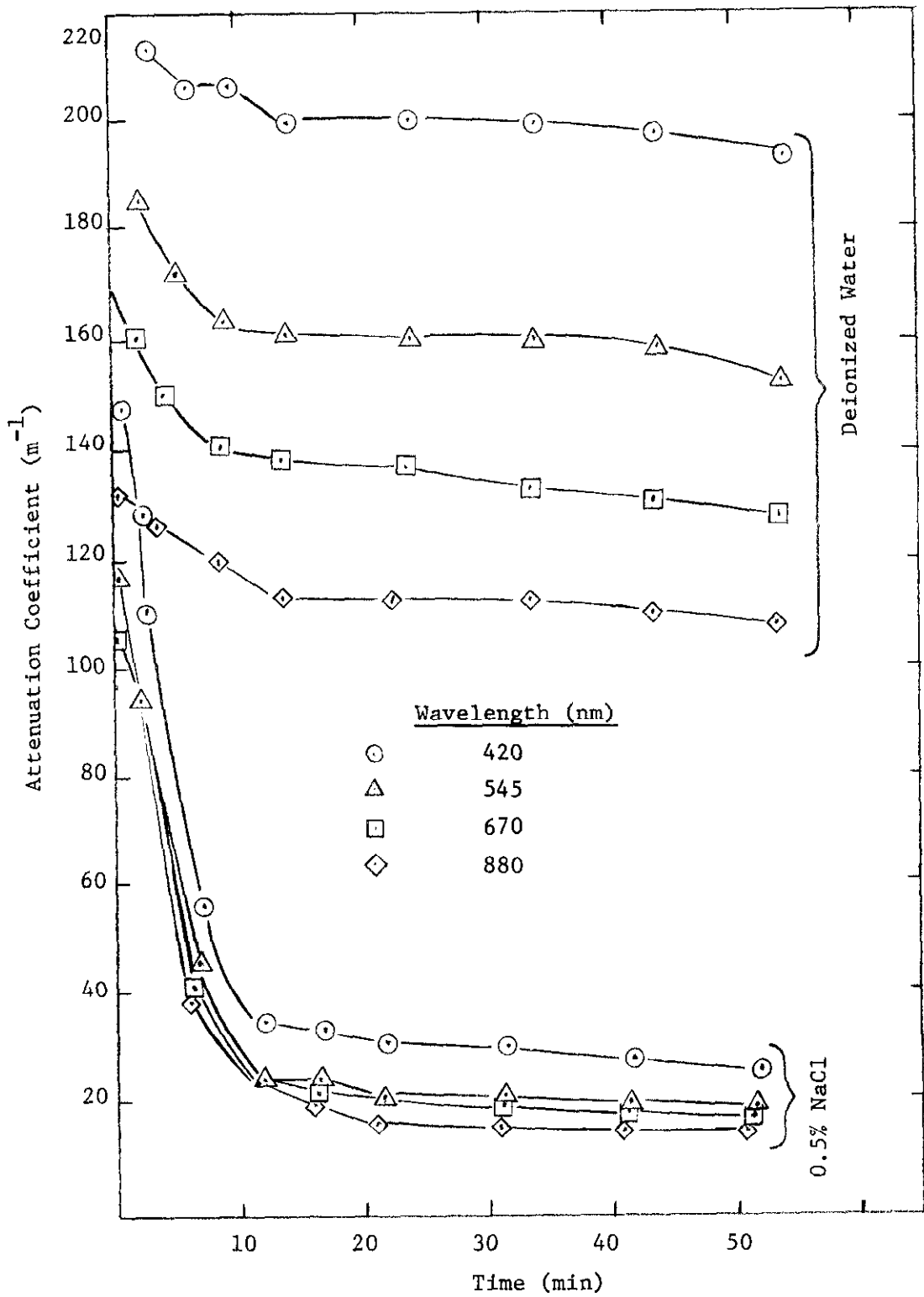


FIGURE 6. TURBIDITY OF KAOLINITE SUSPENSIONS IN TWO TEST WATERS AT FOUR WAVELENGTHS

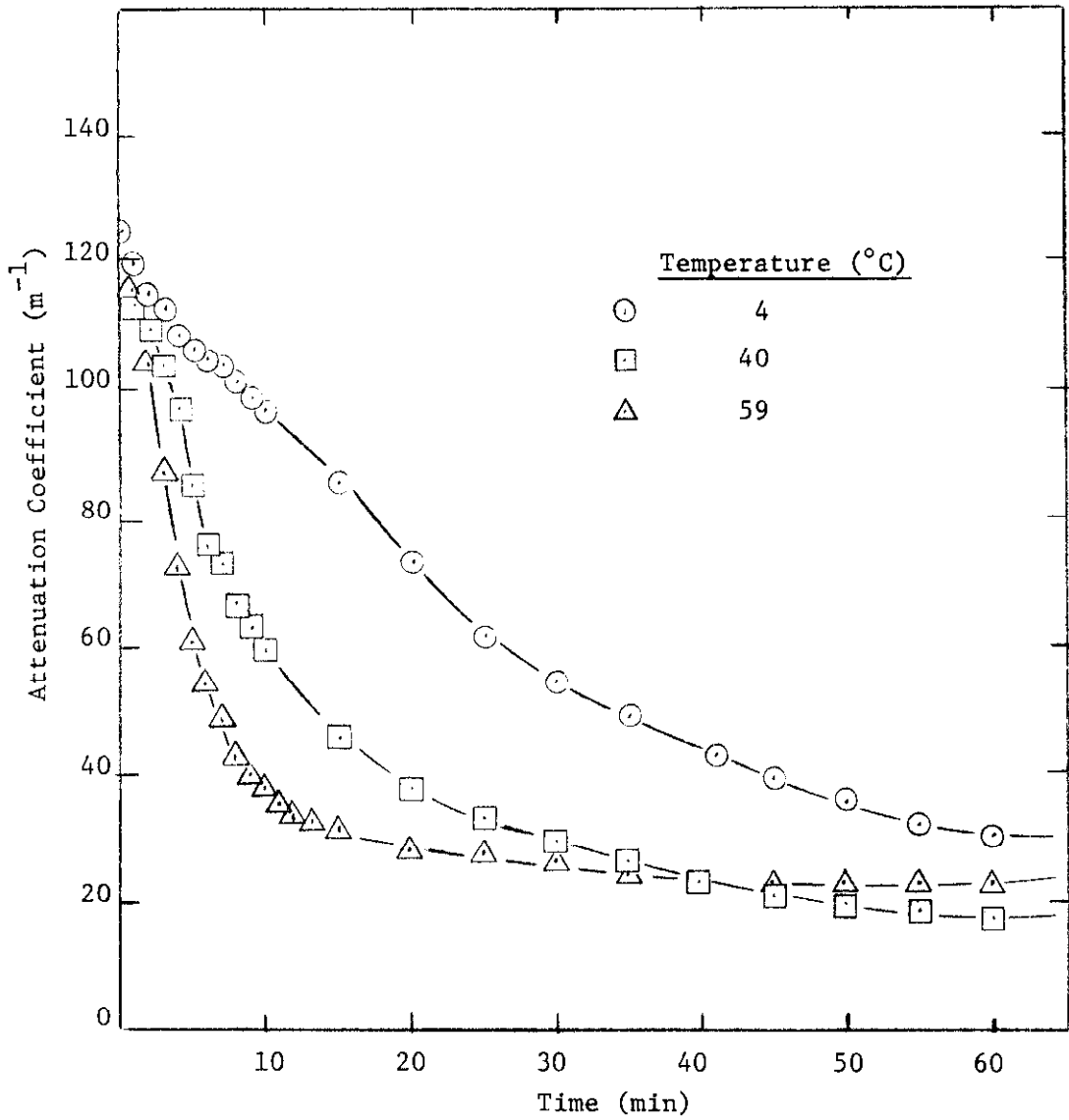


FIGURE 7. TURBIDITY OF KAOLINITE SUSPENSIONS IN 0.5% SODIUM CHLORIDE SOLUTION, SETTLING AT THREE DIFFERENT TEMPERATURES

to turbulent diffusion. To deduce values of settling velocities from the jar-test data, it is important that the latter mode of transport be either known or, preferably, negligible.

96. Tests with fairly low concentrations of clay-free, nonfloculent silt (VIX), which should settle as individual particles according to Stokes' Law, were made to estimate the extent of eddy mixing as opposed to gravitational settling in the jar tests. Four series of tests, at two different initial silt concentrations and two different salinities (deionized water and salt water), were made at several different stirring rates. Light-attenuation values were measured as a function of time for each. The curves in Figure 8 show, for each of the four combinations, turbidity after 30 min as a function of stirring rate. Turbidities were only slightly greater for stirring rates up to 30 rpm than for zero stirring rates; but beyond 30 rpm they increased substantially. For stirring rates up to 30 rpm there is apparently no substantial eddy mixing, and the transition at 30 rpm is interpreted as a changeover from laminar to turbulent stirring.

97. Since the jar tests were conducted at stirring speeds well below 30 rpm, it can be assumed that eddy diffusion was essentially absent. However, the increase in turbidity observed between 0 and 10 rpm suggests that minor turbulence does exist at very low stirring rates, possibly due to the presence of the light probes in the jars. Because of this effect, the lack of precise stirring rate control in the range of 2-5 rpm might be one source of variability in measured turbidities. The fact that α vs. time plots almost always yielded smooth curves indicates that this effect was averaged out over the time span of the experiments, although the absolute values of the curves may have been affected by variations in the stirring rate.

Stratification in jar tests

98. Another important consideration in interpreting jar-test results is whether any stratification existed during the rapid-mixing and dispersal period. Ideally, mixing would have been fully turbulent and suspensions homogeneous to insure the validity of comparisons between the various suspensions tested. If mixing was not adequate to

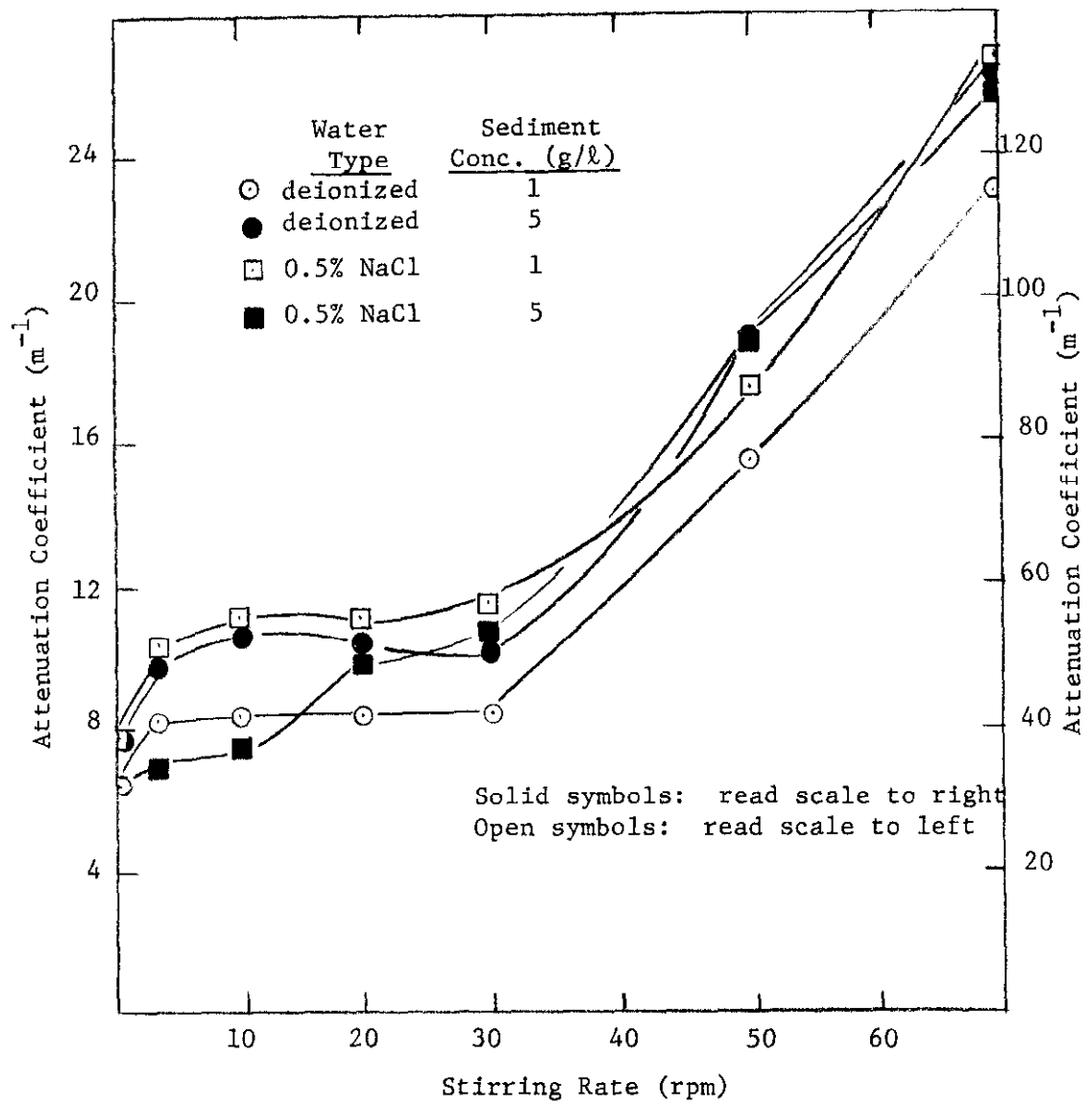


FIGURE 8. TURBIDITY OF SILT SUSPENSIONS AFTER 30 MIN OF SETTLING AS A FUNCTION OF STIRRING RATE DURING SETTLING

fully and evenly disperse the sediments, larger particles would have been more concentrated toward the bottom of the suspensions.

99. To test this possibility, two natural sediments were dispersed in the usual manner, and the top half of each suspension was drained off while stirring continued. Suspended solids determinations were then made for the top and bottom halves of both suspensions. In both cases, the top halves were found to be about 20% lower in suspended solids than were the bottom halves. Thus, some stratification does appear to have existed during the rapid-mixing period of jar tests.

100. Although these tests indicate incomplete homogenization of sediment suspensions during jar tests, it is likely that the turbidity results were only minimally affected. This is because the stratification must have been essentially limited to large silt particles. Smaller silt particles and clays, which contribute most to optical turbidity, were almost certainly well dispersed. Insofar as the initial concentration affects flocculation rates, varying amounts of stratification between different test suspensions could have had a slight effect on the measured rate of settling. However, other evidence suggests that coarse silt particles settle essentially independently of the clays, and therefore this effect was probably not important.

Electrolyte concentration

101. In Figures 9, 10, and 11 the settling curves for kaolinite, illite, and montmorillonite (1 g/ℓ clay) at various sea salt concentrations are shown. These experiments bracket the response of the three clay samples to sea salt solutions, from essentially no flocculation to very rapid flocculation and settling. One interesting observation from these data is the continuous decrease of α_0 with increasing salinity for kaolinite and illite, and the slight increase in α_0 with increasing salinity for montmorillonite. These results may be indicative of the presence of flocs even at the 100-rpm stirring rate at which zero-time readings were taken.

Correlation of light transmission, light scattering, suspended solids

102. Turbidity is commonly quantified by measuring light transmission, light scattering, or suspended solids. Each of these three

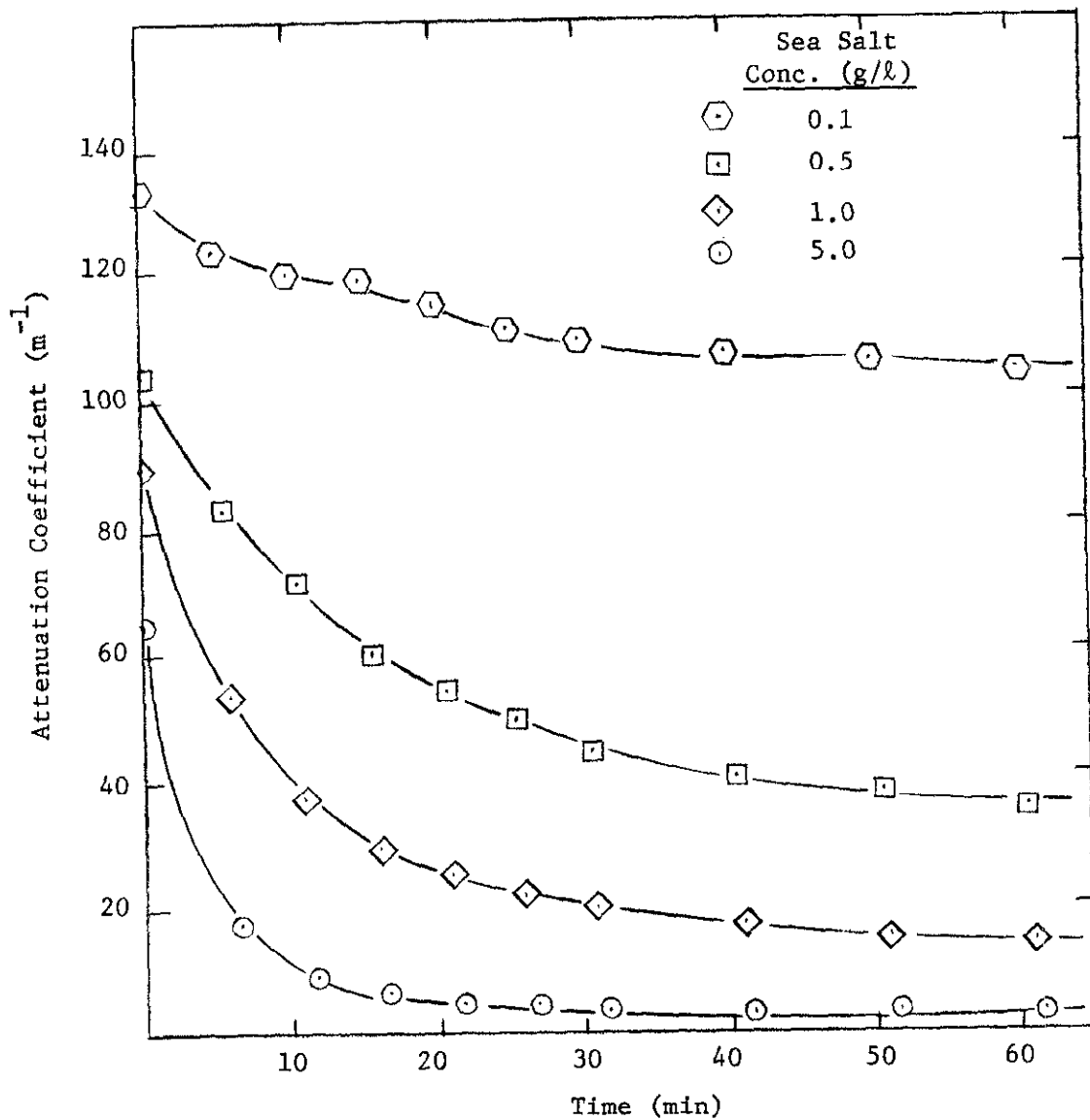


FIGURE 9. TURBIDITY OF KAOLINITE SUSPENSIONS AT VARIOUS SEA SALT CONCENTRATIONS

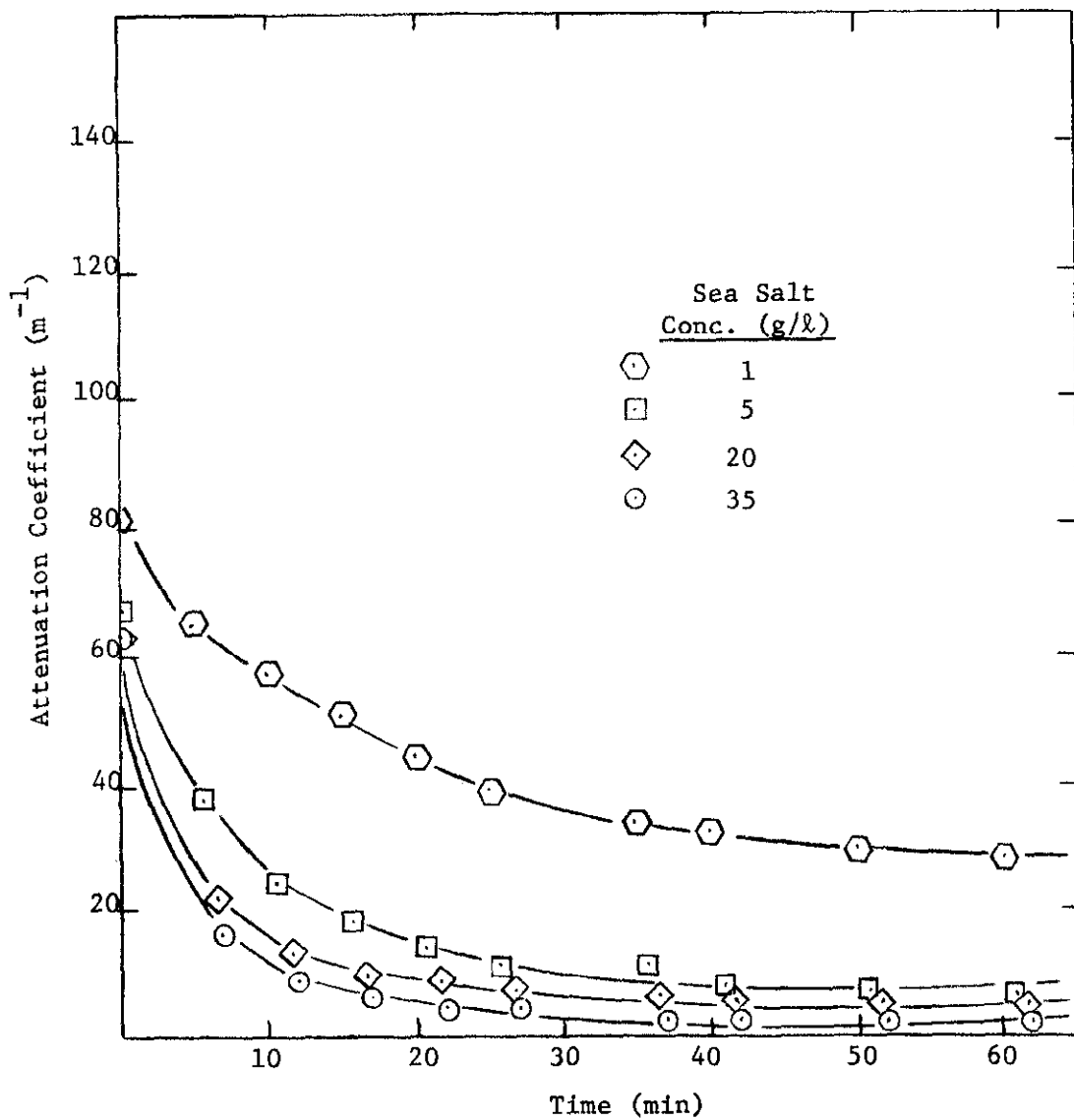


FIGURE 10. TURBIDITY OF ILLITE SUSPENSIONS AT VARIOUS SEA SALT CONCENTRATIONS

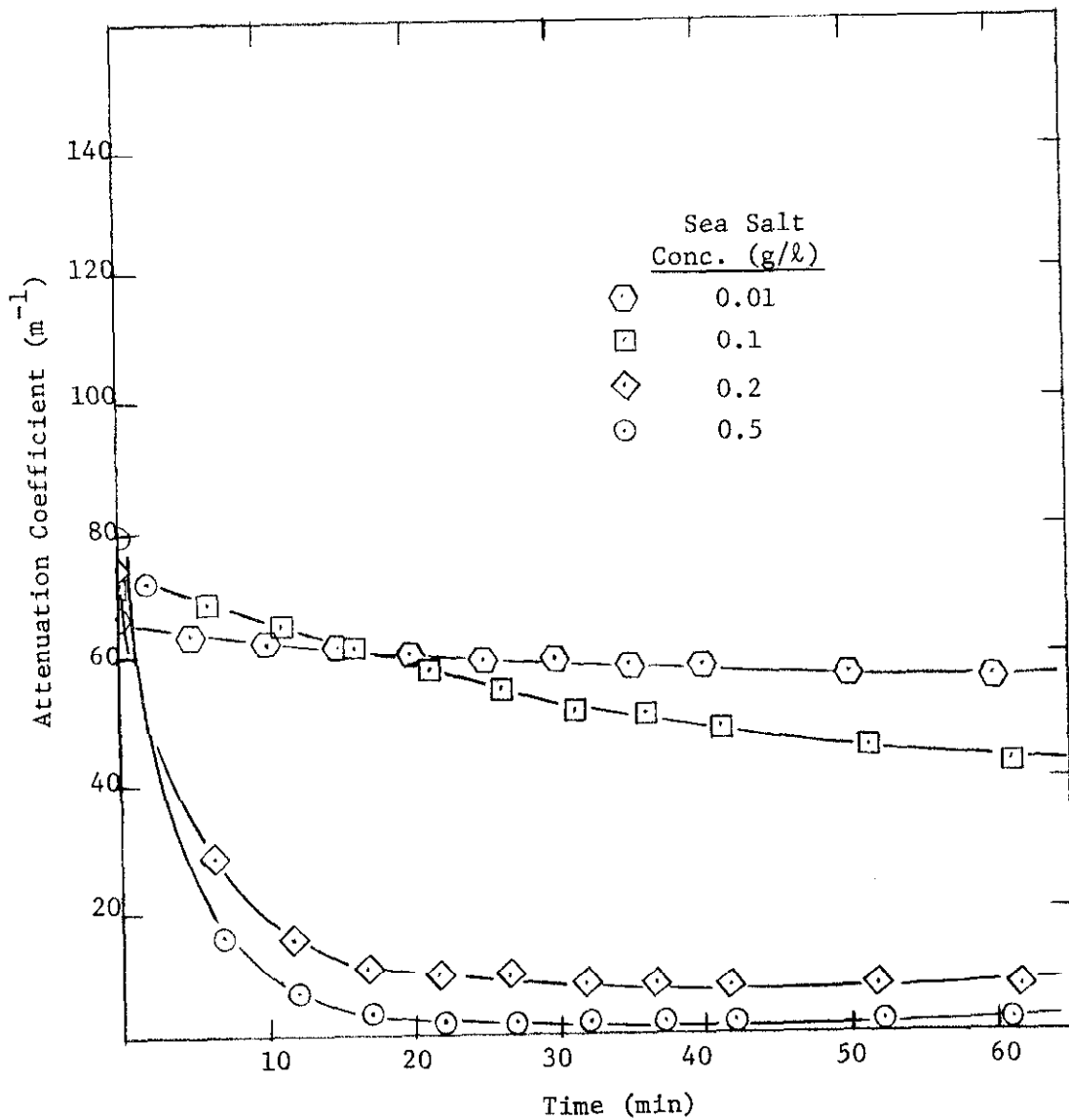


FIGURE 11. TURBIDITY OF MONTMORILLONITE SUSPENSIONS AT VARIOUS SEA SALT CONCENTRATIONS

methods may be particularly suitable for specific applications, but because of differences in measurement techniques and the physical properties of suspended materials they do not necessarily yield equivalent results. In this study, jar-test turbidities were measured by light transmission. In order to determine how well these data relate to the actual settling of suspended solids and to evaluate the usefulness of light scattering measurements, replicate test samples were analyzed for light transmission, light scattering, and suspended solids. The data are plotted in Figures 12-14.

103. Simple linear regression techniques were applied to the data to determine the correlations between the three measurements. A functional dependence of the following form was assumed:

$$Y = a + bX + e \quad (10)$$

where X and Y are measured suspended solids and turbidity values, respectively; a and b are mathematically determined coefficients; and e is the random experimental error which accounts for all variation in Y not explained by a, b, and X. The correlation coefficient, r, is a measure of the degree of closeness of the linear relationship between X and Y, while the square of the correlation coefficient, r^2 , may be described as the proportion of the variance of Y which is explained by the regression. The regression equations and statistical parameters are given in Table 3. Clays and natural sediments were considered separately to characterize any differences between them.

104. The equations for clays and natural sediments were statistically equivalent at the 1% significance level when comparing the attenuation coefficient (α) with suspended solids. Therefore, only one equation is given. The correlation coefficient is high, indicating a rather good fit. Light scattering (FTU) gives a reasonably good correlation with suspended solids for clays, but not quite as good a fit for natural sediments. Furthermore, the clays and natural sediments do seem to give statistically distinct curves, suggesting that light scattering is a function of the type of material in suspension as well as

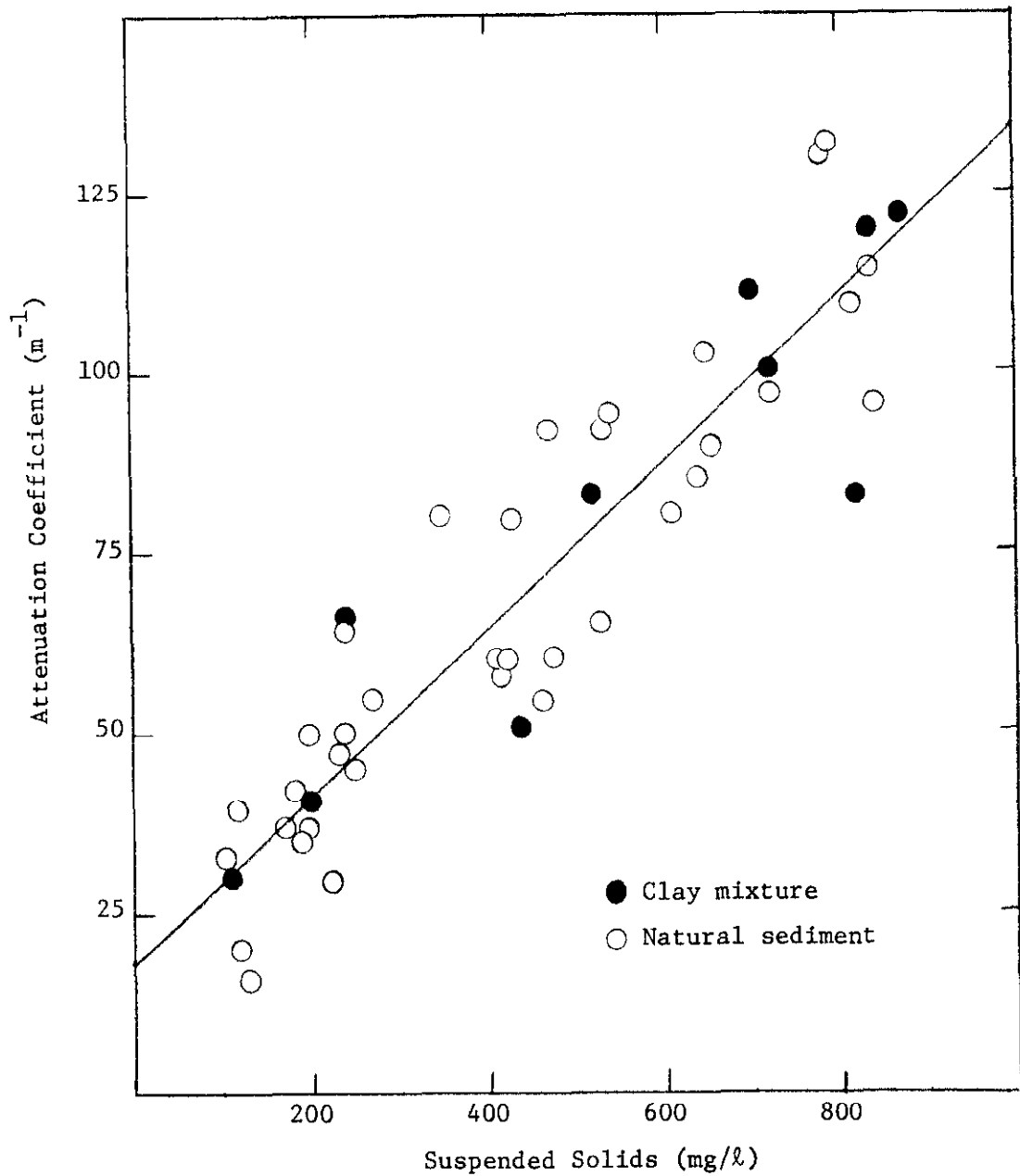


FIGURE 12. LIGHT ATTENUATION AS A FUNCTION OF SUSPENDED SOLIDS FOR CLAYS AND NATURAL SEDIMENTS

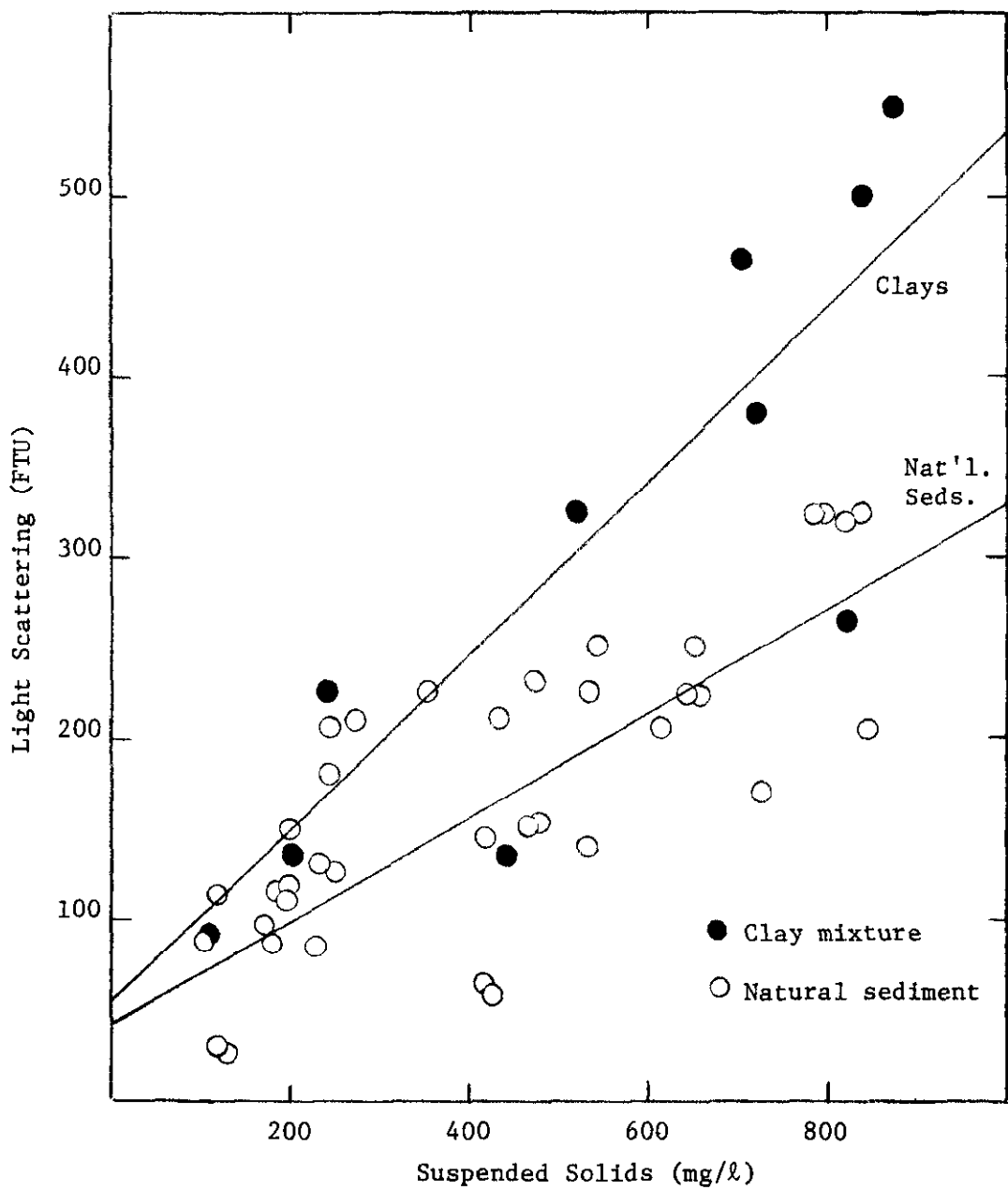


FIGURE 13. LIGHT SCATTERING AS A FUNCTION OF SUSPENDED SOLIDS FOR CLAYS AND NATURAL SEDIMENTS

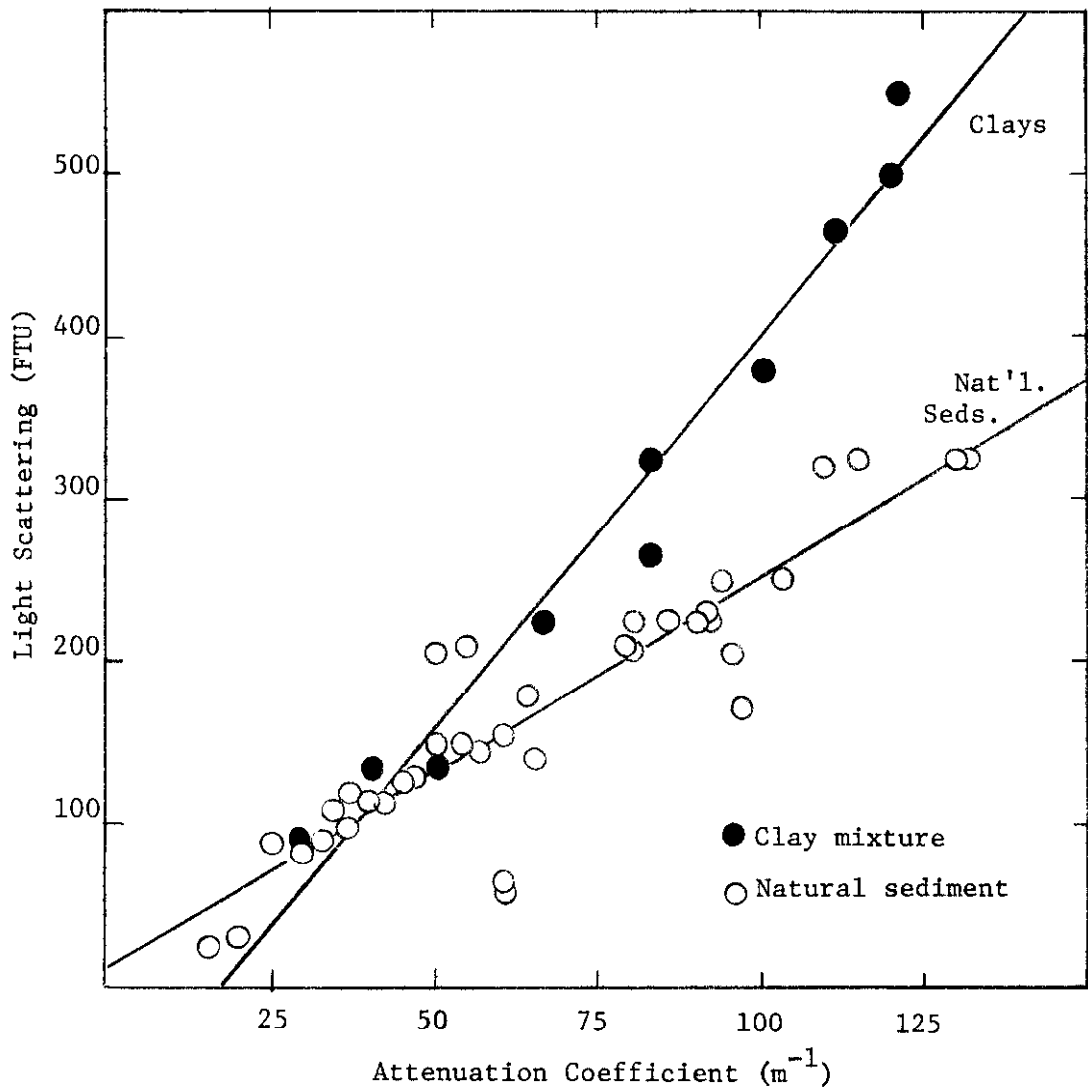


FIGURE 14. LIGHT SCATTERING AS A FUNCTION OF LIGHT ATTENUATION FOR CLAYS AND NATURAL SEDIMENTS

Table 3

Regression Equations for α , FTU, and SS

<u>Samples</u>	<u>Regression</u> [*]	<u>Significance Parameters</u> ^{**}
clays and natural sediments	$\alpha = (17.9 \pm 3.8) + (0.116 \pm 0.007)SS$	SEE = 12.6, $r = 0.919$, $r^2 = 0.84$ $F_{0.01} = 7.2$, $F(1,47) = 243$
clays	FTU = $(43 \pm 65) + (0.49 \pm 0.11)SS$	SEE = 92, $r = 0.849$, $r^2 = 0.72$ $F_{0.01} = 10.0$, $F(1,10) = 21$
natural sediments	FTU = $(58 \pm 18) + (0.27 \pm 0.04)SS$	SEE = 52, $r = 0.777$, $r^2 = 0.60$ $F_{0.01} = 7.4$, $F(1,37) = 53$
clays	FTU = $(-84 \pm 28) + (4.83 \pm 0.32)\alpha$	SEE = 32, $r = 0.983$, $r^2 = 0.97$ $F_{0.01} = 10.0$, $F(1,10) = 230$
natural sediments	FTU = $(12 \pm 14) + (2.38 \pm 0.19)\alpha$	SEE = 36, $r = 0.903$, $r^2 = 0.82$ $F_{0.01} = 7.4$, $F(1,36) = 154$

* Regression coefficients given with standard errors

** SEE = standard error of estimate

r = correlation coefficient

$F_{0.01}$ = tabulated F-value for each regression

$F(k,d.f.)$ = calculated F-value for regression

d.f. = degrees of freedom.

k = number of independent variables for each regression

its concentration. This effect may be due in large part to the color of the sediments. The darker, organic-bearing natural sediments are stronger light absorbers than the clays and consequently scatter less light per unit weight than do the clays. A similar effect is observed when comparing light scattering (FTU) with attenuation (α), and distinct curves are derived for clays and natural sediments. For clays, where scattering is the major contributor to light attenuation, the two measurements are well correlated. However, for natural sediments the correlation is not as good, possibly due to the absorption of light by organic matter without a concomitant increase in scattering.

105. In summary, light transmission measurements seem to provide a better indication of suspended solids concentration than do light scattering measurements, at least for the materials studied here. Although the correlation is good, however, the standard error of the estimate is still relatively large, and caution must be exercised when estimating suspended solids from light attenuation or vice versa. The equations provided here should not be used to draw conclusions regarding suspensions of other types of materials without further evidence indicating the relationship between suspended solids, transmission, and scattering.

Clays and Clay Mixtures

Turbidity characteristics

106. The turbidity-time curves for kaolinite in five waters (Figure 15) demonstrate the typical features of turbidity reduction as a function of time for clays tested in the factorial experiment. Turbidity is high and settling is minimal over the period of 60 min in soft waters. In hard water, the settling rate is enhanced; and in saline waters, turbidity is effectively reduced (at the 6-cm depth of the light probe) within 60 min. The results for illite are similar to those for kaolinite, although illite settles less rapidly in saline waters. The montmorillonite suspensions also remain turbid in soft waters but attain >95% reduction in turbidity in 15 min in hard and saline waters. For mixtures of the three clay samples, the most striking result is that the presence of montmorillonite always leads to extremely rapid

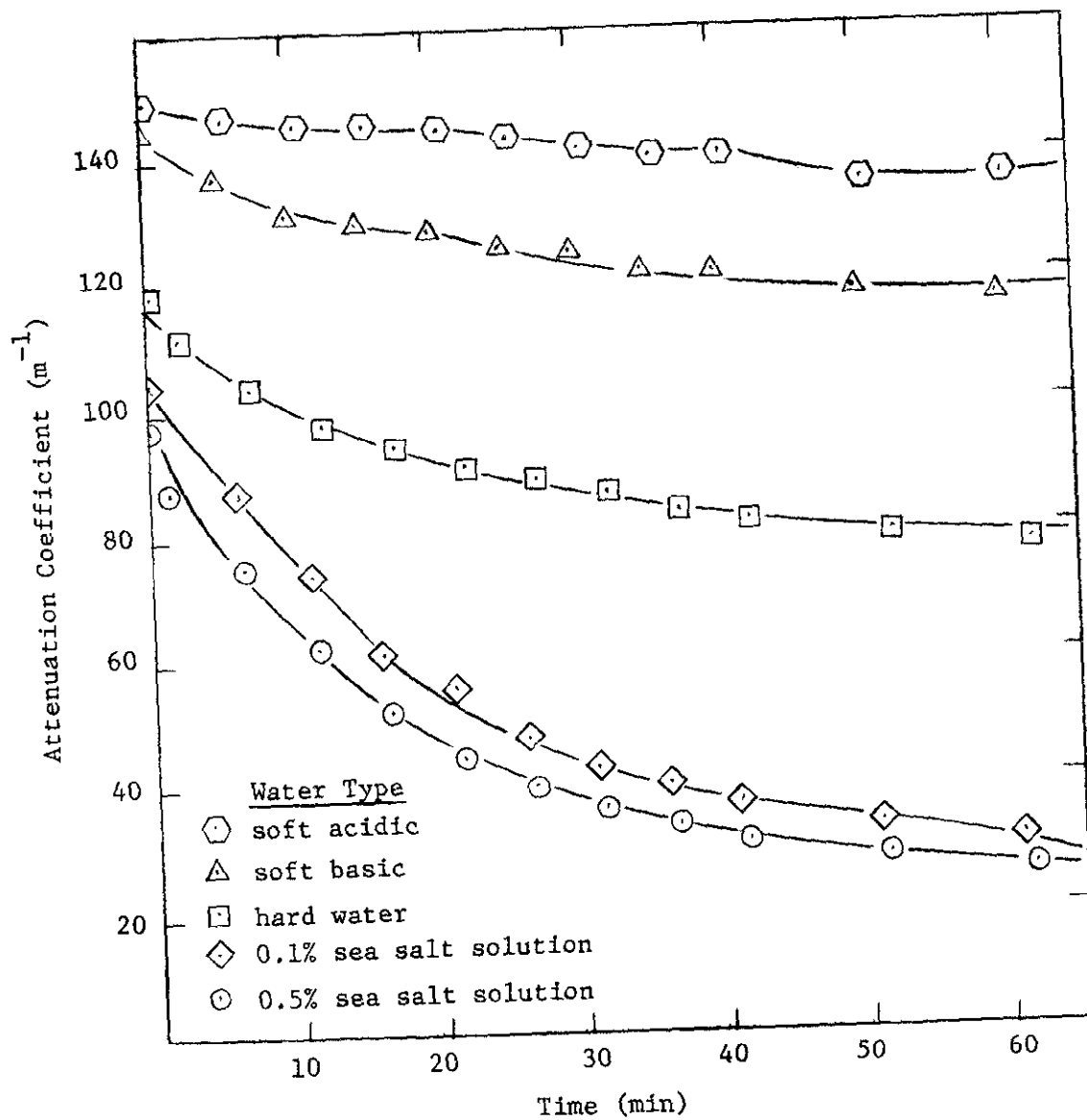


FIGURE 15. TURBIDITY OF KAOLINITE SUSPENSIONS IN FIVE TEST WATERS

turbidity reduction in hard and saline waters. In Figure 16, the curves for kaolinite, montmorillonite, and the kaolinite-montmorillonite mixture (KM) in 0.5% sea salt are compared. The effect of montmorillonite in increasing the turbidity reduction rate is evident since the turbidity of the KM mixture is reduced more rapidly than would be expected based upon the average of the individual component curves. A similar effect was found for other tests in which montmorillonite was a component of the clay mixture.

107. Values of α at zero time and after 15, 30, 45, and 60 minutes of settling for all clay experiments are tabulated in Appendix E. Also included in the appendix are the values of $1/t_{67}$ which were used to characterize the settling properties for regression analyses. The importance of flocculation can be seen by comparing the residual turbidity in soft waters, hard water, and saline waters for the clays and clay mixtures at various times. Lower residual turbidities result from more rapid settling of suspended solids and are therefore indicative of flocculation.

Replicate tests

108. Replicate tests were performed for the three-part clay mixture (KIM) in 0.1% sea salt and hard water and for the three two-part clay mixtures (KI, KM, IM) in 0.1% sea salt (see Appendix F). X-ray diffraction results indicate that illite tends to remain in suspension slightly longer than kaolinite and montmorillonite since it is enriched in the samples of supernatant suspension. However, the apparent increase is only slightly greater than the estimated error limits of the technique ($\sim 5\%$).

109. The zeta potential of KIM in hard water is significantly lower than that in 0.1% sea salt, probably due to the presence of divalent cations in the hard water. Although one might expect coagulation to be more rapid with a lower zeta potential, the observed settling time to one-half α_0 is slightly longer in hard water than in salt water. The discrepancy seems to indicate that the electrostatic potential barrier is not the limiting factor in coagulation of the clays. Thus zeta potential measurement does not appear to be a useful means of predicting sedimentation rates.

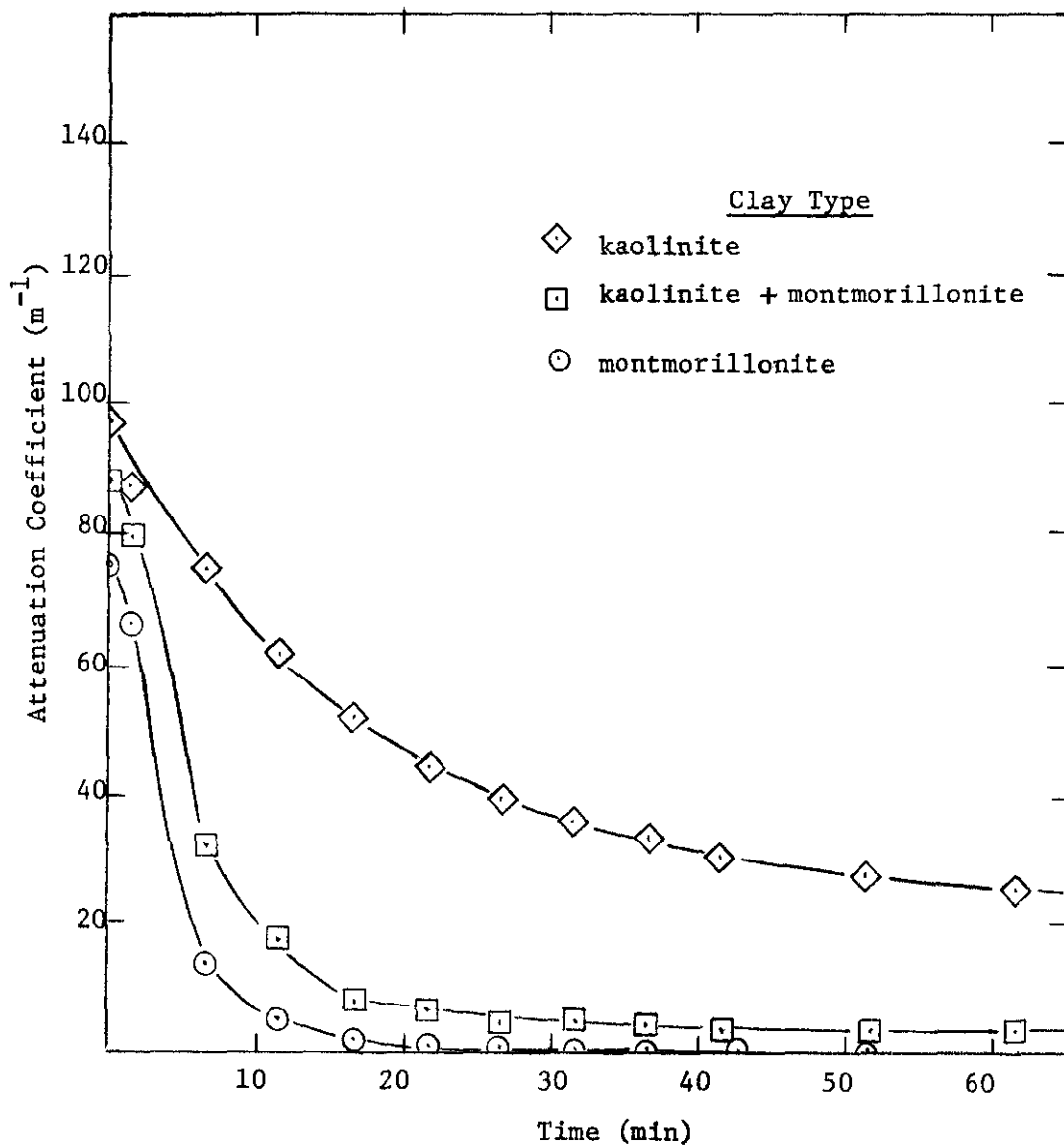


FIGURE 16. TURBIDITY OF KAOLINITE, MONTMORILLONITE, AND KAOLINITE + MONTMORILLONITE MIXTURE IN 0.5% SEA SALT SOLUTION

Statistical analysis of clay
and clay mixture turbidity data

110. Clay sedimentation data were statistically analyzed by stepwise linear regression techniques (see paragraphs 48-52). Separate regressions were performed for two dependent variables [$1/t_{67}$ and $\ln(1/t_{67})$], and the data were further divided to consider freshwater results alone, saltwater data alone, and combined freshwater and saltwater data together. This approach was used to provide the greatest insight into the relative importance of factors controlling particle settling under a variety of conditions. No a priori preference is given to the results for either $1/t$ or $\ln(1/t)$ regressions, but similarities or differences between them must be considered in the context of the complete experimental plan. Analysis of the freshwater and saltwater data alone was useful in identifying factors which might otherwise have been missed due to the strict criteria for statistical significance. Results of the statistical analyses are summarized in Table 4.

111. Ten independent variables were considered: water hardness (H; 0 = no hardness, 1 = 200 mg/l hardness), water salinity (S; in g/l), water pH (0 = acidic pH, 1 = basic pH), kaolinite concentration (K; in g/l), illite concentration (I; in g/l), montmorillonite concentration (M; in g/l), kaolinite-illite interaction (KI), kaolinite-montmorillonite interaction (KM), illite-montmorillonite interaction (IM), and kaolinite-illite-montmorillonite interaction (KIM). Initial clay concentration was not tested as a factor since all data were limited to 1 g/l suspensions. The choice of values such as 0 or 1 for hardness and pH was appropriate for determining the statistical significance of these factors. Although the values are arbitrary, their significance is not affected by linear transformations. The regression equations presented in Table 4, however, cannot be used to predict settling rates for conditions other than those used in the jar tests reported here. The purpose of the regression analyses was to identify statistically significant factors affecting turbidity reduction, and not to develop a mathematical relation suitable for general application.

Table 4
Statistical Analysis of Clay and Clay-Mixture Data

<u>Waters</u>	<u>Dependent Variable</u>	<u>Regression*</u>	<u>Significance Parameters**</u>
Fresh	1/t	$1/t = 0.169 + (6.9 \pm 1.7)H$	SEE = 3.63, $r = 0.688$, $r^2 = 0.47$ $F_{0.01} = 8.18$, $F(1,19) = 17.1$
Fresh	$\ln(1/t)$	$\ln(1/t) = -1.83 + (2.8 \pm 0.5)H$	SEE = 1.09, $r = 0.788$, $r^2 = 0.62$ $F_{0.01} = 8.18$, $F(1,19) = 31.2$
Salt	1/t	$1/t = 0.960 + (11.0 \pm 0.5)M + (31 \pm 2)IM + (17 \pm 2)KM + (82 \pm 14)KIM$	SEE = 0.72, $r = 0.995$, $r^2 = 0.99$ $F_{0.01} = 10.56$, $F(1,9) = 32.5$, $F(4,9) = 297$
Salt	$\ln(1/t)$	$\ln(1/t) = -0.109 + (2.5 \pm 0.4)M + (6.7 \pm 1.3)IM + (5.7 \pm 1.3)KM$	SEE = 0.47, $r = 0.955$, $r^2 = 0.91$ $F_{0.01} = 10.04$, $F(1,10) = 17.9$, $F(3,10) = 42$
Combined	1/t	$1/t = 1.789 + (8.2 \pm 2.5)M$	SEE = 5.18, $r = 0.489$, $r^2 = 0.24$ $F_{0.01} = 7.59$, $F(1,33) = 10.35$
Combined	$\ln(1/t)$	$\ln(1/t) = -1.804 + (2.3 \pm 0.7)PH$	SEE = 1.74, $r = 0.475$, $r^2 = 0.23$ $F_{0.01} = 7.55$, $F(1,33) = 9.62$

* Regression coefficients given with standard errors
 ** SEE = standard error of estimate
 r = correlation coefficient
 $F_{0.01}$ = tabulated F-value for last included independent variable in each regression
 $F(1, d.f.)$ = calculated F-value for last included independent variable in each regression
 $F(k, d.f.)$ = calculated F-value for whole regression
 d.f. = degrees of freedom
 k = number of independent variables for each regression

112. The freshwater regressions indicate a strong dependence of settling rate on water hardness. This is consistent with the prediction of clay colloid stability theory that hardness induces coagulation of suspended clay particles.

113. In salt waters there is a strong correlation between settling rate and the presence of montmorillonite, either alone or in mixtures. The interaction effects (IM, KM, KIM) indicate that montmorillonite not only settles rapidly itself in salt waters, but it also acts as an effective flocculating agent for the other clays. The high values of r^2 for both saltwater regressions indicate that essentially all the variability could be ascribed to clay factors and that other variables (in particular, salinity) were relatively unimportant. Of course, the presence of salinity was necessary to induce flocculation. The fact that it does not appear as a significant variable in these regressions simply indicates that the difference between 0.1% and 0.5% salinity had less of an effect than the presence or absence of montmorillonite and its interactions with the other clays.

114. For the combined data set, M and pH appear as the only significant variables for the $1/t$ and $\ln(1/t)$ regressions, respectively. The corresponding correlation coefficients are fairly low ($r < 0.5$), and this is an indication that other important effects have been excluded by the $F_{0.01}$ significance criterion. The appearance of montmorillonite (M) in the $1/t$ regression seems plausible based upon its importance in the saltwater results. However, pH is unlikely to be of real significance. Since only soft fresh waters were run at both acidic and basic pH, this factor would have appeared in the freshwater regressions if it were truly important. Rather, it is believed that the appearance of pH in the regression is a statistical artifact due to the unbalanced experimental design. This unbalance results from the fact that salt and hard waters were always basic in the clay tests, whereas the soft freshwater was tested at both acidic and basic pH. It seems likely, therefore, that the pH factor is actually an expression of the effects of salinity and hardness.

115. The fact that montmorillonite appears as the only significant

factor in the $1/t$ regression while pH appears in the $\ln(1/t)$ regression suggests that both of these terms are important. The difference between the regressions is merely a consequence of weighting of the data and the criteria for significance. Taken together, these results indicate that salinity, hardness, and montmorillonite are probably all important in reducing the turbidity of clay suspensions. The presence of 200 mg/l hardness or salinity is effective in flocculating montmorillonite suspensions. Once flocculation is induced, the montmorillonite appears to interact with the other clays by coagulating them and/or "sweeping out" other clay particles during settling. However, replicate tests indicated that illite was not completely removed along with the other clays. This might be due in part to the relatively coarse grain size of the illite sample. The presence of higher levels of salinity has no further effect on the flocculation of montmorillonite, which would explain why salinity does not appear as a factor in the regressions using saltwater data alone. In the absence of montmorillonite, salinity and hardness are still important factors, resulting in the flocculation of the other clays. However, with montmorillonite present the flocculation of other clays appears to be greatly enhanced.

Silt Tests

116. The settling behavior of the VIX silt sample in five waters was monitored for 1-g/l suspensions. The turbidity was much lower than that of any of the other clays or natural sediments tested, and, as would be expected for a nonclay sediment, there was essentially no flocculation. The VIX sample was added to an equal weight proportion of the KIM clay mixture (total concentration 1 g/l) in order to test for any clay-silt interaction. The settling curves for this mixture were simply an average of the individual curves for KIM and VIX (see Appendix E), thus indicating that no interaction existed. Similar tests with additions of VIX to the Boston Harbor (BH) and Charles River (CR) sediments yielded the same result, i.e., no apparent interaction between clay and silt. Because of the small number of results, no statistical analysis was performed.

Natural Sediments

Turbidity characteristics

117. In general, the response of natural sediments to water hardness and salinity factors is similar to that observed for clays and clay mixtures. Turbidity reduction is minimal over 60 min in soft waters, while water hardness and particularly salinity promote flocculation and therefore more rapid settling of the suspended solids. The turbidity data and reciprocal settling times ($1/t_{67}$) for all experiments are tabulated in Appendix E.

118. In developing a predictive capability for dredging-related turbidity, it is of primary importance to relate the differences in settling behavior of various sediments to their compositional characteristics. In Figures 17 and 18, the settling curves of all eight sediments (at 1 g/l initial concentration) in 0.1% sea salt are compared, both in terms of absolute turbidity values and after normalizing to the initial turbidity. Initial turbidities vary widely, by nearly a factor of two, at constant initial sediment concentration. However, the residual turbidities after 60 min vary by more than a factor of 5 in absolute value and by about a factor of 4 in terms of the fraction of initial turbidity, indicating that the settling rates of various sediments suspended in a single type of water can vary markedly.

119. Although stratification during the initial stirring period of jar tests might account for part of the variation in α_0 , it is probably not the major contributor to this variation. The amount of stratification, and therefore the concentration at the depth of the light probe (6 cm), should be a function of the sediment particle-size distribution. If stratification was a major factor in determining initial turbidity values, one would expect to find a good correlation between α_0 and the mean particle size. No such correlation was found to exist. Furthermore, the effect of stratification in determining α_0 is expected to be minimized by the fact that only larger particles, which contribute least to the optical turbidity, contribute to the concentration gradient.

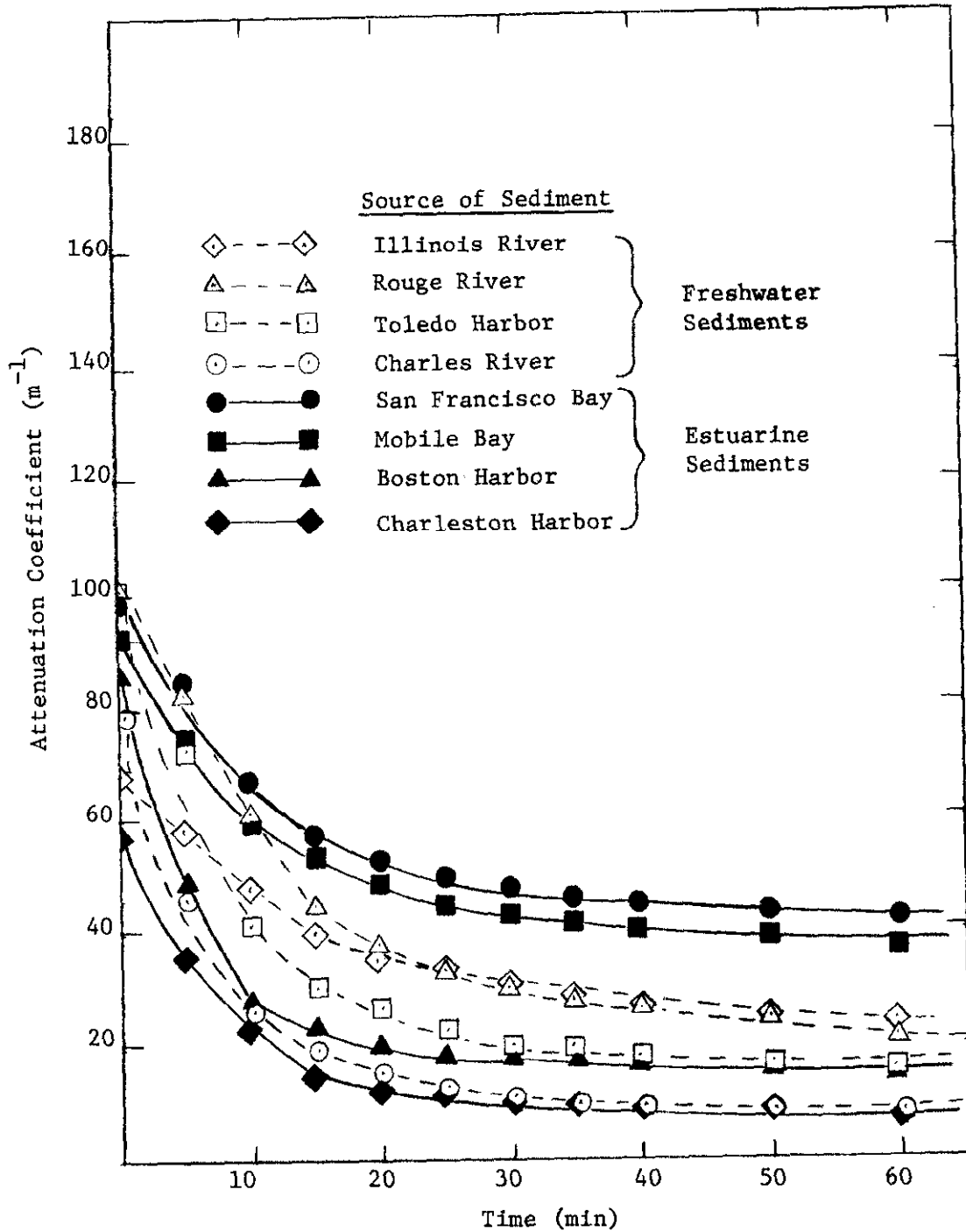


FIGURE 17. TURBIDITY OF EIGHT NATURAL SEDIMENT SUSPENSIONS IN 0.1% SEA SALT SOLUTION

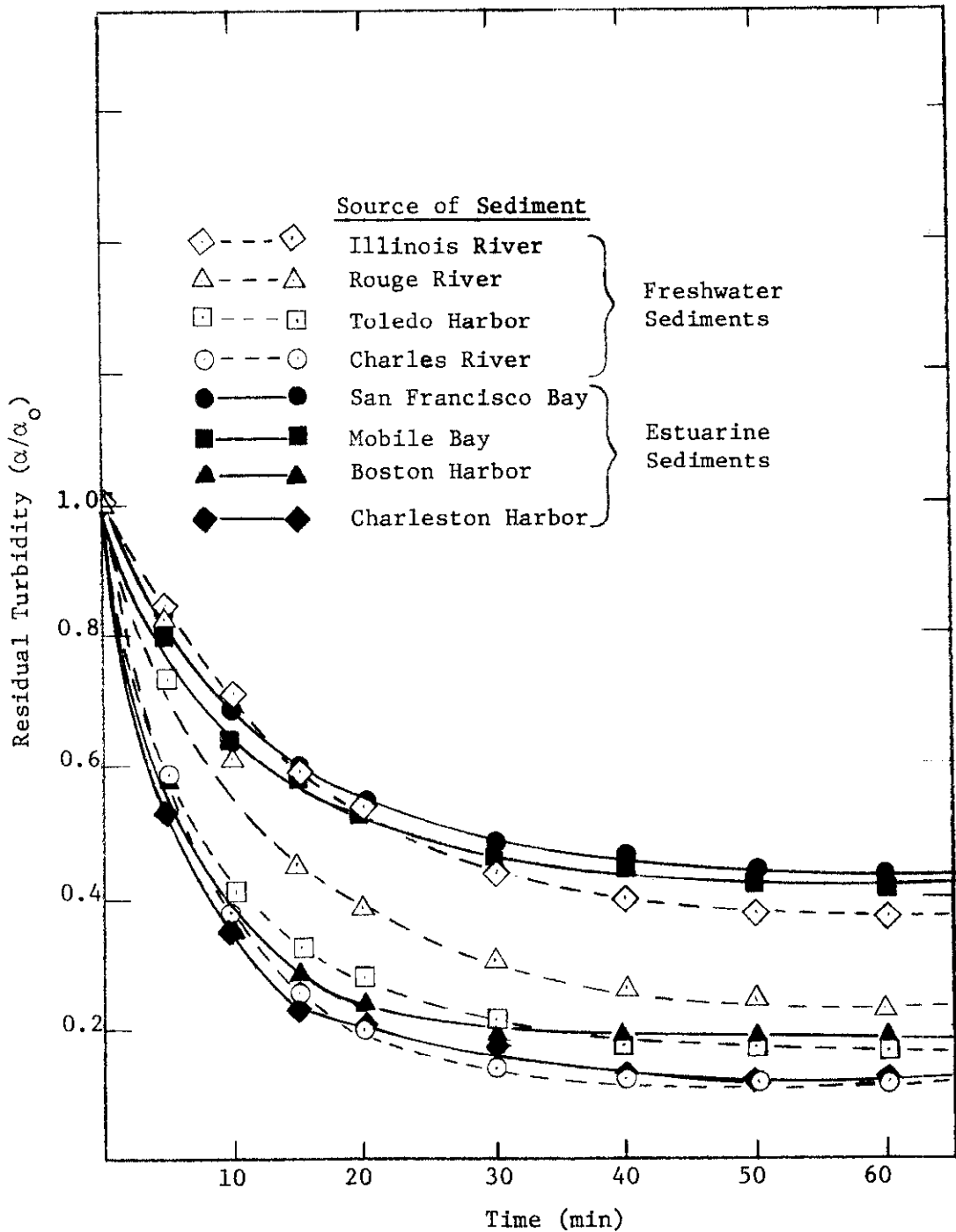


FIGURE 18. RESIDUAL TURBIDITY (α/α_0) OF EIGHT NATURAL SEDIMENT SUSPENSIONS IN 0.1% SEA SALT SOLUTION

120. Firm conclusions relating settling rate to compositional characteristics can be drawn only on the basis of a proper statistical treatment of the data (see below), but several useful observations can be made from Figures 17 and 18. First, the settling rates of the eight sediments do vary over a wide range. This suggests that dredging-related turbidity problems can vary significantly depending on sediment characteristics. Second, certain behavior which might be expected, based on the results of testing with clays and clay mixtures, is not observed in the natural sediments. The presence of montmorillonite (e.g., MB, SF) does not lead to rapid flocculation and settling. Third, the organics content of the sediments may have a major influence on the settling rates (Figure 18). The three sediments lowest in organic carbon (IR, SF, MB) have the slowest settling rates, while the more organic-rich sediments settle more rapidly in salt water. However, the settling rates of these sediments are not linearly correlated with the % organic carbon measurements.

Replicate tests

121. Two different tests were replicated for each of the eight natural sediments to determine whether any sediment components preferentially segregate during sedimentation. Replicate test data are presented in Appendix F, where tests 6-21 are for natural sediments. The significance of changes in sediment composition was evaluated by comparing the values measured for supernatant suspensions (b-samples in Appendix F) with the values for the corresponding original suspensions (a-samples) for each test. The mean difference for each component was calculated by subtracting the mean value of the a-samples from the mean value of the b-samples. Standard deviations for mean differences and levels of significance were computed from a two-way analysis of variance (test numbers, i.e., 6-25; and treatment, i.e., a vs. b). Results are presented in Table 5.

122. The X-ray diffraction data provide information on the settling behavior of the various mineral fractions of the sediments in flocculated and unflocculated suspensions. The data were derived by analyzing aliquots of the material suspended in both deionized water and the appropriate test solution, taken after the specified period of

Table 5

Evaluation of Preferential Settling of Sediment Components

<u>Parameter</u>	<u>Parameter Mean</u>	<u>Mean Change</u>	<u>Standard Deviation of Change</u>	<u>Level of Significance</u>	<u>Number of Data Pairs</u>
1. Quartz (%) [*]	7.0	-0.92	0.96	>0.25	16
2. Organic Carbon (%)	3.8	-0.11	0.12	>0.25	16
3. Kaolinite + Chlorite (%) ^{**}	34.3	-0.56	1.09	>0.25	16
4. Illite (%)	22.0	1.56	1.09	>0.25	16
5. Montmorillonite (%)	12.2	1.70	2.09	>0.25	8
6. Zeta Potential (mv)	-20.7	0.36	0.21	>0.25	16
7. Particle Diameter (microns)	2.81	-2.20	0.72	~0.02	7
8. Weight % <2 μ	15.66	5.00	3.03	>0.25	16

* Values for % quartz indicate relative peak area, not wt. %.

** Kaolinite and chlorite were not differentiated in this analysis.

settling for each replicate test. Results obtained for deionized water suspensions are reported as zero-time samples in Appendix F (6a, 7a, 8a, etc.), while the flocculated suspensions are listed as 6b, 7b, 8b, etc. This approach was used for two reasons. First, the large amount of silt in the bulk sediment samples makes it difficult to obtain accurate intensity data for the clay minerals. Removing the coarse, nonclay fraction by settling is thus beneficial for quantifying the clays and necessary for making an unbiased comparison with the clay mineralogy of supernatant suspensions (b-samples), where gravity settling tends to remove much of the silt during the course of the test. A second purpose for this procedure was to derive useful information on the possibility of interactions between clay and silt.

123. Although the silt fraction may comprise several minerals, the relative peak area of quartz (Q) can be used as an indicator of the proportion of silt in the suspensions. Comparison of the results for each replicate test (see Appendix F and Table 5) indicates that there is no significant change in the proportion of quartz between a- and b-samples (unflocculated vs. flocculated suspensions). The most likely explanation for this trend is that silt particles large enough to settle out in the appropriate time period for each test ($> \sim 20 \mu$ for the shortest experiments, $> 4.5 \mu$ for the longest settling times) were not affected by flocculation and settled independently of the clays. Smaller silt particles, however, must settle in association with the clays for this interpretation to be valid. It is difficult to evaluate the errors associated with these particular measurements. Therefore, although the proposed explanation is consistent with the replicate test observations, as well as turbidity tests of clay and silt mixtures, it may not be the only valid interpretation. It should also be noted that in two tests (No. 6 and 10) there is an apparent change in Q, in one case decreasing and in the other case increasing. It is doubtful that any significance can be attached to these results.

124. The results for the clay mineralogy and organic carbon contents do not show any clear evidence of preferential settling from the water. The observed average changes are all significantly less than

their respective standard deviations which are, in turn, all small enough to be at least largely attributable to experimental error. In only two cases, tests 12 and 21, the increase in illite between a- and b-samples appears significant, possibly indicating slower settling. In several tests, the fractional changes in organic carbon content seem large (>25% of the starting value). However, after comparing the values obtained for suspensions which should give identical results (6a and 7a, 8a and 9a, etc.), the absolute changes appear to be largely within the experimental error of the test procedures. Certainly no consistent change in the organic carbon content of the suspended solids is apparent.

125. The zeta potentials of particles in the supernatant suspensions after settling has taken place are not significantly different from those measured at zero time, suggesting that their settling rate is unrelated to the electrostatic potential. This suggestion is further supported by the fact that zeta potentials measured in hard water were significantly lower than those measured in 0.1% sea salt, while settling rates in hard water were always slower than in sea salt. If reduction in electrostatic potential was the key factor in promoting flocculation, the lower zeta potentials (as in hard water) would correlate with more rapid settling. The opposite situation was observed here.

126. Particle-size analyses of the initial and supernatant suspensions indicated a decrease in the mean particle size with time, which was significant at about the 2% level. This trend results from the more rapid settling of coarser particles in the suspensions relative to fine silt and clays. It is consistent with the suggestion made above that silt particles settled independently of the clays.

Statistical analysis of natural sediment turbidity data

127. Sedimentation data for natural sediments were analyzed by stepwise linear regression techniques (see paragraphs 48-52). Three data sets were separately analyzed: freshwater data, saltwater data, and combined freshwater and saltwater data. Two dependent variables

were separately analyzed: $1/t_{67}$ and $\ln(1/t_{67})$. Thirteen independent variables were tested simultaneously: initial sediment concentration (Conc; in g/l), wt. % kaolinite (K), wt. % illite (I), wt. % montmorillonite (M), wt. % chlorite (C), wt. % $>2 \mu$, wt. % organic carbon (Org), water salinity (S; in g/l), water hardness (H; 0 = no hardness, 1 = 200 mg/l hardness), water pH (0 = acidic pH, 1 = basic pH), montmorillonite-organics interaction (M x Org), salinity-organics interaction (S x Org), and pH-organics interaction (pH x Org). Several other interaction terms were shown in preliminary analyses to be statistically insignificant. The results are summarized in Table 6.

128. For fresh waters, the $1/t$ regression yields no significant factors, whereas the $\ln(1/t)$ regression suggests that the particle-size distribution of the suspended sediment (% $>2 \mu$), water hardness, and chlorite content of the sediment are all significant factors controlling settling rates. Due to the small number (four) of sediments used in the freshwater analyses, these results must be viewed with some caution. A strong dependence of settling rate on the sediment particle-size distribution indicates that, in fresh water, the settling of unflocculated particles is the most important factor accounting for turbidity reduction. The positive correlation with water hardness is consistent with theories of colloid stability. Dependence of settling rate on chlorite concentration was unexpected on the basis of the literature survey and may be a statistical artifact due to the small number of sediments tested. The absence of % organics or of the clays montmorillonite, illite, or kaolinite is consistent with the theory, proposed below, that in fresh water the sediment clay fraction is covered with natural organics which mask the properties of the pure clays. This might explain why montmorillonite, which was found to flocculate and settle rapidly in hard water when testing pure clays, behaved quite differently in the natural sediments.

129. In salt waters, the significant factors controlling settling rates were the initial sediment concentration, % organic carbon, and the interaction of organics with salinity. The importance of sediment concentration is consistent with colloid stability theories which indicate

Table 6
Statistical Analysis of Natural Sediment Sedimentation Data

Data Set	Dependent Variable	Regression Equations*	Parameters of Statistical Significance**
Fresh Water	l/t	$l/t = 0.90 \pm 2.25$	
Fresh Water	$\ln(l/t)$	$\ln(l/t) = -10.29 + (0.105 \pm 0.017)(\% > 2 \mu) + (0.92 \pm 0.20)(H) + (0.16 \pm 0.05)(\text{Chlorite})$	SEE = 0.58, $r = 0.836$, $r^2 = 0.70$ $F_{0.01} \approx 7.64$, $F(1,28) = 10.65$, $F(3,28) = 23.7$
Salt Water	l/t	$l/t = -4.80 + (4.58 \pm 0.77)(\text{Conc}) + (0.63 \pm 0.16)(S \times \text{Org})$	SEE = 12.4, $r = 0.671$, $r^2 = 0.45$ $F_{0.01} \approx 7.08$, $F(1,61) = 16.2$, $F(2,61) = 25.9$
Salt Water	$\ln(l/t)$	$\ln(l/t) = 0.47 + (0.37 \pm 0.05)(\text{Conc}) + (0.18 \pm 0.05)(\text{Org})$	SEE = 0.86, $r = 0.698$, $r^2 = 0.49$ $F_{0.01} \approx 7.08$, $F(1,61) = 13.5$, $F(2,61) = 29.9$
Combined Waters	l/t	$l/t = -4.17 + (0.82 \pm 0.13)(S \times \text{Org}) + 3.13(\text{Conc})$	SEE = 11.5, $r = 0.645$, $r^2 = 0.42$ $F_{0.01} \approx 6.95$, $F(1,93) = 29.0$, $F(2,93) = 34.1$
Combined Waters	$\ln(l/t)$	$\ln(l/t) = -2.29 + (0.38 \pm 0.07)(S) + (0.27 \pm 0.06)(\text{Conc}) + (1.60 \pm 0.38)(\text{pH}) + (0.15 \pm 0.05)(\text{Org})$	SEE = 1.28, $r = 0.713$, $r^2 = 0.51$ $F_{0.01} \approx 6.95$, $F(1,91) = 7.38$, $F(4,91) = 25.7$

* Regression coefficients given with standard errors

** SEE = standard error of estimate

r = correlation coefficient

$F_{0.01}$ = tabulated F-value for last included independent variable in each regression

$F(1, d.f.)$ = calculated F-value for last included independent variable in each regression

$F(k, d.f.)$ = calculated F-value for whole regression

d.f. = degrees of freedom

k = number of independent variables for each regression

a strong dependence of flocculation rate on the particle number density (i.e., concentration). Higher concentration results in a greater number of interparticle collisions and therefore more rapid agglomeration. However, this factor may represent the effect of increased concentration of dissolved organic matter, originating in the sediment, on particle agglomeration. The positive correlation of settling rate with organic content (both as a main and interaction effect) is also consistent with a theory in which a protective colloid (natural organics adsorbed on clays), stable in fresh water, is destabilized in saline waters, allowing the clays to coagulate. Greater destabilization in more saline water would account for the salinity-organics interaction effect. This interaction term may, however, be an expression of nonlinearity in the dependence of settling rate on salinity and/or organics, rather than a true interaction. The experimental design utilized in this study does not allow a more precise determination of the nature of clay-organic interactions or the mechanistic role of dissolved and suspended organic matter in promoting flocculation of dredged material. However, the importance of the sediment organic content itself is clearly demonstrated by these results.

130. Regressions with the combined freshwater and saltwater data set provide a good test of salinity effects in that they include data at zero salinity as well as 1 and 5 g/l of sea salt. The appearance of salinity as an important factor in combined waters but not in salt waters indicates that though salinity has a strong effect on settling rates, only occasionally does 5 g/l produce a much stronger effect than 1 g/l. Once again the dependence on sediment concentration and % organics is apparent. The apparent correlation with pH is most likely an artifact of the unbalanced experimental design, where fresh waters were run at acidic and basic pH, but salt waters were always basic. Thus, the pH term probably expresses an effect due to salinity in this analysis.

Summary and Discussion

Summary of jar-test results

131. Jar tests were run with clays, silt, and natural sediments to determine the effects of a variety of physicochemical factors on particle agglomeration and settling rates. These results were statistically analyzed by stepwise linear regression methods. The principal conclusions of these analyses are summarized in the following paragraphs.

132. Clays. Tests with samples of illite, kaolinite, and montmorillonite revealed that the three clays responded differently to the same water compositions. In salt waters, illite settled most slowly, while montmorillonite settled most rapidly; in soft fresh waters, illite settled most rapidly, probably due to its relatively coarse particle size. However, because of the overwhelming influence of montmorillonite on turbidity reduction in saline and hard waters, no statistical difference was found between kaolinite and illite in linear regression analyses. Kaolinite and illite showed responses to different waters which were more similar to one another than to montmorillonite.

133. In fresh waters, the presence of hardness (200 mg/l) led to a significant increase in settling rates. In salt waters (1 ppt and 5 ppt), the presence of montmorillonite was the most important factor leading to turbidity reduction. When both fresh- and saltwater data were analyzed together, both montmorillonite and salinity were found to be significant factors. The latter result indicates that while salinity induces flocculation of all clays, settling was much more rapid with montmorillonite present than in its absence. The montmorillonite apparently "sweeps out" other suspended particles as it settles.

134. Silt tests. In several tests where an essentially clay-free silt sample was added to clays or natural sediments, no interaction was found between the silt and clay or sediment particles. In all cases, the added silt settled independently of the other suspended particles.

135. Natural sediments. The four freshwater and four estuarine sediments studied displayed a wide range of responses to identical water compositions, indicating that sediment compositional characteristics

have an important effect on settling properties. This effect was principally ascribed to the sediment organics content. Settling rates were not found to be dependent upon the clay mineralogy.

136. For data obtained in fresh waters, particle size and hardness were significant factors. The particle-size effect indicates that where flocculation does not occur (i.e., in soft waters) turbidity reduction is dependent upon gravity settling of individual particles. Thus, turbidity reduction of fine-grained sediments in soft, fresh waters would be expected to be extremely slow.

137. In salt waters, three factors were found to be important: initial sediment concentration, % organic carbon, and salinity-organics interaction. The concentration factor may be the result of faster agglomeration due to increased interparticle collisions. However, it is also possible that this factor is an expression of the effect of increased concentration of dissolved organic matter, originating in the sediment, on particle agglomeration. The salinity-organics interaction suggests that stable clay-organic complexes may be destabilized to a greater degree in waters of higher salinity, although this term may also reflect nonlinearity in the dependence of settling rate on salinity and/or organics.

138. The combined fresh- and saltwater data analysis indicates that salinity, sediment concentration, and % organic carbon all have a positive effect on turbidity reduction. The fact that salinity appears as a significant factor in the combined waters analysis but not in the saltwater analysis indicates that low levels of salinity (1 ppt) are effective in inducing flocculation and that 5 ppt salt does not have a significantly greater effect than does 1 ppt salt.

Comparison of clays with natural sediments

139. The analysis of results for clay and natural sediment tests indicates that water hardness and salinity are important factors in reducing the turbidity of both types of suspensions. However, the strong dependence on the presence of montmorillonite found in the clay tests was not apparent in the natural sediment suspensions. Rather, the natural organics content appears to be the predominant compositional factor responsible for the settling behavior of natural sediments.

140. Two possible explanations are suggested for the apparent difference found in the effect of montmorillonite between clay and natural sediment tests. First, the overwhelming importance of % organic carbon in the natural sediment analyses suggests that organics may mask the properties of suspended clay particles. A second possibility is that the behavior of the particular montmorillonite sample tested was determined by some factor other than the mineralogy itself. For instance, the extremely fine particle size of this sample relative to all other samples studied may have been responsible for its peculiar behavior.

141. Regardless of the mechanism involved in this distinction, it can be concluded that clay data does not appear to be particularly useful in modeling natural sediment systems. Clay mineralogy may exert a more subtle influence on the settling behavior of suspended sediments, but its importance is probably small relative to other factors.

Other sources of variability

142. The regression analyses shown in Tables 4 and 6 were based on a strict criterion for significance (F-test for 1% significance level) in order to identify the most important and unequivocal factors affecting observed settling rates. The r^2 parameter for these regressions indicates the fraction of the variability in the data which can be attributed to the independent variables in the equations. Thus, for the combined water data for natural sediments, only about 40-50% of the observed variability is actually due to the effects found to be significant. Removing the significance criterion results in regressions with r^2 in the range of perhaps 50-60%, but the remainder of the variability is unexplained by the factors considered in this study. Thus, it is necessary to consider what other sources of variability may have affected the jar-test results.

143. One possibility is that variation in the stirring speed during settling tests (see paragraph 97) contributed to experimental variability. Both turbulent diffusion and flocculation induced by liquid shear could have been influenced by this factor. Other sources

of variability might include laboratory vibration, incomplete homogenization of suspensions during the rapid-mix period, aging of sediments, and sediment heterogeneity. Unfortunately it was not possible, with the test plan utilized, to evaluate the relative importance of these or other factors affecting the jar tests.

144. Much of the unexplained variability may result from the use of linear regression equations. Since the proper functional relationship between dependent and independent variables was not known, linear functions were assumed. It is important to remember that this statistical analysis was only intended to determine which factors were significant in affecting turbidity reduction, and no attempt was made to quantitatively model the relationship between sediment-water factors and turbidity.

Replicate test conclusions

145. The replicate tests were designed to study the nature of turbidity and the changes which occur with time as suspensions settle. Data on the particle-size distribution, clay mineralogy, organic carbon content, and zeta potential of 25 test suspensions were collected both before and after settling had occurred and were analyzed to determine whether any significant segregation of sediment components took place.

146. Relatively large silt particles ($>20 \mu$) were found to settle independently of clays. Smaller silt particles ($2-20 \mu$), however, may be involved in flocculation and become incorporated into agglomerates. Other than this segregation due to particle-size effects, most sediments appeared to settle with their various components associated. This is consistent with the view that clay-organic aggregates are formed in suspensions of natural sediments. Zeta potential measurements similarly support this suggestion, since settling rates were found to be independent of the particles' electrostatic potential. Thus, natural organics seem to play a major role in the settling behavior of suspended sediments. These observations reinforce the conclusion of the statistical analyses presented above indicating the importance of the sediment organic carbon content in determining the rate of turbidity reduction.

147. Although there may have been some minor segregation of components in individual tests, there was certainly no consistent pattern observed. Furthermore, there was no identifiable sediment component found to be responsible for persistent turbidity.

Implications for dredging

148. Jar tests and statistical analyses have shown that the characteristics of dredged material and the composition of waters into which it is discharged significantly affect the settling rate of suspended particles. Various suspended sediments behave quite differently under similar water conditions, and any particular sediment behaves differently when suspended in waters of various compositions. Since turbidity is due primarily to the very slow settling rates of fine silt and clay particles in dredged material, factors influencing the particle agglomeration (and, therefore, settling) rates must be taken into account in any effort to predict the extent of turbidity problems. Unfortunately, no simple linear relationship was found between the rate of turbidity reduction and easily measurable sediment and water compositional factors. In order to determine particle settling rates under different conditions, it is therefore necessary to perform jar tests using samples of dredged material suspended in the waters into which they are to be discharged.

149. The evolution of turbidity plumes is dependent upon hydrodynamic factors as well as particle settling rates, and the extent to which plume profiles are affected by sediment-water characteristics must be considered in light of these effects (see Part V, below). Nevertheless, a number of qualitative judgements based upon jar-test results can be made. First, in fresh waters, the presence of hardness (200 mg/l) does promote flocculation and therefore may lead to some reduction in turbidity. However, this is a relatively mild effect, and its importance in determining the extent of downstream turbidity may be small relative to hydrodynamic factors.

150. Second, the presence of low levels of salinity (1-5 ppt) significantly reduces turbidity for most suspended sediments. Turbidity problems would therefore be expected to be less severe in estuarine waters than in fresh waters.

151. Third, the initial concentration of dredged material discharges may be important in affecting the resultant turbidity. Laboratory tests indicated that increased sediment concentration led to more rapid turbidity reduction, but it is difficult to extrapolate these results to field situations. At real dredge discharges, most slurries start out at very high concentrations (as high as 10-20% solids by weight) but concentrations in the water column are rapidly reduced to less than 1% within a short distance from the discharge point. Further study is needed to determine the effects of high initial concentrations as well as variability in the concentration of the dredge effluent.

152. Finally, based upon experience with jar tests it seems likely that variability in field conditions can significantly affect turbidity problems. Factors such as the extent of turbulent mixing in the dredge pipe, the state of the material when it is discharged, and sediment heterogeneity may exert important influences on particle settling rates and therefore downstream turbidity. Extensive comparisons between field and laboratory observations are needed to determine the relative magnitude of such effects and whether the use of jar-test data is a practical means of predicting turbidity.

PART V: TURBIDITY PLUME MODEL

153. A turbidity plume model based on jar-test data was developed as a means of predicting the concentration of suspended sediment downstream from a line source (hydraulic pipeline dredge discharging in open water) as a function of sedimentation data (from jar tests) and hydraulic parameters (e.g. eddy diffusion, current velocity). In this section the derivation of the mathematical model, the utilization of jar-test data, the numerical solution method, and a sample calculation are presented. Details of the computer program are presented in Appendix G.

154. The turbidity plume model described here predicts the downstream concentration gradient of silt and colloidal-size fractions of dredged sediments discharged in waters characterized by unidirectional constant flow, essentially infinite width, constant depth, and infinite length. Density gradient settling, salt wedges, narrow channels, tidal flows, and complex circulation patterns are beyond the scope of the model in its present state of development. The model has been tested by comparing plumes predicted on the basis of jar-test data for Mobile Bay sediment with previously published observations of turbidity plumes from this locality.¹⁷ However, further validation through laboratory experiments and comparison with other field observations is required.

Material Balance Relationship

155. Downstream from a dredging site the residual turbidity will be determined by a balance between several sediment transport mechanisms. These are:

- a. Removal by downward settling with ultimate removal by deposition at the bottom (Note: In the case of flocculating sediment, e.g., clays in saline water, flocs will be formed with settling velocities much greater than those for individual particles).
- b. Upward transport by vertical eddy diffusion in the direction of decreasing concentration gradient (i.e., upward from the bottom).

- c. Dispersion by eddy diffusion in the lateral direction.
- d. Dispersion by both bulk advection (convection) and eddy diffusion in the downstream direction.

156. The differential material balance at any downstream point is given by the following equation:

$$\underbrace{\frac{\partial}{\partial x} (uc)}_{\text{downstream advection}} + \underbrace{\frac{\partial}{\partial y} [\int wf(w) dw]}_{\text{vertical sedimentation}} - \underbrace{\frac{\partial}{\partial x} (E_x \frac{\partial c}{\partial x}) - \frac{\partial}{\partial y} (E_y \frac{\partial c}{\partial y}) - \frac{\partial}{\partial z} (E_z \frac{\partial c}{\partial z})}_{\text{eddy diffusion}} = 0 \quad (11)$$

where

x = downstream coordinate, m

y = vertical coordinate, m

z = lateral coordinate, m

u = current velocity at any point, m/sec

c = sediment concentration, kg/m³

w = settling velocity, m/sec

f(w) = settling-velocity frequency distribution, (sediment mass/w) vs. w

E_x, E_y, E_z = eddy diffusivities in x, y, and z directions, m²/sec

This relationship is based on the assumption that flow is steady, uniform, and fully turbulent, and that eddy diffusion can be characterized by Fick's Law with eddy diffusion coefficients.

157. Many investigators have used an equation of this kind, in one form or another, to study distribution of negatively buoyant particles downstream of a particle source in a turbulent flow, both in the atmosphere²⁴⁻²⁶ and in water flows.²⁷⁻³¹

158. For Equation 11 to be useful in the plume model, further simplifying assumptions must be made:

- a. Eddy diffusion in the downstream direction is negligible compared to the other two diffusive transport terms. Thus,

$$\frac{\partial}{\partial x} \left(E_x \frac{\partial c}{\partial x} \right) = 0 \quad (12)$$

- b. For fully turbulent flow the velocity profile will be flat, especially outside the relatively thin near-bottom zone. Hence, it can be assumed that u is constant and equal to the mean velocity (U):

$$\frac{\partial}{\partial x} (uc) = U \frac{\partial c}{\partial x} \quad (13)$$

- c. Eddy diffusivity E_y can be related to vertical position in the flow by assuming that E_y is about the same as the diffusion coefficient E_M for fluid momentum. This assumption is made in deriving the classical suspended-load equation, which has been the most successful approach to steady suspended-sediment transport. It is the fine fraction of the sediment that will be of greatest importance in the evolution of near-surface turbidity downstream of a dredging site, and it has been found that E_y and E_M are almost equal for laboratory channel flows transporting fine sediment.²⁹ An expression for E_M as a function of distance, y , above the bottom can be derived using three equations. The first is obtained by differentiating the logarithmic velocity profile:

$$U = \frac{u_*}{\kappa} \ln \frac{y}{h} \quad (14)$$

The second is the definition of E_M :

$$\tau_t = \rho E_M \frac{du}{dy} \quad (15)$$

The third is the vertical distribution of shear stress, assuming that τ_t accounts for almost all of the shear stress at positions not close to the bottom:

$$\tau_t = \tau_o \left(1 - \frac{y}{h} \right) \quad (16)$$

Combining Equations 14-16,

$$E_M = \kappa u_* y \left(1 - \frac{y}{h} \right) \quad (17)$$

where

- u_* = the shear velocity, equal to $(\tau_o/\rho)^{1/2}$, m/sec
- κ = von Karman constant, approximately equal to 0.4
- h = channel depth, m
- τ_t = turbulent shear stress, N/m^2
- ρ = density, kg/m^3
- E_M = eddy viscosity, m^2/sec
- τ_o = shear stress at the bottom boundary, N/m^2

Equation 17 should hold everywhere except very near the bottom, where E_M must go to zero in a slightly different manner than predicted by Equation 17 because of the presence of a viscous-dominated layer. E_M thus varies parabolically from zero at the surface and bottom to a maximum at mid-depth. Equation 17 has been verified experimentally²⁹ using dye diffusion in clear-water laboratory channel flow. To make Equation 17 useful for the plume model, it is necessary to use the empirical relationship between mean flow velocity and boundary shear stress,

$$\tau_o = \frac{f}{8} \rho U^2 \quad (18)$$

where f is the friction factor. Substituting Equation 18 into Equation 17, and using a value of 0.02 for f , which is a good estimate for the range of Reynolds numbers, flow depths, and bottom roughnesses likely to be involved in natural flows,

$$E_M = 0.02 Uy(1 - \frac{y}{h}) = E_y \quad (19)$$

- d. Based on experimental studies, summarized by Fischer,³² over most of the flow depth except very near the bottom the lateral eddy diffusivity E_z is approximately constant, and given by the equation

$$E_z = 0.2hu_* \quad (20)$$

Using Equations 17-19, this can be written in terms of the maximum value of E_y (at mid-depth):

$$E_z \approx 2.2(E_y)_{\max} \quad (21)$$

With these assumptions, the initial material balance relationship (Equation 11) becomes

$$U \frac{\partial c}{\partial x} + \frac{\partial}{\partial y} [\int w f(w) dw] - \frac{\partial}{\partial y} (E_y \frac{\partial c}{\partial y}) - \frac{\partial}{\partial z} (E_z \frac{\partial c}{\partial z}) = 0 \quad (22)$$

with E_y given by Equation 19, and E_z given by Equations 20 and 21.

159. Equation 22 differs from similar convection-diffusion-settling equations in the form of the settling term. If all the sediment had the same settling velocity, this term would reduce to $\partial(wc)/\partial y$. When the sediment has a range of settling velocities, vertical flux due to settling then involves contributions over this entire range, and must therefore be written as an integral (to be evaluated between values of w less than and greater than all the settling velocities represented in the sediment).

160. For nonflocculent sediment, the settling velocity of each particle will be invariant with respect to time and position. Thus, the field of total concentration at points downstream of the source can be found by solving Equation 22 with a settling term $w \frac{\partial c}{\partial y}$ for each sediment size present and then superimposing the results (weighted with respect to the initial concentration of particles in each size range) to obtain total concentration at each point downstream.

161. The problem is far more complicated when the sediment is flocculating as it diffuses and settles. The settling characteristics of the sediment vary with both time and local $f(w)$ itself, by virtue of the effect of shear/collision and differential settling on the rate and nature of flocculation. That is, the distribution $f(w)$ in the integral in Equation 22 is bound up with the very process the equation characterizes; and for Equation 22 to be solved rigorously, $f(w)$ would be expressed as a highly complicated function of concentration (c) and position (x, y, z). In fact, Equation 22 cannot be solved without some simplifying assumption about this flocculation process. This simplification is developed in the following section.

Estimation of Settling Velocities from Jar-Test Data

Absence of eddy diffusion in jar tests

162. The jar tests were designed to characterize the settling properties of representative sediments in a simplified laboratory situation that involved water compositions and shear rates that are realistic in terms of the natural environment. An important consideration in use of the jar-test data is the relative importance of downward flux of sediment due to gravitational settling and upward flux due to turbulent diffusion. To deduce values of settling velocities from the jar-test data, it is important that the latter mode of transport be either known or, preferably, negligible. Tests with fairly low concentrations of clay-free, nonflocculent silt, which should settle as individual particles according to Stokes' Law, were made in order to determine the extent of eddy mixing as opposed to gravitational settling in the jar tests (see paragraphs 96-97). These tests demonstrated that eddy diffusion was essentially absent for the slow stirring speeds at which jar tests were conducted, and the latter can therefore be used to determine particle settling velocities.

Development of settling-velocity distributions

163. Dredged material may contain flocculent (clay) and nonflocculent (silt, sand) particles. For nonflocculent sediment, particle agglomeration does not occur, and the particle settling velocities are dependent only on the initial particle-size distribution. The settling-velocity distribution in jar tests can be determined from the measured curve of sediment concentration as a function of time by the same principle as is used in determination of sediment size distribution by settling-velocity analysis. However, for flocculent sediment, particle agglomeration causes the initial particle-size distribution to change with time. There is thus no simple procedure for determining settling velocity which can be applied to the plume model unless it is assumed that the sediment attains a steady state of flocculation (time-invariant distribution of settling velocities) in a time that is short relative to the time scale of evolution of the plume profile downstream of

the source. This is probably not very realistic with respect to either the jar tests or the natural plume, but this assumption must be made in order to extract information from the jar tests which will allow approximate modeling of plume evolution. Fortunately this assumption is most realistic for the smallest settling velocities and therefore for near-surface turbidity. That is, both in the jar tests and in the natural plume the larger flocs are rapidly fractionated downward from the finer material. The residual fine material which tends to remain near the surface has a settling-velocity distribution that is determined mainly by the early stages of flocculation, before most of the fractionation occurs, and changes only slowly thereafter.

164. In addition to the stipulation of a time-invariant settling-velocity distribution, two additional assumptions are required to derive settling velocities from jar-test data. First, the suspensions are assumed to be initially uniform and consist of particles with a range of settling velocities. Although some stratification probably existed during the rapid-mix period of jar tests, this is not expected to have significantly affected measured turbidities because the light attenuation is most sensitive to the smallest particles present, which are believed to have been uniformly dispersed. Therefore, although the assumption of initial uniformity was not rigorously met, the practical effect of this problem is most likely negligible. Second, the correlation between light attenuation and suspended solids concentration is assumed to hold for all stages of plume development. In fact, light attenuation is affected by the flocculation state of the suspended particles as well as their concentration and may vary between locations depending upon the physical characteristics of the suspended material. The use of turbidity vs. time curves to deduce suspended solids concentration is, nevertheless, an acceptable procedure for the purposes of the plume model and is not expected to result in substantial errors. Alternatively, rather than determining actual particle settling-velocity distributions, the following procedure might be viewed abstractly as defining a turbidity-reduction function.

165. As shown by Stokes' Law (Equation 1), particle settling velocity is a function of particle size. Each sediment fraction with particles of a certain size and settling velocity, w , will take a different time ($t = H/w$) to settle entirely past an arbitrary depth, H . Thus, as progressively smaller size fractions settle past the depth of the light probe in jar tests the turbidity is reduced, producing a curve such as that shown in Figure 19. This curve of concentration versus time at level H can then be converted to a cumulative distribution curve for w . The initial particle concentration of the suspension is c_0 ; then, after time t , the concentration at level H will be $c = c_0 - Zc_0 = c_0(1-Z)$, where Z is the fraction of the sediment with settling velocity greater than H/t . Using $t = H/w$, the measured concentration curve $c = c(t)$ can be transformed into a curve $c = c(H/w)$, giving c versus w . Setting the values of c from this curve equal to $c_0(1-Z)$, a relationship for Z versus w is obtained that is the desired cumulative frequency distribution for settling velocity (as in Figure 20).

166. This operation can be carried out with reasonable accuracy by selecting ten to twenty points from a jar-test curve (Figure 19), making the simple computations indicated above, and replotting (Figure 20), as demonstrated in the example below. Progressively smaller segments of the settling curve are used in order to include more fractions with low settling velocities and fewer with high settling velocities. This provides the type of distribution most useful for plume prediction since it is the fractions with small settling velocities which cause persistent turbidity.

167. In order to demonstrate the derivation of a settling-velocity distribution, consider the jar-test curve for Mobile Bay sediment at 5 g/l initial concentration in 0.5% sea salt solution (Figure 19). The initial turbidity (α) is 405 m^{-1} . After 5 min (300 sec), the turbidity is reduced to 71 m^{-1} , or 17.5% of the initial value. At this point 82.5% of the suspended material has settled past the depth of the light probe (0.06 m) and therefore has a settling velocity $w \geq 2 \times 10^{-4} \text{ m/sec}$. The fraction, Z , of particles with $w \geq H/t$ is thus 0.825, and the point can be plotted on the cumulative distribution curve (Figure

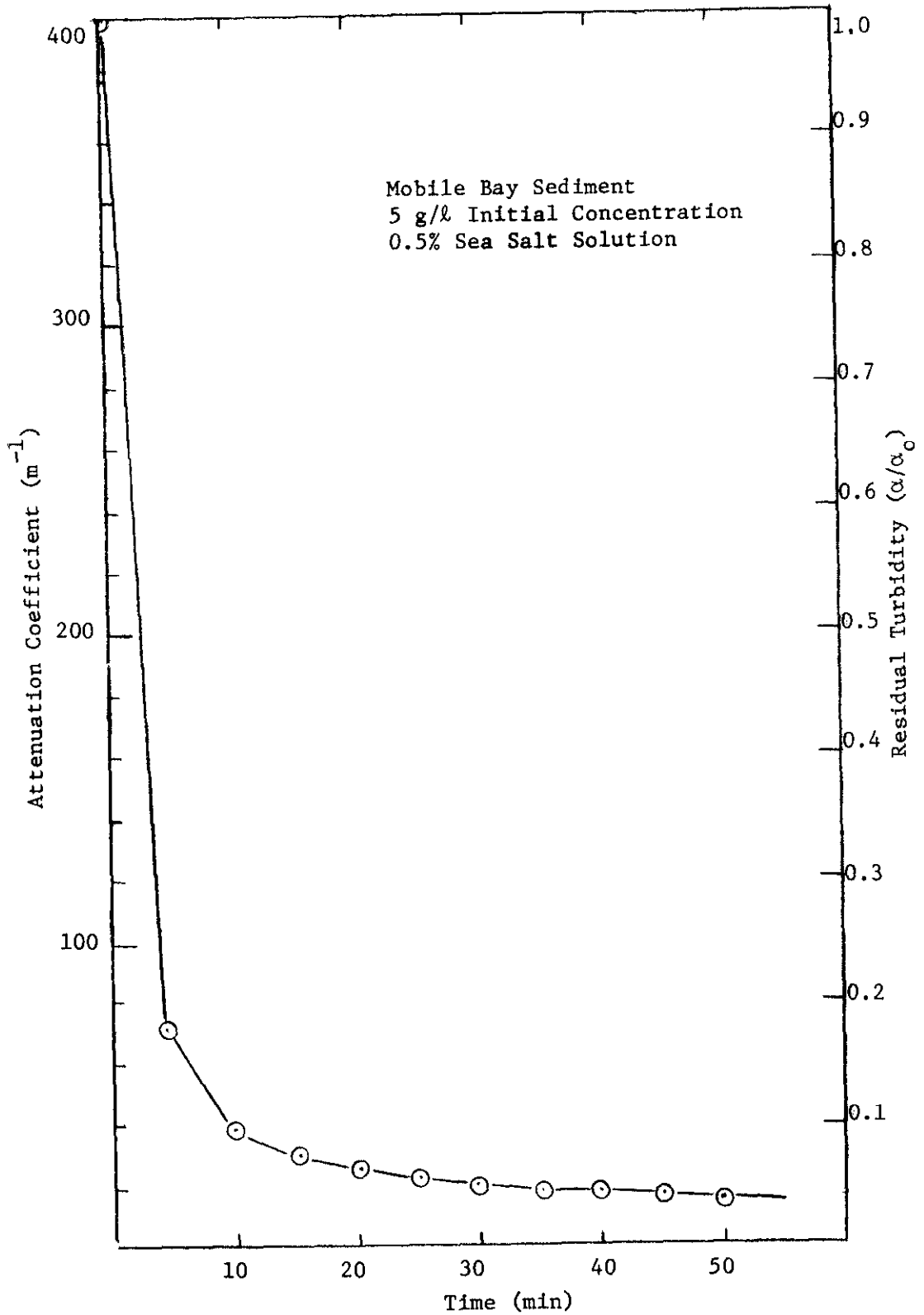


FIGURE 19. TURBIDITY OF MOBILE BAY SEDIMENT IN 0.5% SEA SALT SOLUTION

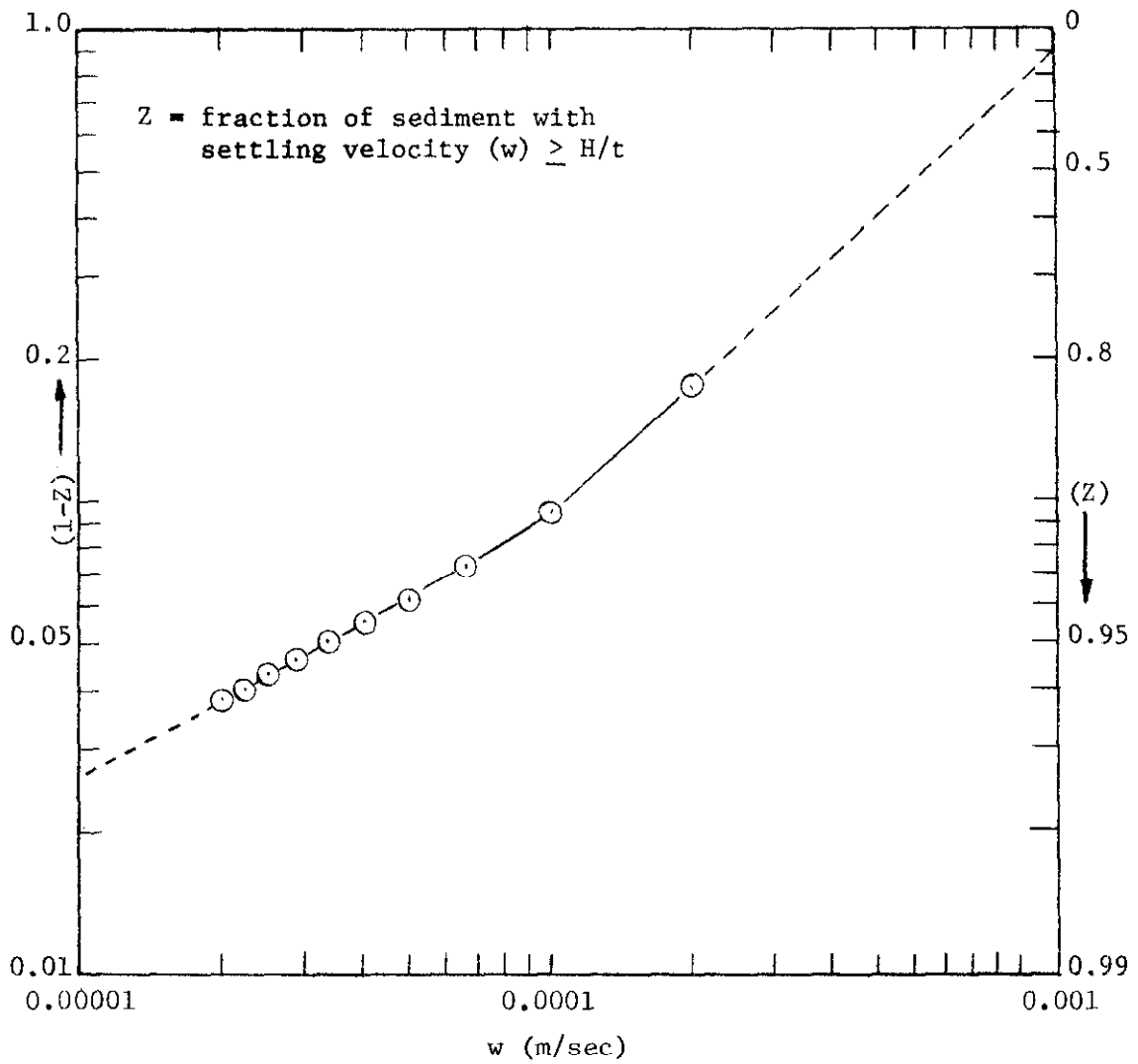


FIGURE 20. CUMULATIVE SETTLING-VELOCITY DISTRIBUTION FOR MOBILE BAY SEDIMENT

20). After 10 min of settling, the turbidity reaches 9.5% of the initial value. The cumulative fraction of the initial material which has settled beyond the light probe at this time is 0.905, and this fraction has settling velocity $w \geq 1 \times 10^{-4}$ m/sec. This process is continued until at least 95-98% turbidity reduction or 2 hr of settling has been accounted for.

168. From the cumulative distribution curve a table of settling-velocity fractions is created, as in Table 7. The distribution curve is divided into a number of segments, each representing a weight fraction of the sediment. For each weight fraction, the settling velocity corresponding to the mean value of Z for that segment is determined by reading directly from the cumulative distribution curve. For example, for the first 20% weight fraction of the sediment, the mean value of Z is 0.1, and the corresponding settling velocity is 124×10^{-5} m/sec. The mean value of Z for the next 10% fraction is 0.25, and this fraction has a mean settling velocity of 100×10^{-5} m/sec. Thus, the mean settling velocities for this example correspond to the times when the cumulative % settled was 10%, 25%, 35%, ..., 92.5%, and 97.5%. The exact intervals used for this procedure are arbitrary, but should be chosen to provide more sediment fractions with low settling velocities than with high settling velocities.

169. With the simplification developed in the preceding paragraphs, the settling term in Equation 22 can be written $w \partial c / \partial y$, with the understanding that the resulting equation,

$$U \frac{\partial c}{\partial x} + w \frac{\partial c}{\partial y} - \frac{\partial}{\partial y} (E_y \frac{\partial c}{\partial y}) - \frac{\partial}{\partial z} (E_z \frac{\partial c}{\partial z}) = 0 \quad (23)$$

is to be solved for each settling-velocity fraction in the sediment, with the appropriate settling velocity (w_i) and initial concentration (c_o)_i for that sediment fraction. All other terms will remain the same, i.e., U, E_y, and E_z. The profile of total suspended sediment concentration is obtained by adding the concentration profiles for the ten (or more) sediment fractions.

Table 7
Settling-Velocity Distribution

<u>Weight Fraction</u>	<u>Mean Z</u>	<u>Settling Velocity (m/sec)</u>
First 20% settled	0.1	124 x 10 ⁻⁵
Next 10% settled	0.25	100
Next 10% settled	0.35	86
Next 10% settled	0.45	73
Next 10% settled	0.55	58
Next 10% settled	0.65	45
Next 10% settled	0.75	30
Next 5% settled	0.825	20
Next 5% settled	0.875	14
Next 5% settled	0.925	7.1
Next 5% settled	0.975	0.95

Numerical Solution of the Material Balance Equation

Geometry and boundary conditions

170. A steady, uniform, infinitely wide flow is assumed with a vertical line source of suspended sediment extending from the surface to the bottom, continuously emitting sediment at a given strength per unit height. This source strength can be converted to an initial concentration by assuming that this sediment is initially concentrated into a vertical column of width b , which is small relative to the depth, h . (A point source located at or below the surface could also be modeled.) The upstream boundary condition is therefore $c = c_0$ at $x = 0$, $|z| \leq b$, $y \leq h$.

171. Physically, the boundary condition at the surface should specify that there is no net flux of sediment across the surface. The best way to specify this is

$$E_y \frac{\partial c}{\partial y} + wc = 0 \quad (24)$$

which means that at a level just below the surface the upward flux due to vertical diffusion is just balanced by downward flux due to settling.

172. For simplicity, it is assumed that all the sediment reaching the bottom is deposited and that there is no reentrainment. The bottom boundary condition is then

$$E_y \frac{\partial c}{\partial y} = 0 \quad (25)$$

which means that all the sediment supplied to a layer just above the bottom by settling is deposited rather than re-mixed upward.

Numerical solution

173. Equation 23 has been solved numerically under the boundary conditions given above by a finite difference method.²⁷ The calculation begins with a given initial concentration at the open-water disposal site, which is located at $x = 0$ and lies between lateral limits $z = -b$ and $z = b$; the initial concentration may vary with the depth y . The calculation proceeds step by step downstream; over each step Δx , a

finite difference model of the equation is used to compute the concentrations at the end of the step from the concentrations at the start; the boundary conditions on the top and bottom surfaces enter at each step to give a well-defined algorithm. Two aspects of this algorithm deserve particular mention.

174. First, the finite difference model, as well as the relation between Δx and the vertical meshwidth Δy , must be chosen in such a way that stability is preserved as the calculation progresses. In other words, instabilities of a purely numerical origin must be excluded. For that purpose an implicit system was selected, representing the diffusion term $\partial/\partial x (E_x \partial c/\partial x)$ by finite differences at the new stage $x + \Delta x$ rather than at the given stage x . This allows Δx to be large enough for an efficient algorithm; otherwise the stability requirement would force an extremely small Δx and would require a tremendous number of steps to move the calculation downstream. The implicit system requires the solution of N coupled equations at each step; $N = H/\Delta y$ is the number of levels in the vertical direction, and the system can be solved quite inexpensively.

175. Second, it was possible to distinguish separately the effect of lateral diffusion and to make use of the analytical solution for the diffusion equation in combination with the numerical solution described above. A pure lateral diffusion would be described by

$$\frac{\partial}{\partial x} (uC) = \frac{\partial}{\partial z} \left(E_z \frac{\partial C}{\partial z} \right) \quad (26)$$

where C represents the concentration for the two-dimensional (x, z) problem, and the boundary condition $c = c_0$ at $x = 0$, $-b \leq z \leq b$ is satisfied. The solution to this reduced equation is given by

$$C(x, z) = \left(\frac{4\pi x E_z}{u} \right)^{-1/2} \int_{-b}^b \exp \left[-\frac{(z-v)^2 u}{4x E_z} \right] dv \quad (27)$$

A change of variables connects this to the "error function" (erf) which

is available in an IBM subroutine. This is possible for a fixed E_z , and experimental data indicate that the lateral diffusion coefficient is indeed fairly constant except near the bottom surface; fortunately concentrations near that surface are much less important to predict and have a negligible effect on values near the top.

176. To use this analytical result in the solution of the full three-dimensional equation, the equation is written symbolically as

$$u \frac{\partial c}{\partial x} = (L_y + L_z) c \quad (28)$$

where L_z represents the lateral diffusion ($E_z \partial^2 / \partial z^2$), and L_y represents the sedimentation and vertical diffusion. Keeping $C(x,z)$ for the analytical solution described above and writing $C'(x,y)$ for the solution of the two-dimensional problem which ignores L_z , the required solution (after matching the initial conditions) is

$$c(x,y,z) = C(x,z) C'(x,y) \quad (29)$$

It is easy to verify that this satisfies the equation:

$$u \frac{\partial c}{\partial x} = \frac{\partial C}{\partial x} C' + uC \frac{\partial C'}{\partial x} = E \frac{\partial^2 C}{\partial z^2} C' + C(L_y C') = (L_y + L_z) c \quad (30)$$

because L_y and L_z affect only C' and C , respectively. Therefore, it is possible to compute $C(x,z)$ analytically and $C'(x,y)$ numerically and to combine these two results to obtain a good numerical approximation to the full three-dimensional concentration field $c(x,y,z)$.

Computer Program and Sample Calculation

177. A FORTRAN IV computer program was written to perform the calculations described above (see Appendix G for details on program use). As inputs to the program, current velocity, stream depth, settling-velocity distribution (given as any number of sediment fractions, each

with a particular concentration and fall velocity), and three computational parameters must be specified. The program output consists of four parts: (1) a section showing the vertical distribution of sediment downstream for each sediment fraction (in the absence of lateral spreading); (2) the summation of vertical slices for all sediment fractions; (3) the lateral spreading coefficients; and (4) five horizontal slices through the full three-dimensional plume at pre-selected depths. A sample calculation and comparison with turbidity plumes observed in Mobile Bay are presented below.

Mobile Bay observations

178. May¹⁷ described numerous turbidity plumes resulting from shell dredging and channel dredging in Mobile Bay. Unfortunately, many of the plumes were subjected to high winds, shifting currents, or other complexities, and in some cases the data are simply too sparse or scattered to make comparison with predicted plumes worthwhile. May's observations of shell dredging on 13 October 1972 provide the best basis for comparison with the model predictions. These data consist of turbidity measurements (by light scattering, in JTU) at a depth of 5 feet (1.5 m) to a distance of about 5000 feet (1500 m) down current from the discharge. Winds were light and, although the current was not given, it was said to be near low tide at the time of sampling. A current velocity of 0.1 or 0.2 m/sec (0.2 or 0.4 knot) was assumed. May also states that the background turbidity was quite low and the plume was visible for a total distance of about 10,000 feet (3000 m).

Plume model calculation

179. Jar-test data for sediment collected in Mobile Bay during this study were used to derive the settling-velocity distribution input into the computer program. The data obtained in tests at 5 g/l initial sediment concentration in 5 g/l sea salt solution were felt to be most applicable to the observed conditions. Although salinity was not specified on 13 October 1972, other observations were in the range of 2-12 ppt (g/l). The initial sediment concentration is also uncertain, but 5 g/l is probably a realistic value.

180. The derivation of a settling-velocity distribution from the appropriate jar-test data was given previously (see paragraphs 167-168). The 11 sediment fractions shown in Table 7 were input into the computer program, along with the water depth, 3m, and current velocity.

181. The program first uses the numerical solution method to calculate two-dimensional (downstream-vertical) profiles for each sediment fraction. An example is shown in Figure 21. The 11 profiles were then summed to give the complete two-dimensional concentration profile, shown in Figure 22. This gives the hypothetical downstream concentration in the absence of any lateral spreading.

182. Several interesting features can be noted from this figure. First, at 1600 m downstream, more than 12% of the initial material is still in suspension at the surface, although much of this will have dispersed laterally. Second, the presence of this material at the surface is due to the effects of eddy diffusion upward. For simple gravity settling (i.e., no upward diffusion), all suspended material would have settled past the 0.15-m depth at 1600 m downstream, based on the settling rate of the slowest settling fraction and the input current velocity.

183. The computer program next calculates lateral spreading factors using the analytical solution described in paragraph 175. These factors, shown in Figure 23, are then applied to the vertical concentration profile, and the three-dimensional plume is output as horizontal sections at specified depths. The surface concentration distribution for the present case is displayed in Figure 24.

Comparison of observed and predicted plumes

184. The predicted and observed downstream concentration profiles for the 13 October 1972 data are compared in Figure 25. Here the center-line concentration (% of c_0) for the model plume at a depth of 1.5 m (interpolated from output depths of 1.2 m and 1.8 m) is shown for current velocities of 0.1 and 0.2 m/sec. The field data display much variability indicative of migration, or meandering of the natural plume. To account for this, the observed center-line concentrations shown in Figure 25 were taken to be the highest values at each distance downstream from the discharge (see Figure 6 in May's report¹⁷). These also

INPUTS:U=	THETA=1.00 XL= 0.50										Distance Downstream (m)	
	0.10	100.0	200.0	300.0	400.0	500.0	600.0	700.0	800.0	900.0		
0.0	0.0	0.0	0.0	0.0	0.0	0.0	0.0	0.0	0.0	0.0	0.0	0.0
0.15	4.59	4.53	4.43	4.31	4.20	4.10	4.00	3.90	3.80	3.71	3.62	3.53
0.30	4.70	4.54	4.42	4.30	4.20	4.10	4.00	3.90	3.80	3.71	3.62	3.53
0.45	4.76	4.60	4.48	4.37	4.26	4.16	4.05	3.96	3.86	3.77	3.67	3.58
0.60	4.80	4.63	4.53	4.41	4.30	4.20	4.10	4.00	3.90	3.81	3.71	3.62
0.75	4.85	4.69	4.59	4.48	4.37	4.26	4.16	4.06	3.96	3.86	3.77	3.68
1.00	4.87	4.74	4.62	4.50	4.39	4.29	4.18	4.08	3.98	3.88	3.79	3.70
1.25	4.89	4.76	4.64	4.53	4.42	4.31	4.22	4.12	4.02	3.92	3.83	3.74
1.50	4.91	4.80	4.68	4.56	4.45	4.34	4.24	4.13	4.03	3.94	3.84	3.75
1.75	4.92	4.81	4.69	4.58	4.47	4.36	4.25	4.15	4.05	3.95	3.85	3.76
2.00	4.94	4.83	4.71	4.59	4.48	4.37	4.27	4.16	4.06	3.96	3.87	3.78
2.25	4.95	4.85	4.73	4.61	4.50	4.39	4.29	4.18	4.09	3.99	3.89	3.80
2.50	4.96	4.86	4.75	4.63	4.52	4.41	4.30	4.20	4.11	4.01	3.91	3.81
2.75	4.97	4.87	4.77	4.65	4.54	4.43	4.33	4.22	4.12	4.02	3.92	3.83
3.00	4.97	4.88	4.79	4.67	4.56	4.45	4.35	4.24	4.14	4.04	3.94	3.84
AVG	4.88	4.76	4.65	4.54	4.43	4.32	4.21	4.11	4.01	3.91	3.82	3.72

FIGURE 21. TWO-DIMENSIONAL CONCENTRATION DISTRIBUTION FOR ONE SEDIMENT FRACTION (NO LATERAL SPREADING)

INPUTS:U=	SUMMATION OF SUSPENDED SEDIMENTS										Distance Downstream (m)	
	0.0	100.0	200.0	300.0	400.0	500.0	600.0	700.0	800.0	900.0		
0.0	0.0	0.0	0.0	0.0	0.0	0.0	0.0	0.0	0.0	0.0	0.0	0.0
0.15	44.29	35.68	30.52	26.91	24.18	22.03	20.29	18.84	17.61	16.56	15.65	14.85
0.30	50.63	40.51	33.97	29.52	26.24	23.71	21.69	20.02	18.63	17.45	16.43	15.54
0.45	51.70	41.58	35.04	30.59	27.30	24.77	22.65	20.83	19.35	18.04	16.95	16.00
0.60	52.81	42.69	36.15	31.70	28.41	25.88	23.69	21.85	20.37	19.04	17.94	17.00
0.75	53.92	43.80	37.26	32.81	29.52	26.99	24.80	22.97	21.48	20.14	18.94	18.00
1.00	55.03	44.91	38.37	33.92	30.63	28.10	26.03	24.20	22.71	21.37	20.17	19.20
1.25	56.14	46.02	39.48	35.03	31.74	29.21	27.17	25.34	23.85	22.51	21.31	20.40
1.50	57.25	47.13	40.59	36.14	32.85	30.32	28.28	26.45	24.96	23.62	22.42	21.50
1.75	58.36	48.24	41.70	37.25	33.96	31.43	29.39	27.66	26.17	24.83	23.63	22.70
2.00	59.47	49.35	42.81	38.36	35.07	32.54	30.50	28.77	27.28	25.94	24.74	23.80
2.25	60.58	50.46	43.92	39.47	36.18	33.65	31.61	29.88	28.39	27.05	25.85	24.90
2.50	61.69	51.57	45.03	40.58	37.29	34.76	32.72	30.99	29.50	28.16	26.96	26.00
2.75	62.80	52.68	46.14	41.69	38.40	35.87	33.79	32.10	30.61	29.27	28.07	27.00
3.00	63.91	53.79	47.25	42.80	39.51	36.98	34.80	33.21	31.72	30.48	29.28	28.00
AVG	55.03	46.56	40.59	36.14	32.85	30.32	28.28	26.45	24.96	23.62	22.42	21.50

FIGURE 22. SUMMATION OF TWO-DIMENSIONAL CONCENTRATION DISTRIBUTIONS FOR ALL SEDIMENT FRACTIONS (NO LATERAL SPREADING)

0.0	1.000	0.462	0.337	0.278	0.242	0.217	0.198	0.184	0.172	0.163	0.154	0.147	0.141	0.136	0.131	0.126	0.122	0.119	0.115
1.00	0.0	0.237	0.236	0.218	0.201	0.187	0.175	0.165	0.157	0.150	0.143	0.138	0.132	0.128	0.124	0.120	0.117	0.114	0.111
2.00	0.0	0.001	0.001	0.031	0.046	0.057	0.065	0.071	0.074	0.077	0.079	0.080	0.080	0.081	0.081	0.080	0.080	0.080	0.079
3.00	0.0	0.000	0.000	0.006	0.013	0.020	0.027	0.034	0.039	0.043	0.047	0.050	0.052	0.054	0.055	0.057	0.058	0.058	0.059
4.00	0.0	0.0	0.000	0.001	0.002	0.005	0.009	0.013	0.017	0.020	0.024	0.027	0.030	0.032	0.034	0.036	0.038	0.039	0.041
5.00	0.0	0.0	0.000	0.000	0.000	0.001	0.002	0.004	0.006	0.008	0.010	0.013	0.015	0.017	0.019	0.021	0.023	0.024	0.026
6.00	0.0	0.0	0.000	0.000	0.000	0.000	0.000	0.001	0.002	0.003	0.004	0.005	0.007	0.008	0.009	0.011	0.012	0.014	0.015
7.00	0.0	0.0	0.0	0.000	0.000	0.000	0.000	0.000	0.000	0.001	0.001	0.002	0.003	0.003	0.004	0.005	0.006	0.007	0.008
8.00	0.0	0.0	0.0	0.0	0.000	0.000	0.000	0.000	0.000	0.000	0.000	0.000	0.001	0.001	0.002	0.002	0.003	0.003	0.004
9.00	0.0	0.0	0.0	0.0	0.0	0.000	0.000	0.000	0.000	0.000	0.000	0.000	0.000	0.000	0.001	0.001	0.001	0.001	0.002
10.00	0.0	0.0	0.0	0.0	0.0	0.0	0.000	0.000	0.000	0.000	0.000	0.000	0.000	0.000	0.000	0.000	0.000	0.000	0.001
11.00	0.0	0.0	0.0	0.0	0.0	0.0	0.0	0.0	0.0	0.000	0.000	0.000	0.000	0.000	0.000	0.000	0.000	0.000	0.000
12.00	0.0	0.0	0.0	0.0	0.0	0.0	0.0	0.0	0.0	0.000	0.000	0.000	0.000	0.000	0.000	0.000	0.000	0.000	0.000
13.00	0.0	0.0	0.0	0.0	0.0	0.0	0.0	0.0	0.0	0.000	0.000	0.000	0.000	0.000	0.000	0.000	0.000	0.000	0.000
14.00	0.0	0.0	0.0	0.0	0.0	0.0	0.0	0.0	0.0	0.000	0.000	0.000	0.000	0.000	0.000	0.000	0.000	0.000	0.000
15.00	0.0	0.0	0.0	0.0	0.0	0.0	0.0	0.0	0.0	0.0	0.0	0.000	0.000	0.000	0.000	0.000	0.000	0.000	0.000
16.00	0.0	0.0	0.0	0.0	0.0	0.0	0.0	0.0	0.0	0.0	0.0	0.0	0.0	0.0	0.000	0.000	0.000	0.000	0.000
17.00	0.0	0.0	0.0	0.0	0.0	0.0	0.0	0.0	0.0	0.0	0.0	0.0	0.0	0.0	0.0	0.000	0.000	0.000	0.000
18.00	0.0	0.0	0.0	0.0	0.0	0.0	0.0	0.0	0.0	0.0	0.0	0.0	0.0	0.0	0.0	0.0	0.000	0.000	0.000
19.00	0.0	0.0	0.0	0.0	0.0	0.0	0.0	0.0	0.0	0.0	0.0	0.0	0.0	0.0	0.0	0.0	0.0	0.0	0.000
20.00	0.0	0.0	0.0	0.0	0.0	0.0	0.0	0.0	0.0	0.0	0.0	0.0	0.0	0.0	0.0	0.0	0.0	0.0	0.000

Distance Downstream \longrightarrow

FIGURE 23. TABLE OF LATERAL SPREADING FACTORS

DISTRIBUTION OF SEDIMENT IN HORIZONTAL PLANE AT DEPTH 0.0 (PARTS PER HUNDRED THOUSAND)

Depth (m)	100.0	200.0	300.0	400.0	500.0	600.0	700.0	800.0	900.0	01000.0	01100.0	01200.0	01300.0	01400.0	01500.0	01600.0	01700.0	01800.0
20.00	0	0	0	0	0	0	0	0	0	0	0	0	0	0	0	0	0	0
19.00	0	0	0	0	0	0	0	0	0	0	0	0	0	0	0	0	0	0
18.00	0	0	0	0	0	0	0	0	0	0	0	0	0	0	0	0	0	0
17.00	0	0	0	0	0	0	0	0	0	0	0	0	0	0	0	0	0	0
16.00	0	0	0	0	0	0	0	0	0	0	0	0	0	0	0	0	0	0
15.00	0	0	0	0	0	0	0	0	0	0	0	0	0	0	0	0	0	0
14.00	0	0	0	0	0	0	0	0	0	0	0	0	0	0	0	0	0	0
13.00	0	0	0	0	0	0	0	0	0	0	0	0	0	0	0	0	0	0
12.00	0	0	0	0	0	0	0	0	0	0	0	0	0	0	0	0	0	0
11.00	0	0	0	0	0	0	0	0	0	0	0	0	0	0	0	0	0	0
10.00	0	0	0	0	0	0	0	0	0	0	0	0	0	0	0	0	0	0
9.00	0	0	0	0	0	0	0	0	0	0	0	0	0	0	0	0	0	0
8.00	0	0	0	0	0	0	0	0	0	0	0	0	0	0	0	0	0	0
7.00	0	0	0	0	0	0	0	0	0	0	0	0	0	0	0	0	0	0
6.00	0	0	0	0	0	0	0	0	0	0	0	0	0	0	0	0	0	0
5.00	0	0	0	0	0	0	0	0	0	0	0	0	0	0	0	0	0	0
4.00	0	0	0	0	0	0	0	0	0	0	0	0	0	0	0	0	0	0
3.00	0	0	0	0	0	0	0	0	0	0	0	0	0	0	0	0	0	0
2.00	0	0	0	0	0	0	0	0	0	0	0	0	0	0	0	0	0	0
1.00	0	0	0	0	0	0	0	0	0	0	0	0	0	0	0	0	0	0
0.00	10000	0	0	0	0	0	0	0	0	0	0	0	0	0	0	0	0	0

0.0 100.0 200.0 300.0 400.0 500.0 600.0 700.0 800.0 900.0 01000.0 01100.0 01200.0 01300.0 01400.0 01500.0 01600.0 01700.0 01800.0

Distance Downstream (m)

FIGURE 24. SURFACE CONCENTRATION DISTRIBUTION

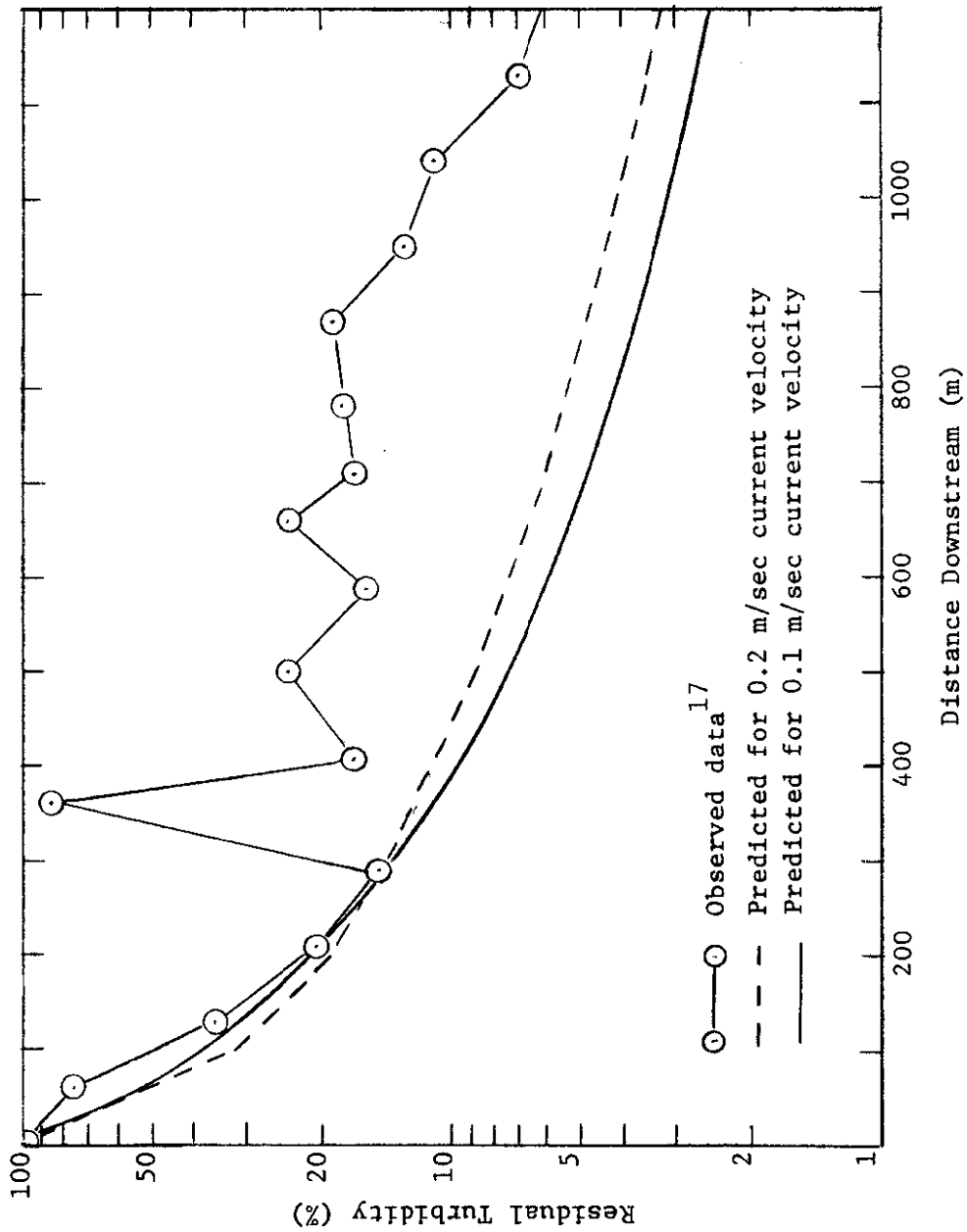


FIGURE 25. COMPARISON OF PREDICTED AND OBSERVED CENTER-LINE CONCENTRATIONS FOR MOBILE BAY TURBIDITY PLUMES

are expressed as the percentage of the initial turbidity (value closest to the discharge).

185. The field observations and model predictions compare favorably for the first 300 m (or first 80-85% reduction in turbidity). Subsequently, however, a sudden increase in turbidity level is found. According to May¹⁷ (p. 31), this was "possibly due to disturbance by a passing boat." It appears that stations farther downstream were likewise affected by this disturbance. However, the decay of the natural plume beyond this disturbance is not unlike that of the model prediction, suggesting that the model does provide a reasonable approximation of the turbidity reduction. If one were to renormalize the observed turbidity at 500 m to match that of the model at this distance, the curves downstream from this point would agree fairly well.

186. No attempt has been made to compare the model's prediction of lateral spreading with that of the observed plume. In the models calculated here, the initial width of the discharge is only 1 m. Positive levels of turbidity are predicted to reach about 10-15 m to either side of the centerline at 1800 m downstream. However, real discharges may be spread quite rapidly by turbulence near the source. Subsequent diffusive spreading is likely to be much less rapid and may approximate that predicted by the plume model. However, further testing is required to evaluate this aspect of the model.

187. Discharges from shell dredging on 30 September 1971 and 21 January 1972 described by May were also modeled with the computer program. The field data were not considered suitable for a quantitative comparison with the model predictions, but a qualitative evaluation can be made. The models indicate reductions of at least 90% of the initial turbidity within the first few hundred meters, which is in agreement with the field observations. It should be noted that "initial turbidity" refers to the turbidity at a point somewhat downstream from the actual discharge, after bulk settling of the relatively high-density slurry has occurred and concentrations on the order of 1 to 5 g/l are found. May notes that this generally occurs within about 100-200 feet (30-60 m) of the discharge.

Other results of plume modeling

188. Several interesting observations were made in the course of plume modeling which bear on the evolution of turbidity plumes and the applicability of the model to dredging situations. These were the result of testing the effects of varying the initial concentration profile, the input settling-velocity distribution, and the current velocity.

189. The source configuration used to model the discharge from a hydraulic pipeline dredge assumes essentially instantaneous bulk settling of much of the relatively high-solids-content, high-density slurry, creating a vertical column as the apparent source. Since the source is programmed as a series of cells, each with its own initial concentration, in practice the source geometry and strength can be varied, and the program could also be used to model the dispersion from a point source (at any depth) or a discontinuous line source. Two different initial vertical concentration profiles were used in the models studied for Mobile Bay turbidity plumes. The first configuration held concentration constant from surface to bottom at the source. The second was an exponentially increasing concentration profile which yielded a bottom concentration twice that of the surface. In all models, there was very little difference in the center-line concentrations beyond a few hundred meters downstream, regardless of the initial source profile.

190. Apparently, removal of the rapid settling components and upward diffusion of the slowest settling components result in the establishment of a quasi-equilibrium independent of the initial source profile. Downstream vertical profiles display similar increasing concentration with depth, due to settling, for both types of input source profiles.

191. A second significant feature of the modeling studies is that the use of different settling curves as input to the program has a major effect on downstream concentrations. Settling-velocity distributions for the Illinois River and Boston Harbor sediments were input in order to examine the variation in turbidity plumes which might

be expected for a broad range of dredged sediments discharged under identical conditions. The jar-test curves chosen were those obtained at 5 g/l sediment concentration in 0.5% sea salt, where the Illinois River sediment was the slowest settling and Boston Harbor was the fastest settling (except for Charles River, a rather unusual sediment). In addition, a model was run where a hypothetical "zero-settling" sediment was used as input to simulate the limiting case of a slowly settling sediment. This probably gives a reasonable approximation of the behavior of dredged sediment discharged in fresh waters, where flocculation is negligible. It is therefore useful in comparing the extent of possible turbidity problems in freshwater and saltwater disposal areas and in demonstrating the effect of lateral spreading alone on turbidity reduction. All models were run with a depth of 3 m and current velocities of 0.1 and 0.2 m/sec, the same parameters used for the Mobile Bay models.

192. Surface concentrations down the center line of the computer-generated plumes (e.g., Figure 24) are shown in Figure 26. The distance to achieve a 90% reduction in turbidity is more than three times as large for the Illinois River sediment as for Boston Harbor sediment at 0.1 m/sec current velocity. For the case of zero settling, the distance to 90% reduction is about seven times that for the Boston Harbor sediment. At the higher current velocity, these differences are somewhat less. Thus, significant differences can be expected in downstream turbidity levels for various sediments discharged under similar conditions.

193. Figures 25 and 26 also indicate that, at least under certain conditions, the current velocity may have a relatively small effect on downstream center-line turbidities. For both Mobile Bay and Illinois River sediments, doubling the current velocity has only a minor effect on the predicted turbidities. It can also be seen that for slow settling velocities, the downstream concentrations can be greater for low current velocity (0.1 m/sec) than for higher current velocity (0.2 m/sec), the reverse of the situation for high settling velocities. This trend reflects the interrelation between current velocity and lateral diffusivity (Equation 20). For slowly settling sediments, the

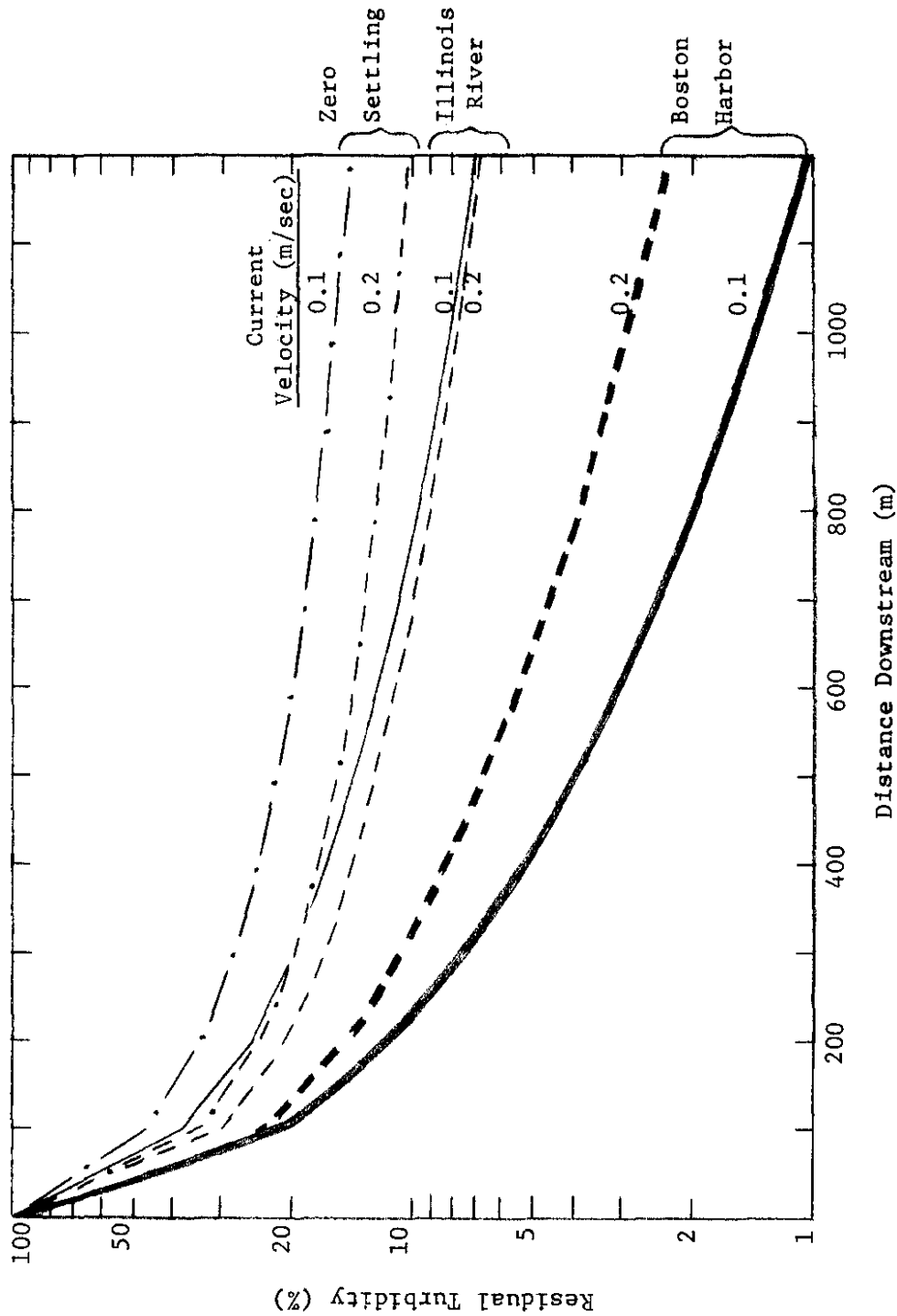


FIGURE 26. PREDICTED CENTER-LINE TURBIDITIES AT THE SURFACE FOR THREE DIFFERENT SETTLING CURVES AT TWO CURRENT VELOCITIES

turbidity reduction is controlled by the lateral diffusion of suspended sediment (a function of current velocity), whereas downward settling and downstream advective transport are the controlling factors for rapidly settling (flocculent) sediments.

194. These results provide a preliminary indication of the relative importance of sediment and hydrologic parameters on turbidity plumes. Further study is required to determine the full range of plumes predicted for a variety of simulated field situations.

Validity of plume model

195. The comparison presented above of observed and predicted turbidity plumes suggests that the model developed under this program may be effective in predicting the extent of dredging-related turbidity problems. Although the assessment of the model's validity has been only preliminary in nature, the essential features of plume evolution (as observed in Mobile Bay) are evident in the computer predictions. The rapid decrease in turbidity near the discharge is followed by a more extended plume at low suspended solids concentrations. The model thus appears to account for the rapid settling of larger particles and/or flocs in the suspended sediment while simulating the slower settling and diffusive transport of smaller particles. This feature indicates that use of jar-test data is reasonable in modeling turbidity plumes.

196. Of course it must be recognized that many uncertainties exist in the application of jar-test data from the present study to the plumes described by May. The nature of the sediment may have been different from that encountered during May's investigation, and no attempt was made to accurately model the concentration of the actual discharge. Still, the results are encouraging and suggest that further verification studies would be worthwhile.

197. Extensive field investigations are required to test the applicability of this model to a variety of dredging conditions. Jar-test data must be obtained for sediment at sites where detailed recording of turbidity plumes is accomplished. Jar tests should be run in actual samples of the receiving water at each site. Of particular importance is the study of the nature of the discharge zone so that jar

tests can be run using realistic concentrations of suspended sediments. In addition, computer-generated models should account for the actual width of the discharge zone to test the model's ability to simulate lateral spreading.

198. The computer models studied here indicate that the settling properties of suspended sediments have a major effect on the predicted extent of turbidity. One approach to verifying this conclusion would be to conduct laboratory flume studies in conjunction with settling-velocity determinations. The appropriateness of the plume model could thus be determined under controlled conditions.

199. Evaluation of the usefulness of this model to field application depends upon whether the underlying assumptions used in its derivation are appropriate to most dredge discharges. Factors such as variability in the nature of the material discharged, configuration of the discharge, current patterns, bottom profiles, and winds may in many cases be important in determining turbidity plumes. Careful field observations must be made and compared with computer predictions to finally determine the extent to which this model can be applied as a predictive tool.

PART VI: APPLICATIONS TO FIELD USE

200. The methods utilized in this study to characterize the settling behavior of suspended sediments can be applied to field use as a means of predicting the extent and duration of turbidity resulting from dredging operations. Turbidity is a function of sediment and water compositional parameters as well as the hydrologic features at particular dredging sites. In the statistical analyses, it was shown that water salinity, sediment organics content, and initial sediment concentration were major significant factors affecting settling rates. However, the range in water compositions encountered in actual dredging operations varies over a much wider range than that which could be considered here. Furthermore, the effects of sediment and water compositional characteristics appear to be highly complex and cannot be specified with adequate precision by simple linear models. It is therefore suggested that the most appropriate means for predicting the turbidity generation potential of dredged sediments is to perform jar tests on a slurried sample of the actual sediment to be dredged in its receiving water. The jar tests will result in the derivation of a settling rate for the sediment-water combination, which can then be used as input to the turbidity plume computer program. The final output provides an estimate of the expected turbidity levels downstream from the discharge point. The recommended procedures for obtaining the necessary information are described in the following sections. The reader is cautioned that these procedures are based only upon laboratory experimentation and must be field-tested before being applied.

Sediment and Water Sampling

201. Bottom sediments can be sampled by a variety of means. Where dredging is limited to removal of relatively homogeneous recently shoaled material, a grab sample should provide adequate sampling of the sediment to be tested. For soft bottoms in quiescent waters, an Ekman-type sampler is sufficient, but where strong currents exist and/or the

bottom sediment is more consolidated, the heavier Petersen-type grab may be required. If a new dredge cut is to be made into possibly inhomogeneous older sediment, a coring-type sampler should be considered so that the variation in sediment type can be adequately sampled. In any case, several samples should be obtained from a particular area and composited to form a representative site sample. A few liters of sediment is more than enough to perform the necessary tests.

202. Sediment samples should always be kept refrigerated to minimize degradation of the organic matter. In the field this is best accomplished by packing the sediment in an insulated container with ice. Care should be taken to ensure that the samples are not frozen, since freezing can change the settling properties measured in jar tests. Dry ice should not be used as a refrigerant, as this may result in freezing of the sediments.

203. If any rocks, shells, or fibrous plant matter are present, these must be removed by wet sieving. Although such materials are often included in dredged sediments, they tend to have a negligible effect on turbidity, and they do interfere with laboratory testing procedures. It is therefore preferable that they be eliminated. An 18- or 20-mesh sieve (sieve opening \approx 1 mm) provides a reasonable screening of unwanted material. Thorough mixing of individual samples or composite samples is essential in the preparation of sediments for turbidity testing. The moisture content of the sediment must be determined in order to express measurements on a dry weight basis. This is done by drying a pre-weighed sample of wet sediment (1-5 g wet weight) in an oven at 105°C for about 2 hr. The moisture content is then calculated as follows:

$$\% \text{ moisture} = \frac{\text{wet weight} - \text{dry weight}}{\text{wet weight}} \times 100 \quad (31)$$

Any weight of wet sediment can be expressed on a dry weight basis through the following conversion:

$$\text{dry weight} = \text{wet weight} \times \left(1 - \frac{\% \text{ moisture}}{100}\right) \quad (31a)$$

204. In lakes and rivers, surface waters can be sampled adequately with a clean bucket. However, in estuaries it is necessary to sample the water column at two or more depths since salinities can be quite variable. For this purpose, Van Dorn or Kemmerer-type bottles are satisfactory.

Jar-Test Procedures

205. The recommended procedure for performing jar tests consists of first dispersing the test sediment in the disposal site water during a 30-min rapid-mix period, followed by monitoring of the light transmission of the suspension as settling occurs. Although systems other than that described in this report can be utilized, the measurement of light transmission using fixed light probes is both convenient and experimentally desirable. This is because light transmission provides a better correlation with suspended solids than does light scattering.

206. In performing the light transmission measurement, the system must be calibrated to read 100% transmission in pure water. This can be done by either a meter adjustment or by calculation of a calibration factor for each jar. Wet sediment (weight calculated to give the desired dry weight) is added to the test water and the suspension is stirred rapidly (≥ 100 rpm) for 30 min. The weight of sediment chosen for testing is important, since the initial concentration appears to have a significant effect on the settling rate. The maximum concentration measurable depends upon the optical characteristics of the particular system but will likely be in the range of a few grams per liter. This is similar to concentrations likely to be found within a few hundred yards of a typical dredge discharge point. Since the effect of increasing concentration appears to be more rapid settling, data obtained at 1 g/l or 5 g/l concentration can be considered to provide minimum settling rates. At higher initial concentrations, settling could be more rapid but is unlikely to be less rapid.

207. After 30 min of rapid stirring, initial turbidity readings are taken, and the slow-stirring phase is begun. Transmission readings are converted to attenuation coefficients according to the following formula:

$$\alpha = \frac{\ln (100/T)}{L} \quad (32)$$

where T is the light transmission (in %); L is the light path length (in m); and α is expressed in units of $[m^{-1}]$. Transmission readings should be taken at one min, three min, five min, and then at five-min intervals until either 95% reduction from α_0 has been achieved, or two hr has passed. A plot of α vs. time is then prepared for each jar test.

Turbidity Plume Modeling

208. Predicted turbidity plumes can be generated from jar-test data following the procedures outlined in Part V and using the computer program described in Appendix G. Jar-test data are first converted to a settling-velocity distribution (see para. 167) for the dredged sediment dispersed in its receiving water. This distribution is then input into the computer program along with the channel depth and current velocity. The program output includes horizontal sections at several depths through the plume which can be evaluated to estimate the extent of downstream turbidity problems.

209. In order to adequately model the potential turbidity problems at a dredging site, it is recommended that a number of different models be run. Input data resulting from several jar tests, possibly using several different sediment samples from a particular area and two or more initial concentrations, should be used to account for variability in sediment characteristics and slurry concentrations. A range of initial discharge configurations, depths, and current velocities might also be run to determine the limits on estimated turbidity plumes for a given field situation.

210. If the range of sites likely to require modeling can be adequately specified, typical plumes can be modeled and the data reduced to a series of graphic displays. A separate series of graphs might be prepared for each concentration contour desired, e.g., 0.01, 0.1, and 1 g/l of suspended sediment above background levels. Such a series of graphs would be patterned after a similar series for atmospheric diffusion estimates.³³ Since a range of non-zero fall velocities is encountered in turbidity plume calculations, the dispersion estimate procedure is complex relative to the case of atmospheric diffusion, where the assumption of zero fall velocity is appropriate. It would therefore be necessary to clearly define the range of conditions of most interest, calculate typical turbidity plumes, and then decide on the best scheme for graphical presentation of the results.

Conclusions

211. The turbidity resulting from open-water discharges of dredged material is dependent upon many factors. These include both physical parameters such as current velocity, winds, discharge configuration, and solids concentration of the slurry and physicochemical properties of colloidal suspensions which affect the settling rates of fine particles dispersed in water. Laboratory jar testing of three clays and eight natural sediments in a variety of waters has confirmed that the settling rates of dredged material discharged in different waters around the country can be expected to vary widely as a result of sediment and water compositional characteristics. A turbidity plume model which accounts for sediment settling rates as well as hydrologic factors was developed and has shown that these variable settling rates can lead to major differences in the extent of turbidity downstream from dredge discharges.

212. Settling rates of suspended sediments were found to vary strongly with the composition of waters in which they were dispersed. Turbidity was extremely persistent in soft fresh waters, but hardness levels typical of natural fresh waters (200 mg/l of dissolved solids) led to a small increase in the rate of turbidity reduction. Low levels of salinity (1-5 ppt) were sufficient to induce flocculation and consequent rapid turbidity reduction. The pH of the test solutions had no effect on observed turbidities.

213. The three clays and eight natural sediments tested also displayed a wide range in responses to any particular water type, indicating that settling properties are strongly influenced by sediment composition. The organics content was found to be the predominant compositional factor affecting the settling rates of natural sediments, with higher organics levels responsible for more rapid turbidity reduction. Clay mineralogy was not found to have an important effect. Although the behavior of montmorillonite was quite distinct from that

of illite and kaolinite in tests with pure clays, no such dependence on clay type was apparent for the natural sediments. This suggests that experiments with clays are not particularly useful for modeling natural sediment systems.

214. The initial sediment concentration also had a major effect on settling rates. Higher initial concentrations led to more rapid turbidity reduction in the range studied (1-5 g/l). This may be due to the increased rate of interparticle collisions in the more concentrated suspensions or to the effect of increased concentration of dissolved organic matter originating in the sediment. It is difficult to extrapolate this finding to field situations, where concentrations in discharged slurries may be substantially higher and extremely variable. Further study is needed to resolve this problem.

215. Experiments designed to define the nature of turbidity indicated that no significant segregation of sediment components took place as settling proceeded, with the exception of the independent settling of coarse silt particles. This finding suggests that clay-organic aggregates may be formed when sediment suspensions are destabilized by saline (or hard) waters. Together with other results, this indicates the importance of sediment organics in determining the settling properties of discharged dredged material.

216. The wide variation in settling rates expected to be found for dredged material discharged under different conditions makes it imperative that settling properties be accounted for when predicting the extent of possible turbidity problems. However, simple linear models relating settling rates to sediment and water compositional factors are inadequate to accurately model these properties. Therefore, it is necessary to determine the settling velocities individually for dredged sediments dispersed in their receiving waters, using laboratory jar tests or other similar procedures.

217. The predictive model developed during this investigation utilizes jar-test data as input and thus implicitly accounts for flocculation of suspended sediments. Preliminary testing indicates that the model predictions compare favorably with the limited amount of

field data available. Furthermore, the results suggest that the particle settling rates of dredged material suspensions can indeed be a factor of major importance in determining the extent of downstream turbidity.

Recommendations

218. Further study is recommended in several areas to enhance the predictive capability developed under the present program. First, coordinated laboratory and field efforts are required to validate the turbidity plume model. Hydraulic flume studies are recommended to test the reliability of the model under well-controlled laboratory conditions. In addition, jar tests with actual dredged sediments and receiving waters should be run concurrently with detailed field observations of turbidity plumes at several dredging sites. Comparison of predicted and observed plumes in this way is required to determine the practical applicability of the model. Also, study of the turbidity predictions generated by the model under a wider range of input conditions would be useful and might lead to the development of graphical methods for field application.

219. Second, further development of the jar-test method is recommended to optimize its practical use in turbidity prediction. The potential use of simplified apparatus and test procedures should be examined to determine the simplest method capable of producing accurate and reproducible settling data.

220. Third, further basic research on the factors controlling turbidity would be valuable. In particular, the effects of various organic materials and clay-organic interactions need to be studied to determine more precisely the dependence of turbidity on the composition of dredged material. A more complex test plan and statistical techniques should be applied to determine functional relationships between turbidity reduction and sediment-water components.

221. Finally, based upon the above studies, a field manual for use by Corps personnel can be developed. Such a manual would reflect

the experience gained by this and future programs to provide the most practical and reliable means of predicting the extent of dredging-related turbidity.

REFERENCES

1. Black, A. P. and Vilaret, M. R., "Effect of Particle Size on Turbidity Removal," Journal of the American Water Works Association, Vol. 61, No. 4, 1969, pp. 209-214.
2. Hahn, H. H. and Stumm, W., "The Role of Coagulation in Natural Waters," American Journal of Science, Vol. 268, 1970, pp. 354-368.
3. Edzwald, J. K., Upchurch, J. B., and O'Melia, C. R., "Coagulation in Estuaries," Environmental Science and Technology, Vol. 8, 1974, pp. 58-63.
4. Edzwald, J. K. and O'Melia, C. R., "Clay Distributions in Recent Estuarine Sediments," Clays and Clay Minerals, Vol. 23, 1975, pp. 39-44.
5. Jacobs, M. B. and Ewing, M., "Mineral Source and Transport in Waters of the Gulf of Mexico and Caribbean Sea," Science, Vol. 163, 1969, pp. 805-809.
6. van Olphen, H., An Introduction to Clay Colloid Chemistry, Wiley Interscience Publishers, New York, 1963.
7. Overbeek, J. T. G., "Colloid and Surface Chemistry: Part 2, Lyophobic Colloids," Study Guide, Department of Chemical Engineering and Center for Advanced Engineering Study, Massachusetts Institute of Technology, 1972.
8. Swartzen-Allen, S. L. and Matijevic, E., "Surface and Colloid Chemistry of Clays," Chemical Reviews, Vol. 74, No. 3, 1974.
9. Whitehouse, U. G., Jeffrey, L. M., and Debbrecht, J. D., "Differential Settling Tendencies of Clay Minerals in Saline Waters," Proc. 7th National Conference on Clays and Clay Minerals, 1958, pp. 1-79.
10. Narkis, N., Rebhun, M., and Sperber, H., "Flocculation of Clay Suspensions in the Presence of Humic and Fulvic Acids," Israel Journal of Chemistry, Vol. 6, 1968, pp. 295-305.
11. Neis, U. and Hahn, H. H., "Differential Coagulation of Silica, Clays, and Metal Oxides," Institut für Siedlungswasserwirtschaft, Universität Karlsruhe, Federal Republic of Germany (to be published).
12. Le Bell, J. C., Hurskainen, V. T., and Stenius, P. J., "The Influence of Sodium Lignosulphonates on the Stability of Kaolin Dispersions," (to be published in Journal of Colloid and Interface Science).

13. Krone, R. B., "A Field Study of Flocculation as a Factor in Estuarial Shoaling Processes," Technical Bulletin No. 19, prepared for the Committee on Tidal Hydraulics, Corps of Engineers, U. S. Army, 1972.
14. Birkner, F. B. and Morgan, J. J., "Polymer Flocculation Kinetics of Dilute Colloidal Suspensions," Journal of the American Water Works Association, 1968, pp. 175-191.
15. Etter, R. J. et al., "Depositional Behavior of Kaolinite in Turbulent Flow," Journal of the Hydraulics Division, Proceedings of the American Society of Civil Engineers, 1968, pp. 1439-1452.
16. Weast, R. C., ed., Handbook of Chemistry and Physics, 49th Edition, Chemical Rubber Co., Cleveland, 1968.
17. May, E. B., "Environmental Effects of Hydraulic Dredging in Estuaries," Alabama Marine Resources Bulletin, No. 9, 1973.
18. Douglas, L. A. and Fiessinger, F., "Degradation of Clay Minerals by H₂O₂ Treatments to Oxidize Organic Matter," Clays and Clay Minerals, Vol. 19, 1971, pp. 67-68.
19. McCarthy, J. C., Pyle, T. E., and Griffin, G. M., "Light Transmissivity, Suspended Sediments and the Legal Definition of Turbidity," Estuarine and Coastal Marine Science, Vol. 2, 1974, pp. 291-299.
20. Brown, G., ed., The X-Ray Identification and Crystal Structures of Clay Minerals, Mineralogical Society (Clay Minerals Group), London, 1961.
21. Frink, C. R., "The Effects of Wash Solvents on Cation-Exchange Capacity Measurements," Soil Science Society Proceedings, Vol. 28, 1964, pp. 506-511.
22. Kim, W., Ludwig, H. F., and Bishop, W. D., "Cation-Exchange Capacity and pH in the Coagulation Process," Journal of the American Waterworks Association, Vol. 57, No. 3, 1965, pp. 327-348.
23. Martin, R. T., "Reference Chlorite Characterization for Chlorite Identification in Soil Clays," in Clays and Clay Minerals, Proceedings of the Third National Conference on Clays and Clay Minerals, W. O. Milligan, ed., 1955, pp. 117-145.
24. Stewart, R. E., "Atmospheric Diffusion of Particulate Matter Released from an Elevated Continuous Source," Journal of Applied Meteorology, Vol. 17, 1960, pp. 425-432.
25. Smith, F. B., "The Problem of Deposition in Atmospheric Diffusion of Particulate Matter," Journal of Atmospheric Science, Vol. 19, 1962, pp. 429-434.

26. Csanady, G. T., "Turbulent Diffusion of Heavy Particles in the Atmosphere," Journal of Atmospheric Science, Vol. 20, 1963, pp. 201-208.
27. Sayre, W. W., "Dispersion of Silt Particles in Open Channel Flow," Journal of Hydraulics Division, Proceedings of the American Society of Civil Engineers, Vol. 95, No. 3, 1969, pp. 1009-1038.
28. Jobson, H. E. and Sayre, W. W., "Predicting Concentration Profiles in Open Channels," Journal of Hydraulics Division, Proceedings of the American Society of Civil Engineers, Vol. 96, 1970, pp. 1983-1996.
29. Jobson, H. E. and Sayre, W. W., "Vertical Transfer in Open Channel Flow," Journal of Hydraulics Division, Proceedings of the American Society of Civil Engineers, Vol. 96, 1970, pp. 703-724.
30. Christodoulou, G. C., Leimkuhler, W. F., and Ippen, A. T., "Mathematical Model of the Massachusetts Bay, Part III. A Mathematical Model for the Dispersion of Suspended Sediments in Coastal Waters," Massachusetts Institute of Technology, Ralph M. Parsons Laboratory for Water Resources and Hydrodynamics, Report 179, 1974, p. 143.
31. Nihoul, J. C. J. and Adam, Y., "Dispersion and Settling Around a Waste Disposal Point in a Shallow Sea," Journal of Hydraulic Research, Vol. 13, 1975, pp. 171-186.
32. Fischer, H. B., "Longitudinal Dispersion and Turbulent Mixing in Open-Channel Flow," Annual Review of Fluid Mechanics, Vol. 5, 1973, pp. 59-78.
33. Turner, D. B., "Workbook of Atmospheric Dispersion Estimates," U. S. Environmental Protection Agency, Research Triangle Park, North Carolina, July, 1971.
34. Draft Environmental Impact Statement, Mobile Bay Project, U. S. Army Engineers, Mobile District, 1975.
35. Galehouse, J. S., "Sedimentation Analysis," Procedures in Sedimentary Petrology, Carver, R. E. (ed.), John Wiley and Sons, New York, 1971, pp. 69-93.
36. Ingram, R. L., "Sieve Analysis," Procedures in Sedimentary Petrology, Carver, R. E. (ed.), John Wiley and Sons, New York, 1971, pp. 49-68.
37. Drever, J. I., "The Preparation of Oriented Clay Mineral Specimens for X-Ray Diffraction Analysis by a Filter Membrane Peel Technique," American Mineralogist, Vol. 58, pp. 553-554.

38. Biscaye, P. E., "Distinction Between Kaolinite and Chlorite in Recent Sediments by X-Ray Diffraction," American Mineralogist, Vol. 49, 1964, pp. 1281-1289.
39. American Society for Testing and Materials, X-Ray Powder Data File.
40. Biscaye, P. E., "Mineralogy and Sedimentation of Recent Deep-Sea Clay in the Atlantic Ocean and Adjacent Seas and Oceans," Geological Society of America Bulletin, Vol. 76, 1965, pp. 803-832.
41. Wang, W. C., "Determination of Cation-Exchange Capacity of Suspended Sediment," Water Resources Bulletin, Vol. 11, No. 5, 1975, pp. 1052-1057.

APPENDIX G: PLUME MODEL COMPUTER PROGRAM

1. A computer program was developed to predict turbidity plumes according to the model discussed in Part V. This program, shown in Figure G1, was written in IBM FORTRAN IV and should be compatible with most compilers. The program relies upon the IBM Scientific Subroutine Package (SSP) to perform matrix manipulations and to solve the systems of linear differential equations. The subroutines used from this package are ARRAY, CMPRD, and DGELG. Access to these programs or their equivalent is necessary for program execution.

2. The input data consist of any number of suspended sediment fractions, each with an initial concentration and settling velocity. Also specified for each input data record are the current velocity, channel depth, and three computational parameters. The data format is shown in Table G1.

3. There are also several program defaults which can be overridden, if desired, by changing the FORTRAN code (Table G2). These include the initial discharge half-width, distance between steps in the lateral and downstream directions, and the initial vertical concentration profile.

4. The program has been run on an IBM 370/158 computer, requiring a core size of 75K. Execution of the program with 10 input sediment fractions uses about 40 seconds of CPU time and costs roughly \$4.00.

5. As an example of the use of the turbidity plume program, a complete listing of input and output data for one run is shown in Figures G2-G20. This model corresponds to the plume prediction for Mobile Bay sediment discussed in paragraphs 179-187 of the main text.

6. Eleven sediment fractions were input (Fig. G2). A current velocity of 0.2 m/sec and channel depth of 3 m were used. The values of XN, THETA, and NSTEP were 20.0, 1.0, and 36.0, respectively.

7. The program output consists of: (1) a two-dimensional (downstream-vertical) concentration distribution for each of the 11 sediment fractions (Figs. G3-G13); (2) the summation of all suspended sediment fractions (Fig. G14); (3) the table of lateral spreading

factors (Fig. G15); and (4) 5 horizontal slices through the three-dimensional plume at depths of 0, 0.6, 1.2, 1.8, and 2.4 m (Figs. G16-G20).

Table G1
Input Data Format

<u>Column</u>	<u>Program Symbol</u>	<u>Format</u>	<u>Value</u>
1-10	U	F10.0	Current velocity (m/sec)
11-20	W	F10.0	Settling velocity of this sediment fraction (m/sec)
21-30	H	F10.0	Channel depth (m)
31-40	CO	F10.0	Concentration of this sediment fraction (% of total)
41-50	XN	F10.0	Number of depths
51-60	THETA	F10.0	Model stability factor (set to 1.0)
61-70	NSTEP	I10	Number of downstream steps (<u>49</u>)

Table G2
Program Defaults

<u>Variable</u>	<u>Program Symbol</u>	<u>Default Value</u>
Initial discharge half-width	XL	0.5 m
Distance between steps in the lateral direction	DELZ	1.0 m
Distance between steps in the downstream direction	DELX	50 m
Initial vertical concentration profile	C(I,1)	Constant and equal to CO

```

0001 REAL #8 B8,MP
0002 REAL #4 IA,MA,ML,IIA D(20,20),IA(20,20),MA(20,20),
0003 DIMENSION C(20,50),ML(400),RL(400),B(20),MPI(400),IIA(20,20)
1 IRA(20,20),CJ(20),ADFLX(50),Z(21,50),AVG(50),CSUM(20,50)
0004 DIMENSION ADELX(50),IOUT(50)
0005 DIMENSION AVGSUM(50),B8(20),IOUT(50)
0006 DATA CSUM/1000*0./
0007 DATA IA/400*0./,D/400*0./,IIA/400*0./,Z/1050*0./,AVGSUM/50*0./
0008 ELY=.02*U*Y*(1.-Y/H)
0009 DO 10 I=1,20
0010 IA(I,I)=1.
0011 IIA(I,I)=-1.
0012 IF (I.GT.1) IIA(I,I-1)=1.
0013 CONTINUE
0014 READ(5,1000,END=99) U,W,H,CO,XN,THETA,NSTEP
0015 IF (XN.GT.20.) XN=20
0016 IF (NSTEP.GT.49) NSTEP=49
0017 XL=0.5
0018 NSTEPI=NSTEP+1
0019 WRITE(6,1001) U,W,H,CO,XN,THETA,XL
0020 FORMAT(6F10.0,110)
0021 FORMAT('11 INPUTS: ',U=' ',F6.2,' W=' ',F7.6,' H=' ',F5.1,
1 ' CO=' ',F6.1,' XN=' ',F3.0,' THETA=' ',F4.2,' XL=' ',F5.2)
0022 N=XN
0023 DELY=H/XN
0024 DELZ=1.0000
0025 CONZ=2.2
0026 DELI2=1./((DELY*DELY)
0027 AVGSUM(1)=AVGSUM(1)+CO
0028 DELX=50.
0029 INC=2
0030 IF (NSTEPI/INC.GT.20) INC=NSTEPI/20
0031 DO 501 J=1,NSTEPI
0032 ADELX(J)={J-1}*DELX
0033 AVG(J)=0.
0034 CONTINUE
0035 DO 500 I=1,N

```

FIGURE G1. TURBIDITY PLUME MODEL COMPUTER PROGRAM

```

0036 ADELY(I)=(I-1)*DELY
0037 IF (I-1)*DELZ.LE.XL) Z(I,1)=I.
0038 CONTINUE
0039 EZ=0.005*H*U *CONZ
0040 FOREZ=4.*EZ
0041 DO 680 J=1,NSTEP
0042 FOREX=SQRT(ADELX(J+1)*FOREZ)
0043 DO 680 IZ=1,21
0044 AZ=(IZ-1)*DELZ
0045 TOP=(AZ+XL)/FOREX
0046 BOT=(AZ-XL)/FCREX
0047 Z(IZ,J+1)=0.5*(ERF(TOP)-ERF(BOT))
0048 CONTINUE
0049 DO 100 I=1,20
0050 C(I,1)=CO
0051 CONTINUE
0052 AVG(1)=CO
0053 D(1,1)=-E(1.5*DELY)
0054 D(1,2)=E(1.5*DELY)
0055 N1=N-1
0056 DO 200 I=2,N1
0057 X1=(2*I-1)*.5*DELY
0058 X2=(2*I+1)*.5*DELY
0059 D(I,I-1)=E(X1)
0060 D(I,I)=-E(X1)-E(X2)
0061 D(I,I+1)=E(X2)
0062 CONTINUE
0063 D(N,N)=-E((XN-.5)*DELY)
0064 D(N,N-1)=-D(N,N)
0065 DO 300 I=1,N
0066 DO 300 J=1,N
0067 D(I,J)=DELY2*D(I,J)
0068 MA(I,J)=U/DELX*IA(I,J)-THETA*D(I,J)
0069 RA(I,J)=U/DELX*IA(I,J)+(1.-THETA)*D(I,J)+W*IIA(I,J)/DELY
0070 CONTINUE
0071 CALL ARRAY(2,N,N,20,20,ML,MA)
0072 CALL ARRAY(2,N,N,20,20,RL,RA)

```

FIGURE G1. (CONTINUED)

```

0073 DO 400 J=1,NSTEP
0074 DO 405 I=1,N
0075 CJ(I)=C(I,J)
0076 CSUM(I,J)=CSUM(I,J)+CJ(I)
0077 CONTINUE
0078 CALL GMPRD(RL,CJ,8,N,N,I)
0079 DO 406 I=1,400
0080 MP(I)=ML(I)
0081 CONTINUE
0082 DO 407 I=1,20
0083 B8(I)=B(I)
0084 CONTINUE
0085 CALL DGEELG(B8,MP,N,I,.00000001,IER)
0086 IF (IER.GT.0) WRITE(7,4747) IER,J
0087 FORMAT(' LOST OF SIGNIFICANCE AT PIVOT ',I3,' IN STEP ',I3)
0088 DO 399 K=1,N
0089 C(K,J+1)=B8(K)
0090 AVG(J+1)=B8(K)+AVG(J+1)
0091 CONTINUE
0092 AVG(J+1)=AVG(J+1)/XN
0093 AVGSUM(J+1)=AVGSUM(J+1)+AVG(J+1)
0094 CONTINUE
0095 WRITE(6,5001)(ADELX(I),I=1,NSTEP1,INC)
0096 FORMAT(11X,20F6.1,/)
0097 DO 410 I=1,N
0098 CSUM(I,NSTEP1)=CSUM(I,NSTEP1)+C(I,NSTEP1)
0099 WRITE(6,5000) ADELY(I),(C(I,J),J=1,NSTEP1,INC)
0100 FORMAT(3X,F5.2,2X,20F6.2)
0101 CONTINUE
0102 WRITE(6,5003) (AVG(KKK),KKK=1,NSTEP1,INC)
0103 FORMAT(4X,'AVG',3X,20F6.2)
0104 GO TO 11
0105 CONTINUE
0106 WRITE(6,5005)
0107 FORMAT(11H,I40,'SUMMATION OF SUSPENDED SEDIMENTS')
0108 WRITE(6,5001)(ADELX(I),I=1,NSTEP1,INC)
0109 DO 412 I=1,N

```

FIGURE G1. (CONTINUED)

```

0110 WRITE(6,5000) ADELX(I,J),(CSUM(I,J),J=1,NSTEP1,INC)
0111 CONTINUE
0112 WRITE(6,5003) (AVGSUM(KKK),KKK=1,NSTEP1,INC)
0113 WRITE(6,6668)
0114 FORMAT(IH1)
0115 DO 411 I=1,21
0116 AZ=(I-1)*DELZ
0117 WRITE(6,5002) AZ,(Z(I,J),J=1,NSTEP1,INC)
0118 FORMAT(4X,F5.2,2X,2OF6.3)
0119 CONTINUE
0120 DO 800 IY=1,20,4
0121 YVAL=(IY-1)*DELY
0122 WRITE(6,5555) YVAL
0123 FORMAT(IH1,I20,'DISTRIBUTION OF SEDIMENT IN HORIZONTAL PLANE',
1, 'AT DEPTH',F6.2,' (PARTS PER HUNDRED THOUSAND)',//////)
0124 DO 810 IZ=1,21
0125 IAZ=22-IZ
0126 AZ=(-DELZ*(IAZ-1))
0127 DO 801 IX=1,NSTEP1,INC
0128 IOUT(IX)=CSUM(IY,IX)*Z(IAZ,IX)*1000.+0.5
0129 CONTINUE
0130 WRITE(6,6666) AZ,(IOUT(KKK),KKK=1,NSTEP1,INC)
0131 FORMAT(2X,F6.2,2X,20I6)
0132 CONTINUE
0133 DO 802 IZ=2,21
0134 AZ=DELZ*(IZ-1)
0135 DO 803 IX=1,NSTEP1,INC
0136 IOUT(IX)=CSUM(IY,IX)*Z(IZ,IX)*1000.+0.5
0137 CONTINUE
0138 WRITE(6,6666) AZ,(IOUT(KKK),KKK=1,NSTEP1,INC)
0139 CONTINUE
0140 WRITE(6,6667)
0141 FORMAT(//)
0142 WRITE(6,5001) (ADELX(KKK),KKK=1,NSTEP1,INC)
0143 CONTINUE
0144 STOP
0145 END

```

FIGURE G1. (CONCLUDED)

<u>Current Velocity (m/sec)</u>	<u>Settling Velocity (m/sec)</u>	<u>Channel Depth (m)</u>	<u>Conc. of This Fraction (%)</u>	<u>XN</u>	<u>THETA</u>	<u>NSTEP</u>
0.20	0.000009	3.0	5.0	20.0	1.0	36.0
0.20	0.000071	3.0	5.0	20.0	1.0	36.0
0.20	0.000140	3.0	5.0	20.0	1.0	36.0
0.20	0.000200	3.0	5.0	20.0	1.0	36.0
0.20	0.000300	3.0	10.0	20.0	1.0	36.0
0.20	0.000450	3.0	10.0	20.0	1.0	36.0
0.20	0.000580	3.0	10.0	20.0	1.0	36.0
0.20	0.000730	3.0	10.0	20.0	1.0	36.0
0.20	0.000860	3.0	10.0	20.0	1.0	36.0
0.20	0.001000	3.0	10.0	20.0	1.0	36.0
0.20	0.001240	3.0	20.0	20.0	1.0	36.0

FIGURE G2. INPUT DATA FOR MORTLE BAY PLUME MODEL

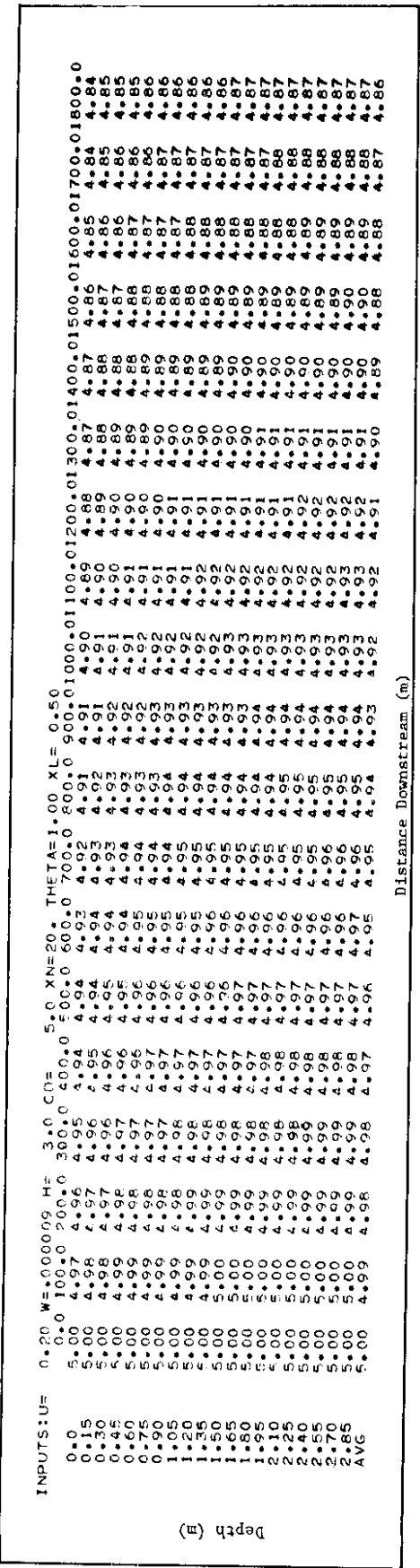


FIGURE G3. TWO-DIMENSIONAL CONCENTRATION DISTRIBUTION FOR FIRST SEDIMENT FRACTION

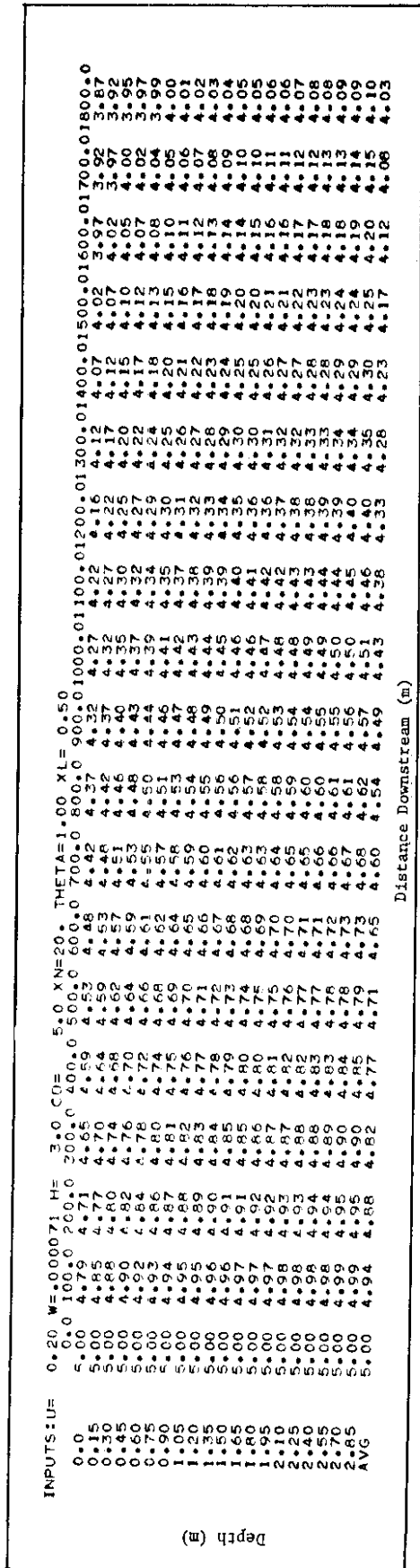


FIGURE G4. TWO-DIMENSIONAL CONCENTRATION DISTRIBUTION FOR SECOND SEDIMENT FRACTION

INPUTS:U#	THETA=1.00 XL= 0.50																				
	0.20	0.100	0.200	0.300	0.400	0.500	0.600	0.700	0.800	0.900	0.1000	0.1000	0.1000	0.1200	0.1300	0.1400	0.1500	0.1600	0.1700	0.1800	0.0
0.0	5.00	4.60	4.55	4.42	4.31	4.21	4.01	3.91	3.82	3.73	3.64	3.55	3.47	3.38	3.30	3.22	3.15	3.07	3.00	3.00	3.00
0.15	5.00	4.70	4.66	4.53	4.43	4.27	4.17	4.07	3.97	3.87	3.78	3.69	3.59	3.50	3.42	3.35	3.27	3.19	3.11	3.03	3.03
0.30	5.00	4.86	4.83	4.70	4.61	4.41	4.31	4.21	4.11	4.01	3.92	3.83	3.73	3.64	3.56	3.49	3.41	3.33	3.25	3.17	3.17
0.45	5.00	4.92	4.89	4.76	4.67	4.45	4.35	4.25	4.15	4.05	3.96	3.87	3.77	3.68	3.60	3.52	3.44	3.36	3.28	3.20	3.20
0.60	5.00	4.88	4.85	4.72	4.63	4.41	4.31	4.21	4.11	4.01	3.92	3.83	3.73	3.64	3.56	3.48	3.40	3.32	3.24	3.16	3.16
0.75	5.00	4.90	4.87	4.74	4.65	4.43	4.33	4.23	4.13	4.03	3.94	3.85	3.75	3.66	3.58	3.50	3.42	3.34	3.26	3.18	3.18
0.90	5.00	4.92	4.89	4.76	4.67	4.45	4.35	4.25	4.15	4.05	3.96	3.87	3.77	3.68	3.60	3.52	3.44	3.36	3.28	3.20	3.20
1.05	5.00	4.93	4.90	4.77	4.68	4.46	4.36	4.26	4.16	4.06	3.97	3.88	3.78	3.69	3.61	3.53	3.45	3.37	3.29	3.21	3.21
1.20	5.00	4.94	4.91	4.78	4.69	4.47	4.37	4.27	4.17	4.07	3.98	3.89	3.79	3.70	3.62	3.54	3.46	3.38	3.30	3.22	3.22
1.35	5.00	4.95	4.92	4.79	4.70	4.48	4.38	4.28	4.18	4.08	3.99	3.90	3.81	3.72	3.64	3.56	3.48	3.40	3.32	3.24	3.24
1.50	5.00	4.96	4.93	4.80	4.71	4.49	4.39	4.29	4.19	4.09	4.00	3.91	3.82	3.73	3.65	3.57	3.49	3.41	3.33	3.25	3.25
1.65	5.00	4.97	4.94	4.81	4.72	4.50	4.40	4.30	4.20	4.10	4.01	3.92	3.83	3.74	3.66	3.58	3.50	3.42	3.34	3.26	3.26
1.80	5.00	4.97	4.94	4.81	4.72	4.50	4.40	4.30	4.20	4.10	4.01	3.92	3.83	3.74	3.66	3.58	3.50	3.42	3.34	3.26	3.26
1.95	5.00	4.98	4.95	4.82	4.73	4.51	4.41	4.31	4.21	4.11	4.02	3.93	3.84	3.75	3.67	3.59	3.51	3.43	3.35	3.27	3.27
2.10	5.00	4.97	4.94	4.81	4.72	4.50	4.40	4.30	4.20	4.10	4.01	3.92	3.83	3.74	3.66	3.58	3.50	3.42	3.34	3.26	3.26
2.25	5.00	4.98	4.95	4.82	4.73	4.51	4.41	4.31	4.21	4.11	4.02	3.93	3.84	3.75	3.67	3.59	3.51	3.43	3.35	3.27	3.27
2.40	5.00	4.97	4.94	4.81	4.72	4.50	4.40	4.30	4.20	4.10	4.01	3.92	3.83	3.74	3.66	3.58	3.50	3.42	3.34	3.26	3.26
2.55	5.00	4.98	4.95	4.82	4.73	4.51	4.41	4.31	4.21	4.11	4.02	3.93	3.84	3.75	3.67	3.59	3.51	3.43	3.35	3.27	3.27
2.70	5.00	4.99	4.96	4.83	4.74	4.52	4.42	4.32	4.22	4.12	4.03	3.94	3.85	3.76	3.68	3.60	3.52	3.44	3.36	3.28	3.28
2.85	5.00	4.98	4.95	4.82	4.73	4.51	4.41	4.31	4.21	4.11	4.02	3.93	3.84	3.75	3.67	3.59	3.51	3.43	3.35	3.27	3.27
AVG		4.88	4.77	4.65	4.54	4.43	4.33	4.22	4.12	4.02	3.93	3.83	3.74	3.65	3.56	3.48	3.40	3.31	3.23	3.15	3.15

Depth (m)

Distance Downstream (m)

FIGURE G5. TWO-DIMENSIONAL CONCENTRATION DISTRIBUTION FOR THIRD SEDIMENT FRACTION

INPUTS:U#	THETA=1.00 XL= 0.50																				
	0.20	0.100	0.200	0.300	0.400	0.500	0.600	0.700	0.800	0.900	1.000	0.1000	0.1200	0.1300	0.1400	0.1500	0.1600	0.1700	0.1800	0.0	
0.0	5.00	4.47	4.21	4.25	4.05	3.90	3.77	3.64	3.51	3.38	3.27	3.16	3.05	2.94	2.84	2.74	2.65	2.56	2.47	2.38	2.38
0.15	5.00	4.58	4.45	4.34	4.14	3.98	3.84	3.71	3.58	3.46	3.34	3.23	3.11	2.99	2.90	2.80	2.70	2.61	2.52	2.43	2.43
0.30	5.00	4.72	4.51	4.39	4.23	4.07	3.94	3.81	3.67	3.55	3.42	3.30	3.19	3.07	2.97	2.87	2.77	2.68	2.58	2.49	2.49
0.45	5.00	4.80	4.60	4.47	4.31	4.15	4.01	3.87	3.74	3.61	3.49	3.36	3.24	3.11	3.00	2.90	2.82	2.72	2.63	2.54	2.54
0.60	5.00	4.84	4.64	4.47	4.34	4.19	4.04	3.90	3.77	3.64	3.51	3.39	3.27	3.14	3.03	2.94	2.84	2.74	2.65	2.56	2.56
0.75	5.00	4.86	4.66	4.49	4.36	4.21	4.07	3.93	3.79	3.66	3.53	3.41	3.29	3.16	3.05	2.96	2.86	2.76	2.67	2.58	2.58
0.90	5.00	4.88	4.71	4.55	4.41	4.26	4.09	3.95	3.81	3.68	3.55	3.43	3.31	3.18	3.07	2.98	2.89	2.79	2.69	2.60	2.60
1.05	5.00	4.89	4.75	4.59	4.43	4.28	4.13	3.99	3.85	3.71	3.57	3.44	3.31	3.19	3.08	2.99	2.90	2.80	2.70	2.60	2.60
1.20	5.00	4.90	4.76	4.60	4.45	4.30	4.15	4.00	3.86	3.73	3.60	3.46	3.34	3.22	3.11	3.02	2.91	2.81	2.71	2.61	2.61
1.35	5.00	4.92	4.78	4.62	4.47	4.31	4.16	4.03	3.89	3.75	3.62	3.49	3.37	3.25	3.14	3.04	2.94	2.83	2.73	2.63	2.63
1.50	5.00	4.94	4.81	4.65	4.50	4.34	4.19	4.06	3.92	3.79	3.66	3.52	3.39	3.27	3.16	3.06	2.95	2.85	2.75	2.65	2.65
1.65	5.00	4.94	4.81	4.65	4.50	4.34	4.19	4.06	3.92	3.79	3.66	3.52	3.39	3.27	3.16	3.06	2.95	2.85	2.75	2.65	2.65
1.80	5.00	4.95	4.82	4.66	4.51	4.35	4.20	4.07	3.94	3.80	3.67	3.54	3.42	3.30	3.19	3.09	2.98	2.88	2.78	2.68	2.68
1.95	5.00	4.96	4.83	4.67	4.52	4.36	4.21	4.08	3.94	3.81	3.68	3.55	3.43	3.31	3.20	3.10	2.99	2.89	2.79	2.69	2.69
2.10	5.00	4.97	4.84	4.68	4.53	4.37	4.22	4.09	3.95	3.81	3.68	3.55	3.43	3.31	3.20	3.10	2.99	2.89	2.79	2.69	2.69
2.25	5.00	4.98	4.85	4.69	4.54	4.38	4.23	4.10	3.96	3.82	3.69	3.56	3.44	3.32	3.21	3.11	3.01	2.91	2.81	2.71	2.71
2.40	5.00	4.98	4.85	4.69	4.54	4.38	4.23	4.10	3.96	3.82	3.69	3.56	3.44	3.32	3.21	3.11	3.01	2.91	2.81	2.71	2.71
2.55	5.00	4.99	4.86	4.70	4.55	4.39	4.24	4.11	3.97	3.83	3.70	3.57	3.45	3.33	3.23	3.13	3.03	2.93	2.83	2.73	2.73
2.70	5.00	4.99	4.86	4.70	4.55	4.39	4.24	4.11	3.97	3.83	3.70	3.57	3.45	3.33	3.23	3.13	3.03	2.93	2.83	2.73	2.73
2.85	5.00	4.98	4.85	4.69	4.54	4.38	4.23	4.10	3.96	3.82	3.69	3.56	3.44	3.32	3.21	3.11	3.01	2.91	2.81	2.71	2.71
AVG		4.83	4.67	4.51	4.35	4.20	4.06	3.91	3.78	3.65	3.52	3.40	3.28	3.17	3.06	2.95	2.85	2.75	2.65	2.55	2.55

Depth (m)

Distance Downstream (m)

FIGURE G6. TWO-DIMENSIONAL CONCENTRATION DISTRIBUTION FOR FOURTH SEDIMENT FRACTION

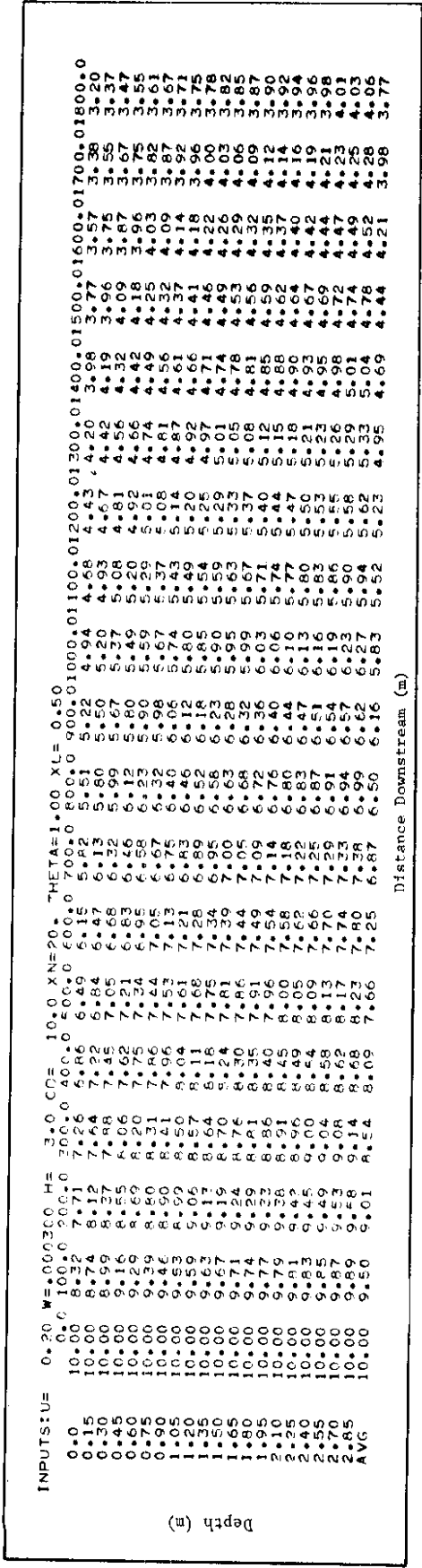


FIGURE G7. TWO-DIMENSIONAL CONCENTRATION DISTRIBUTION FOR FIFTH SEDIMENT FRACTION

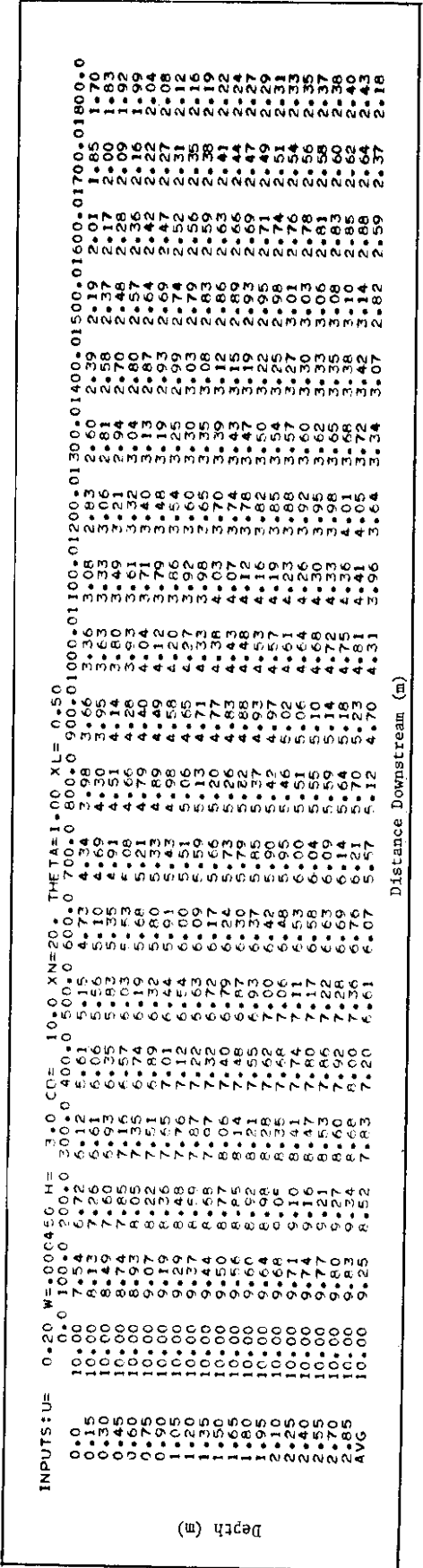


FIGURE G8. TWO-DIMENSIONAL CONCENTRATION DISTRIBUTION FOR SIXTH SEDIMENT FRACTION

INPUTS:UF	0.20	0.40	0.60	0.80	1.00	1.20	1.40	1.60	1.80	2.00	2.20	2.40	2.60	2.80	3.00	3.20	3.40	3.60	3.80	4.00	4.20	4.40	4.60	4.80	5.00	5.20	5.40	5.60	5.80	6.00	6.20	6.40	6.60	6.80	7.00	7.20	7.40	7.60	7.80	8.00	8.20	8.40	8.60	8.80	9.00	9.20	9.40	9.60	9.80	10.00																																																			
Depth (m)	0.0	0.15	0.30	0.45	0.60	0.75	0.90	1.05	1.20	1.35	1.50	1.65	1.80	1.95	2.10	2.25	2.40	2.55	2.70	2.85	3.00	3.15	3.30	3.45	3.60	3.75	3.90	4.05	4.20	4.35	4.50	4.65	4.80	4.95	5.10	5.25	5.40	5.55	5.70	5.85	6.00	6.15	6.30	6.45	6.60	6.75	6.90	7.05	7.20	7.35	7.50	7.65	7.80	7.95	8.10	8.25	8.40	8.55	8.70	8.85	9.00	9.15	9.30	9.45	9.60	9.75	9.90	10.00																																	
Distance Downstream (m)	0.0	10.00	20.00	30.00	40.00	50.00	60.00	70.00	80.00	90.00	100.00	110.00	120.00	130.00	140.00	150.00	160.00	170.00	180.00	190.00	200.00	210.00	220.00	230.00	240.00	250.00	260.00	270.00	280.00	290.00	300.00	310.00	320.00	330.00	340.00	350.00	360.00	370.00	380.00	390.00	400.00	410.00	420.00	430.00	440.00	450.00	460.00	470.00	480.00	490.00	500.00	510.00	520.00	530.00	540.00	550.00	560.00	570.00	580.00	590.00	600.00	610.00	620.00	630.00	640.00	650.00	660.00	670.00	680.00	690.00	700.00	710.00	720.00	730.00	740.00	750.00	760.00	770.00	780.00	790.00	800.00	810.00	820.00	830.00	840.00	850.00	860.00	870.00	880.00	890.00	900.00	910.00	920.00	930.00	940.00	950.00	960.00	970.00	980.00	990.00	1000.00

FIGURE G9. TWO-DIMENSIONAL CONCENTRATION DISTRIBUTION FOR SEVENTH SEDIMENT FRACTION

INPUTS:UF	0.20	0.40	0.60	0.80	1.00	1.20	1.40	1.60	1.80	2.00	2.20	2.40	2.60	2.80	3.00	3.20	3.40	3.60	3.80	4.00	4.20	4.40	4.60	4.80	5.00	5.20	5.40	5.60	5.80	6.00	6.20	6.40	6.60	6.80	7.00	7.20	7.40	7.60	7.80	8.00	8.20	8.40	8.60	8.80	9.00	9.20	9.40	9.60	9.80	10.00																																																			
Depth (m)	0.0	0.15	0.30	0.45	0.60	0.75	0.90	1.05	1.20	1.35	1.50	1.65	1.80	1.95	2.10	2.25	2.40	2.55	2.70	2.85	3.00	3.15	3.30	3.45	3.60	3.75	3.90	4.05	4.20	4.35	4.50	4.65	4.80	4.95	5.10	5.25	5.40	5.55	5.70	5.85	6.00	6.15	6.30	6.45	6.60	6.75	6.90	7.05	7.20	7.35	7.50	7.65	7.80	7.95	8.10	8.25	8.40	8.55	8.70	8.85	9.00	9.15	9.30	9.45	9.60	9.75	9.90	10.00																																	
Distance Downstream (m)	0.0	10.00	20.00	30.00	40.00	50.00	60.00	70.00	80.00	90.00	100.00	110.00	120.00	130.00	140.00	150.00	160.00	170.00	180.00	190.00	200.00	210.00	220.00	230.00	240.00	250.00	260.00	270.00	280.00	290.00	300.00	310.00	320.00	330.00	340.00	350.00	360.00	370.00	380.00	390.00	400.00	410.00	420.00	430.00	440.00	450.00	460.00	470.00	480.00	490.00	500.00	510.00	520.00	530.00	540.00	550.00	560.00	570.00	580.00	590.00	600.00	610.00	620.00	630.00	640.00	650.00	660.00	670.00	680.00	690.00	700.00	710.00	720.00	730.00	740.00	750.00	760.00	770.00	780.00	790.00	800.00	810.00	820.00	830.00	840.00	850.00	860.00	870.00	880.00	890.00	900.00	910.00	920.00	930.00	940.00	950.00	960.00	970.00	980.00	990.00	1000.00

FIGURE G10. TWO-DIMENSIONAL CONCENTRATION DISTRIBUTION FOR EIGHTH SEDIMENT FRACTION

INPUTS:U=	0.20	0.00	100.00	200.00	300.00	400.00	500.00	600.00	700.00	800.00	900.00	1000.00	1100.00	1200.00	1300.00	1400.00	1500.00	1600.00	1700.00	1800.00
Depth (m)	0.00	0.15	0.30	0.45	0.60	0.75	0.90	1.05	1.20	1.35	1.50	1.65	1.80	1.95	2.10	2.25	2.40	2.55	2.70	2.85
W=	0.01240	0.01240	0.01240	0.01240	0.01240	0.01240	0.01240	0.01240	0.01240	0.01240	0.01240	0.01240	0.01240	0.01240	0.01240	0.01240	0.01240	0.01240	0.01240	0.01240
XN=	20.0	50.0	100.0	200.0	400.0	600.0	900.0	1200.0	1500.0	1800.0	2100.0	2400.0	2700.0	3000.0	3300.0	3600.0	3900.0	4200.0	4500.0	4800.0
CD=	3.0	4.0	5.0	6.0	7.0	8.0	9.0	10.0	11.0	12.0	13.0	14.0	15.0	16.0	17.0	18.0	19.0	20.0	21.0	22.0
HE	200.0	200.0	200.0	200.0	200.0	200.0	200.0	200.0	200.0	200.0	200.0	200.0	200.0	200.0	200.0	200.0	200.0	200.0	200.0	200.0
THETA=	1.00	1.00	1.00	1.00	1.00	1.00	1.00	1.00	1.00	1.00	1.00	1.00	1.00	1.00	1.00	1.00	1.00	1.00	1.00	1.00
XL=	0.50	0.50	0.50	0.50	0.50	0.50	0.50	0.50	0.50	0.50	0.50	0.50	0.50	0.50	0.50	0.50	0.50	0.50	0.50	0.50
Distance	Downstream																			

FIGURE G13. TWO-DIMENSIONAL CONCENTRATION DISTRIBUTION FOR ELEVENTH SEDIMENT FRACTION

INPUTS:U=	0.0	100.00	200.00	300.00	400.00	500.00	600.00	700.00	800.00	900.00	1000.00	1100.00	1200.00	1300.00	1400.00	1500.00	1600.00	1700.00	1800.00	
Depth (m)	0.0	0.15	0.30	0.45	0.60	0.75	0.90	1.05	1.20	1.35	1.50	1.65	1.80	1.95	2.10	2.25	2.40	2.55	2.70	2.85
SUMMATION OF	SUSPENDED																			
SEDIMENTS	SEDIMENTS	SEDIMENTS	SEDIMENTS	SEDIMENTS	SEDIMENTS	SEDIMENTS	SEDIMENTS	SEDIMENTS	SEDIMENTS	SEDIMENTS	SEDIMENTS	SEDIMENTS	SEDIMENTS	SEDIMENTS	SEDIMENTS	SEDIMENTS	SEDIMENTS	SEDIMENTS	SEDIMENTS	SEDIMENTS
Distance	Downstream																			

FIGURE G14. SUMMATION OF TWO-DIMENSIONAL CONCENTRATION DISTRIBUTIONS FOR ALL SEDIMENT FRACTIONS

Lateral Distance (m)	Distance Downstream →																				
	0.0	1.00	2.00	3.00	4.00	5.00	6.00	7.00	8.00	9.00	10.00	11.00	12.00	13.00	14.00	15.00	16.00	17.00	18.00	19.00	20.00
0.0	0.000	0.337	0.242	0.198	0.172	0.154	0.141	0.131	0.122	0.115	0.109	0.104	0.100	0.096	0.093	0.089	0.087	0.084	0.082	0.080	0.078
1.00	0.0	0.236	0.201	0.175	0.157	0.143	0.132	0.124	0.117	0.111	0.105	0.101	0.097	0.093	0.090	0.087	0.085	0.082	0.080	0.077	0.075
2.00	0.0	0.091	0.116	0.121	0.119	0.114	0.110	0.105	0.101	0.098	0.094	0.091	0.088	0.086	0.083	0.081	0.079	0.077	0.075	0.073	0.071
3.00	0.0	0.001	0.012	0.027	0.039	0.047	0.052	0.055	0.058	0.059	0.059	0.060	0.060	0.060	0.060	0.060	0.059	0.059	0.059	0.059	0.058
4.00	0.0	0.000	0.012	0.009	0.017	0.024	0.030	0.034	0.038	0.041	0.043	0.044	0.046	0.047	0.047	0.048	0.048	0.048	0.048	0.048	0.048
5.00	0.0	0.000	0.000	0.002	0.006	0.010	0.015	0.019	0.023	0.026	0.028	0.030	0.032	0.034	0.035	0.036	0.037	0.038	0.038	0.038	0.038
6.00	0.0	0.0	0.000	0.000	0.002	0.004	0.007	0.009	0.012	0.015	0.017	0.020	0.021	0.023	0.025	0.026	0.027	0.028	0.028	0.029	0.029
7.00	0.0	0.0	0.000	0.000	0.000	0.001	0.003	0.004	0.006	0.008	0.010	0.012	0.013	0.015	0.017	0.018	0.019	0.020	0.021	0.021	0.021
8.00	0.0	0.0	0.000	0.000	0.000	0.001	0.002	0.002	0.003	0.004	0.005	0.007	0.008	0.009	0.010	0.012	0.013	0.014	0.015	0.015	0.015
9.00	0.0	0.0	0.0	0.000	0.000	0.000	0.000	0.001	0.001	0.002	0.002	0.003	0.004	0.005	0.006	0.007	0.008	0.009	0.010	0.010	0.010
10.00	0.0	0.0	0.0	0.000	0.000	0.000	0.000	0.000	0.000	0.001	0.001	0.001	0.002	0.002	0.003	0.004	0.005	0.006	0.006	0.006	0.006
11.00	0.0	0.0	0.0	0.0	0.0	0.000	0.000	0.000	0.000	0.000	0.000	0.001	0.001	0.001	0.002	0.002	0.003	0.003	0.004	0.004	0.004
12.00	0.0	0.0	0.0	0.0	0.0	0.000	0.000	0.000	0.000	0.000	0.000	0.000	0.000	0.001	0.001	0.001	0.002	0.002	0.003	0.003	0.003
13.00	0.0	0.0	0.0	0.0	0.0	0.000	0.000	0.000	0.000	0.000	0.000	0.000	0.000	0.000	0.001	0.001	0.001	0.002	0.002	0.002	0.002
14.00	0.0	0.0	0.0	0.0	0.0	0.000	0.000	0.000	0.000	0.000	0.000	0.000	0.000	0.000	0.000	0.001	0.001	0.001	0.001	0.001	0.001
15.00	0.0	0.0	0.0	0.0	0.0	0.0	0.000	0.000	0.000	0.000	0.000	0.000	0.000	0.000	0.000	0.000	0.000	0.000	0.000	0.000	0.000
16.00	0.0	0.0	0.0	0.0	0.0	0.0	0.0	0.000	0.000	0.000	0.000	0.000	0.000	0.000	0.000	0.000	0.000	0.000	0.000	0.000	0.000
17.00	0.0	0.0	0.0	0.0	0.0	0.0	0.0	0.0	0.000	0.000	0.000	0.000	0.000	0.000	0.000	0.000	0.000	0.000	0.000	0.000	0.000
18.00	0.0	0.0	0.0	0.0	0.0	0.0	0.0	0.0	0.0	0.000	0.000	0.000	0.000	0.000	0.000	0.000	0.000	0.000	0.000	0.000	0.000
19.00	0.0	0.0	0.0	0.0	0.0	0.0	0.0	0.0	0.0	0.0	0.000	0.000	0.000	0.000	0.000	0.000	0.000	0.000	0.000	0.000	0.000
20.00	0.0	0.0	0.0	0.0	0.0	0.0	0.0	0.0	0.0	0.0	0.0	0.0	0.0	0.0	0.000	0.000	0.000	0.000	0.000	0.000	0.000

FIGURE G15. TABLE OF LATERAL SPREADING FACTORS

DISTRIBUTION OF SEDIMENT IN HORIZONTAL PLANE AT DEPTH 0.0 (PARTS PER HUNDRED THOUSAND)

Lateral Distance (M)	0.0	100.0	200.0	300.0	400.0	500.0	600.0	700.0	800.0	900.0	1000.0	1100.0	1200.0	1300.0	1400.0	1500.0	1600.0	1700.0	1800.0	
-20.00	0	0	0	0	0	0	0	0	0	0	0	0	0	0	0	0	0	0	0	0
-19.00	0	0	0	0	0	0	0	0	0	0	0	0	0	0	0	0	0	0	0	0
-18.00	0	0	0	0	0	0	0	0	0	0	0	0	0	0	0	0	0	0	0	0
-17.00	0	0	0	0	0	0	0	0	0	0	0	0	0	0	0	0	0	0	0	0
-16.00	0	0	0	0	0	0	0	0	0	0	0	0	0	0	0	0	0	0	0	0
-15.00	0	0	0	0	0	0	0	0	0	0	0	0	0	0	0	0	0	0	0	0
-14.00	0	0	0	0	0	0	0	0	0	0	0	0	0	0	0	0	0	0	0	0
-13.00	0	0	0	0	0	0	0	0	0	0	0	0	0	0	0	0	0	0	0	0
-12.00	0	0	0	0	0	0	0	0	0	0	0	0	0	0	0	0	0	0	0	0
-11.00	0	0	0	0	0	0	0	0	0	0	0	0	0	0	0	0	0	0	0	0
-10.00	0	0	0	0	0	0	0	0	0	0	0	0	0	0	0	0	0	0	0	0
-9.00	0	0	0	0	0	0	0	0	0	0	0	0	0	0	0	0	0	0	0	0
-8.00	0	0	0	0	0	0	0	0	0	0	0	0	0	0	0	0	0	0	0	0
-7.00	0	0	0	0	0	0	0	0	0	0	0	0	0	0	0	0	0	0	0	0
-6.00	0	0	0	0	0	0	0	0	0	0	0	0	0	0	0	0	0	0	0	0
-5.00	0	0	0	0	0	0	0	0	0	0	0	0	0	0	0	0	0	0	0	0
-4.00	0	0	0	0	0	0	0	0	0	0	0	0	0	0	0	0	0	0	0	0
-3.00	0	0	0	0	0	0	0	0	0	0	0	0	0	0	0	0	0	0	0	0
-2.00	0	0	0	0	0	0	0	0	0	0	0	0	0	0	0	0	0	0	0	0
-1.00	0	0	0	0	0	0	0	0	0	0	0	0	0	0	0	0	0	0	0	0
0.00	0	0	0	0	0	0	0	0	0	0	0	0	0	0	0	0	0	0	0	0
1.00	0	0	0	0	0	0	0	0	0	0	0	0	0	0	0	0	0	0	0	0
2.00	0	0	0	0	0	0	0	0	0	0	0	0	0	0	0	0	0	0	0	0
3.00	0	0	0	0	0	0	0	0	0	0	0	0	0	0	0	0	0	0	0	0
4.00	0	0	0	0	0	0	0	0	0	0	0	0	0	0	0	0	0	0	0	0
5.00	0	0	0	0	0	0	0	0	0	0	0	0	0	0	0	0	0	0	0	0
6.00	0	0	0	0	0	0	0	0	0	0	0	0	0	0	0	0	0	0	0	0
7.00	0	0	0	0	0	0	0	0	0	0	0	0	0	0	0	0	0	0	0	0
8.00	0	0	0	0	0	0	0	0	0	0	0	0	0	0	0	0	0	0	0	0
9.00	0	0	0	0	0	0	0	0	0	0	0	0	0	0	0	0	0	0	0	0
10.00	0	0	0	0	0	0	0	0	0	0	0	0	0	0	0	0	0	0	0	0
11.00	0	0	0	0	0	0	0	0	0	0	0	0	0	0	0	0	0	0	0	0
12.00	0	0	0	0	0	0	0	0	0	0	0	0	0	0	0	0	0	0	0	0
13.00	0	0	0	0	0	0	0	0	0	0	0	0	0	0	0	0	0	0	0	0
14.00	0	0	0	0	0	0	0	0	0	0	0	0	0	0	0	0	0	0	0	0
15.00	0	0	0	0	0	0	0	0	0	0	0	0	0	0	0	0	0	0	0	0
16.00	0	0	0	0	0	0	0	0	0	0	0	0	0	0	0	0	0	0	0	0
17.00	0	0	0	0	0	0	0	0	0	0	0	0	0	0	0	0	0	0	0	0
18.00	0	0	0	0	0	0	0	0	0	0	0	0	0	0	0	0	0	0	0	0
19.00	0	0	0	0	0	0	0	0	0	0	0	0	0	0	0	0	0	0	0	0
20.00	0	0	0	0	0	0	0	0	0	0	0	0	0	0	0	0	0	0	0	0

0.0 100.0 200.0 300.0 400.0 500.0 600.0 700.0 800.0 900.0 1000.0 1100.0 1200.0 1300.0 1400.0 1500.0 1600.0 1700.0 1800.0

Distance Downstream (m)

FIGURE G16. CONCENTRATION DISTRIBUTION IN HORIZONTAL PLANE AT THE SURFACE

DISTRIBUTION OF SEDIMENT IN HORIZONTAL PLANE AT DEPTH 0.60 (PARTS PER HUNDRED THOUSAND)

Lateral Distance (m)	0.0	100.0	200.0	300.0	400.0	500.0	600.0	700.0	800.0	900.0	01000.0	01100.0	01200.0	01300.0	01400.0	01500.0	01600.0	01700.0	01800.0
-20.00	0	0	0	0	0	0	0	0	0	0	0	0	0	0	0	0	0	0	0
-19.00	0	0	0	0	0	0	0	0	0	0	0	0	0	0	0	0	0	0	0
-18.00	0	0	0	0	0	0	0	0	0	0	0	0	0	0	0	0	0	0	0
-17.00	0	0	0	0	0	0	0	0	0	0	0	0	0	0	0	0	0	0	0
-16.00	0	0	0	0	0	0	0	0	0	0	0	0	0	0	0	0	0	0	0
-15.00	0	0	0	0	0	0	0	0	0	0	0	0	0	0	0	0	0	0	0
-14.00	0	0	0	0	0	0	0	0	0	0	0	0	0	0	0	0	0	0	0
-13.00	0	0	0	0	0	0	0	0	0	0	0	0	0	0	0	0	0	0	0
-12.00	0	0	0	0	0	0	0	0	0	0	0	0	0	0	0	0	0	0	0
-11.00	0	0	0	0	0	0	0	0	0	0	0	0	0	0	0	0	0	0	0
-10.00	0	0	0	0	0	0	0	0	0	0	0	0	0	0	0	0	0	0	0
-9.00	0	0	0	0	0	0	0	0	0	0	0	0	0	0	0	0	0	0	0
-8.00	0	0	0	0	0	0	0	0	0	0	0	0	0	0	0	0	0	0	0
-7.00	0	0	0	0	0	0	0	0	0	0	0	0	0	0	0	0	0	0	0
-6.00	0	0	0	0	0	0	0	0	0	0	0	0	0	0	0	0	0	0	0
-5.00	0	0	0	0	0	0	0	0	0	0	0	0	0	0	0	0	0	0	0
-4.00	0	0	0	0	0	0	0	0	0	0	0	0	0	0	0	0	0	0	0
-3.00	0	0	0	0	0	0	0	0	0	0	0	0	0	0	0	0	0	0	0
-2.00	0	0	0	0	0	0	0	0	0	0	0	0	0	0	0	0	0	0	0
-1.00	0	0	0	0	0	0	0	0	0	0	0	0	0	0	0	0	0	0	0
1.00	1000.00	0	0	0	0	0	0	0	0	0	0	0	0	0	0	0	0	0	0
2.00	0	0	0	0	0	0	0	0	0	0	0	0	0	0	0	0	0	0	0
3.00	0	0	0	0	0	0	0	0	0	0	0	0	0	0	0	0	0	0	0
4.00	0	0	0	0	0	0	0	0	0	0	0	0	0	0	0	0	0	0	0
5.00	0	0	0	0	0	0	0	0	0	0	0	0	0	0	0	0	0	0	0
6.00	0	0	0	0	0	0	0	0	0	0	0	0	0	0	0	0	0	0	0
7.00	0	0	0	0	0	0	0	0	0	0	0	0	0	0	0	0	0	0	0
8.00	0	0	0	0	0	0	0	0	0	0	0	0	0	0	0	0	0	0	0
9.00	0	0	0	0	0	0	0	0	0	0	0	0	0	0	0	0	0	0	0
10.00	0	0	0	0	0	0	0	0	0	0	0	0	0	0	0	0	0	0	0
11.00	0	0	0	0	0	0	0	0	0	0	0	0	0	0	0	0	0	0	0
12.00	0	0	0	0	0	0	0	0	0	0	0	0	0	0	0	0	0	0	0
13.00	0	0	0	0	0	0	0	0	0	0	0	0	0	0	0	0	0	0	0
14.00	0	0	0	0	0	0	0	0	0	0	0	0	0	0	0	0	0	0	0
15.00	0	0	0	0	0	0	0	0	0	0	0	0	0	0	0	0	0	0	0
16.00	0	0	0	0	0	0	0	0	0	0	0	0	0	0	0	0	0	0	0
17.00	0	0	0	0	0	0	0	0	0	0	0	0	0	0	0	0	0	0	0
18.00	0	0	0	0	0	0	0	0	0	0	0	0	0	0	0	0	0	0	0
19.00	0	0	0	0	0	0	0	0	0	0	0	0	0	0	0	0	0	0	0
20.00	0	0	0	0	0	0	0	0	0	0	0	0	0	0	0	0	0	0	0

0.0 100.0 200.0 300.0 400.0 500.0 600.0 700.0 800.0 900.0 01000.0 01100.0 01200.0 01300.0 01400.0 01500.0 01600.0 01700.0 01800.0

Distance Downstream (m)

FIGURE G17. CONCENTRATION DISTRIBUTION IN HORIZONTAL PLANE AT A DEPTH OF 0.6 METER

DISTRIBUTION OF SEDIMENT IN HORIZONTAL PLANE AT DEPTH 1.80 (PARTS PER HUNDRED THOUSAND)

Lateral Distance (m)	0.0	100.0	200.0	300.0	400.0	500.0	600.0	700.0	800.0	900.0	1000.0	1100.0	1200.0	1300.0	1400.0	1500.0	1600.0	1700.0	1800.0	1900.0	2000.0
-20.00	0	0	0	0	0	0	0	0	0	0	0	0	0	0	0	0	0	0	0	0	0
-19.00	0	0	0	0	0	0	0	0	0	0	0	0	0	0	0	0	0	0	0	0	0
-18.00	0	0	0	0	0	0	0	0	0	0	0	0	0	0	0	0	0	0	0	0	0
-17.00	0	0	0	0	0	0	0	0	0	0	0	0	0	0	0	0	0	0	0	0	0
-16.00	0	0	0	0	0	0	0	0	0	0	0	0	0	0	0	0	0	0	0	0	0
-15.00	0	0	0	0	0	0	0	0	0	0	0	0	0	0	0	0	0	0	0	0	0
-14.00	0	0	0	0	0	0	0	0	0	0	0	0	0	0	0	0	0	0	0	0	0
-13.00	0	0	0	0	0	0	0	0	0	0	0	0	0	0	0	0	0	0	0	0	0
-12.00	0	0	0	0	0	0	0	0	0	0	0	0	0	0	0	0	0	0	0	0	0
-11.00	0	0	0	0	0	0	0	0	0	0	0	0	0	0	0	0	0	0	0	0	0
-10.00	0	0	0	0	0	0	0	0	0	0	0	0	0	0	0	0	0	0	0	0	0
-9.00	0	0	0	0	0	0	0	0	0	0	0	0	0	0	0	0	0	0	0	0	0
-8.00	0	0	0	0	0	0	0	0	0	0	0	0	0	0	0	0	0	0	0	0	0
-7.00	0	0	0	0	0	0	0	0	0	0	0	0	0	0	0	0	0	0	0	0	0
-6.00	0	0	0	0	0	0	0	0	0	0	0	0	0	0	0	0	0	0	0	0	0
-5.00	0	0	0	0	0	0	0	0	0	0	0	0	0	0	0	0	0	0	0	0	0
-4.00	0	0	0	0	0	0	0	0	0	0	0	0	0	0	0	0	0	0	0	0	0
-3.00	0	0	0	0	0	0	0	0	0	0	0	0	0	0	0	0	0	0	0	0	0
-2.00	0	0	0	0	0	0	0	0	0	0	0	0	0	0	0	0	0	0	0	0	0
-1.00	0	0	0	0	0	0	0	0	0	0	0	0	0	0	0	0	0	0	0	0	0
0.00	1000	0	0	0	0	0	0	0	0	0	0	0	0	0	0	0	0	0	0	0	0
1.00	0	0	0	0	0	0	0	0	0	0	0	0	0	0	0	0	0	0	0	0	0
2.00	0	0	0	0	0	0	0	0	0	0	0	0	0	0	0	0	0	0	0	0	0
3.00	0	0	0	0	0	0	0	0	0	0	0	0	0	0	0	0	0	0	0	0	0
4.00	0	0	0	0	0	0	0	0	0	0	0	0	0	0	0	0	0	0	0	0	0
5.00	0	0	0	0	0	0	0	0	0	0	0	0	0	0	0	0	0	0	0	0	0
6.00	0	0	0	0	0	0	0	0	0	0	0	0	0	0	0	0	0	0	0	0	0
7.00	0	0	0	0	0	0	0	0	0	0	0	0	0	0	0	0	0	0	0	0	0
8.00	0	0	0	0	0	0	0	0	0	0	0	0	0	0	0	0	0	0	0	0	0
9.00	0	0	0	0	0	0	0	0	0	0	0	0	0	0	0	0	0	0	0	0	0
10.00	0	0	0	0	0	0	0	0	0	0	0	0	0	0	0	0	0	0	0	0	0
11.00	0	0	0	0	0	0	0	0	0	0	0	0	0	0	0	0	0	0	0	0	0
12.00	0	0	0	0	0	0	0	0	0	0	0	0	0	0	0	0	0	0	0	0	0
13.00	0	0	0	0	0	0	0	0	0	0	0	0	0	0	0	0	0	0	0	0	0
14.00	0	0	0	0	0	0	0	0	0	0	0	0	0	0	0	0	0	0	0	0	0
15.00	0	0	0	0	0	0	0	0	0	0	0	0	0	0	0	0	0	0	0	0	0
16.00	0	0	0	0	0	0	0	0	0	0	0	0	0	0	0	0	0	0	0	0	0
17.00	0	0	0	0	0	0	0	0	0	0	0	0	0	0	0	0	0	0	0	0	0
18.00	0	0	0	0	0	0	0	0	0	0	0	0	0	0	0	0	0	0	0	0	0
19.00	0	0	0	0	0	0	0	0	0	0	0	0	0	0	0	0	0	0	0	0	0
20.00	0	0	0	0	0	0	0	0	0	0	0	0	0	0	0	0	0	0	0	0	0

0.0 100.0 200.0 300.0 400.0 500.0 600.0 700.0 800.0 900.0 1000.0 1100.0 1200.0 1300.0 1400.0 1500.0 1600.0 1700.0 1800.0 1900.0 2000.0

Distance Downstream (m)

FIGURE G19. CONCENTRATION DISTRIBUTION IN HORIZONTAL PLANE AT A DEPTH OF 1.8 METERS

DISTRIBUTION OF SEDIMENT IN HORIZONTAL PLANE AT DEPTH 1.80 (PARTS PER HUNDRED THOUSAND)

Lateral Distance (m)	0.0	100.0	200.0	300.0	400.0	500.0	600.0	700.0	800.0	900.0	1000.0	0100.0	01200.0	01300.0	01400.0	01500.0	01600.0	01700.0	01800.0
-20.00	0	0	0	0	0	0	0	0	0	0	0	0	0	0	0	0	0	0	0
-19.00	0	0	0	0	0	0	0	0	0	0	0	0	0	0	0	0	0	0	0
-18.00	0	0	0	0	0	0	0	0	0	0	0	0	0	0	0	0	0	0	0
-17.00	0	0	0	0	0	0	0	0	0	0	0	0	0	0	0	0	0	0	0
-16.00	0	0	0	0	0	0	0	0	0	0	0	0	0	0	0	0	0	0	0
-15.00	0	0	0	0	0	0	0	0	0	0	0	0	0	0	0	0	0	0	0
-14.00	0	0	0	0	0	0	0	0	0	0	0	0	0	0	0	0	0	0	0
-13.00	0	0	0	0	0	0	0	0	0	0	0	0	0	0	0	0	0	0	0
-12.00	0	0	0	0	0	0	0	0	0	0	0	0	0	0	0	0	0	0	0
-11.00	0	0	0	0	0	0	0	0	0	0	0	0	0	0	0	0	0	0	0
-10.00	0	0	0	0	0	0	0	0	0	0	0	0	0	0	0	0	0	0	0
-9.00	0	0	0	0	0	0	0	0	0	0	0	0	0	0	0	0	0	0	0
-8.00	0	0	0	0	0	0	0	0	0	0	0	0	0	0	0	0	0	0	0
-7.00	0	0	0	0	0	0	0	0	0	0	0	0	0	0	0	0	0	0	0
-6.00	0	0	0	0	0	0	0	0	0	0	0	0	0	0	0	0	0	0	0
-5.00	0	0	0	0	0	0	0	0	0	0	0	0	0	0	0	0	0	0	0
-4.00	0	0	0	0	0	0	0	0	0	0	0	0	0	0	0	0	0	0	0
-3.00	0	0	0	0	0	0	0	0	0	0	0	0	0	0	0	0	0	0	0
-2.00	0	0	0	0	0	0	0	0	0	0	0	0	0	0	0	0	0	0	0
-1.00	0	0	0	0	0	0	0	0	0	0	0	0	0	0	0	0	0	0	0
0.00	100000	0	0	0	0	0	0	0	0	0	0	0	0	0	0	0	0	0	0
1.00	0	0	0	0	0	0	0	0	0	0	0	0	0	0	0	0	0	0	0
2.00	0	0	0	0	0	0	0	0	0	0	0	0	0	0	0	0	0	0	0
3.00	0	0	0	0	0	0	0	0	0	0	0	0	0	0	0	0	0	0	0
4.00	0	0	0	0	0	0	0	0	0	0	0	0	0	0	0	0	0	0	0
5.00	0	0	0	0	0	0	0	0	0	0	0	0	0	0	0	0	0	0	0
6.00	0	0	0	0	0	0	0	0	0	0	0	0	0	0	0	0	0	0	0
7.00	0	0	0	0	0	0	0	0	0	0	0	0	0	0	0	0	0	0	0
8.00	0	0	0	0	0	0	0	0	0	0	0	0	0	0	0	0	0	0	0
9.00	0	0	0	0	0	0	0	0	0	0	0	0	0	0	0	0	0	0	0
10.00	0	0	0	0	0	0	0	0	0	0	0	0	0	0	0	0	0	0	0
11.00	0	0	0	0	0	0	0	0	0	0	0	0	0	0	0	0	0	0	0
12.00	0	0	0	0	0	0	0	0	0	0	0	0	0	0	0	0	0	0	0
13.00	0	0	0	0	0	0	0	0	0	0	0	0	0	0	0	0	0	0	0
14.00	0	0	0	0	0	0	0	0	0	0	0	0	0	0	0	0	0	0	0
15.00	0	0	0	0	0	0	0	0	0	0	0	0	0	0	0	0	0	0	0
16.00	0	0	0	0	0	0	0	0	0	0	0	0	0	0	0	0	0	0	0
17.00	0	0	0	0	0	0	0	0	0	0	0	0	0	0	0	0	0	0	0
18.00	0	0	0	0	0	0	0	0	0	0	0	0	0	0	0	0	0	0	0
19.00	0	0	0	0	0	0	0	0	0	0	0	0	0	0	0	0	0	0	0
20.00	0	0	0	0	0	0	0	0	0	0	0	0	0	0	0	0	0	0	0

Distance Downstream (m)

FIGURE G19. CONCENTRATION DISTRIBUTION IN HORIZONTAL PLANE AT A DEPTH OF 1.8 METERS

APPENDIX H: NOTATION

a	Constant in linear regression equation
b	Coefficient to independent variable in linear regression equation
c	Concentration of suspended sediment
$c(x,y,z)$	Three-dimensional concentration distribution
$C(x,z)$	Two-dimensional concentration distribution
$C'(y,z)$	Two-dimensional concentration distribution
d	Particle diameter
e	Random error term in linear regression equation
E_M	Diffusion coefficient for fluid momentum (eddy viscosity)
E_x, E_y, E_z	Eddy diffusivities in x, y, and z directions
f	Friction factor
$f(w)$	Settling-velocity frequency distribution
F	Test of statistical significance
g	Acceleration of gravity
G	Velocity gradient
h	Channel depth
H	Depth below the surface
I	Particle collision frequency due to thermal motion
J	Particle collision frequency due to liquid shear
k	Boltzmann's constant
L	Path length in light transmissometer
L_y, L_z	Vertical and lateral diffusion terms in transport equation
n	Particle number density
P	Particle collision frequency due to differential settling
r	Correlation coefficient
R	Collision radius
t	Time
T	Absolute temperature; also % light transmission
u	Current velocity at any point
u_*	Shear velocity
U	Mean current velocity

V	Relative velocity between settling particles
w	Particle settling velocity
x	Downstream coordinate
X	Independent variable in linear regression equation
y	Vertical coordinate
Y	Dependent variable in linear regression equation
z	Lateral coordinate
Z	Weight fraction of sediment with a particular settling velocity
α	Attenuation coefficient
η	Coefficient of viscosity
θ	Diffraction angle
K	Von Karman constant
ρ	Density
τ_t	Turbulent shear stress
τ_o	Shear stress at the bottom boundary

In accordance with letter from DAEN-RDC, DAEN-ASI dated 22 July 1977, Subject: Facsimile Catalog Cards for Laboratory Technical Publications, a facsimile catalog card in Library of Congress MARC format is reproduced below.

Wechsler, Barry A

A laboratory study of the turbidity generation potential of sediments to be dredged / by Barry A. Wechsler, David R. Cogley, Walden Division of Abcor, Inc., Wilmington, Massachusetts. Vicksburg, Miss. : U. S. Waterways Experiment Station ; Springfield, Va. : available from National Technical Information Service, 1977.

125, p. : ill. ; 27 cm. (Technical report - U. S. Army Engineer Waterways Experiment Station ; D-77-14)

Prepared for Office, Chief of Engineers, U. S. Army, Washington, D. C., under Contract No. DACW39-75-C-0104 (DMRP Work Unit No. 6C01)

References: p. 122-125.

1. Dredged material. 2. Dredging. 3. Particles. 4. Sediment. 5. Settling. 6. Turbidity. I. Cogley, David R., joint author. II. Abcor, Inc. Walden Division. III. United States. Army. Corps of Engineers. IV. Series: United States. Waterways Experiment Station, Vicksburg, Miss. Technical report ; D-77-14. TA7.W34 no.D-77-14